A.D. MDLXII

UNIVERSITY OF SASSARI
FACULTY OF MATHEMATICAL PHYSICAL AND NATURAL SCIENCES
DOCTORAL SCHOOL IN SCIENCE AND CHEMICAL TECHNOLOGY
CHEMICAL SCIENCES
XXIV CYCLE

APPLICATIONS OF THE DIFFRACTION TECHNIQUE IN SOLID STATE CHEMISTRY FROM "AB-INITIO" STRUCTURE SOLUTION TO FINAL STRUCTURE REFINEMENT.
-POWDER AND SINGLE CRYSTAL-

Doctoral Thesis by
Emilio Napolitano

Director:
Prof. B. Suffritti

Supervisor:
Prof. S.Enzo

Academic Year 2010/2011

–Emilio Napolitano–
Application of the Diffraction Technique in Solid State Chemistry from
"ab-initio" Structure Solution to Final Structure Refinement
–Powder and Single Crystal–
Doctoral Thesis in Sciences and Chemical Technology, XXIV cycle
University of Sassari

Pag. 2

Foreword.

This thesis started with the challenging scope of studying the structure of materials used for the hydrogen storage and release with the relevant kinetics paths. This is one of the new frontiers in view of the foreseen declining availability of fossil fuels for the next human generations.

After defending the now classic five-years Italian degree and final dissertation in inorganic chemistry, three years ago my early concern was to enter into the scientific subject for sustainable energy processes on the basis of the previous background and skills acquired, typically chemical inorganic syntheses for new organometallic compounds. Apparently, these two topics are quite apart, but now I believed that a bridge between them not only should be desirable but also necessary.

On the other hand, it was also clear to me that the high-profile environment around me and my supervisors was somewhat limited by the size of the laboratory. The highly interdisciplinary topics involved in the a broad subject like "Materials for Energy and Environment", was calling for a flexible introduction, trying to develop at a good level those abilities which are unavoidable in order to improve further the state-of-art of selected topics. Said in other words this posed the question about which abilities important to know.

Of course structure solution by powder diffraction was an obliged tool to think about, so my earlier approach with the structure of materials was a training on the Rietveld method to follow the kinetics of phase transformations induced by severe ball milling. The selected material was TiO_2, which may be a master inorganic compound in order to learn polymorphism, the structure, geometry, symmetry, i.e., all which is associated to the structure feature of the various compounds. The ability to quantify the amount of each developing phase in the course of the mechanical treatment time elucidated the kinetics of the transformations involved. This work was successfully published and gave to me some confidence about the refinement procedure. It must be recognized that the Rietveld approach is declined in an easy and friendly way thanks to the program MAUD, kindly made available in various improved versions by Dr. Luca Lutterotti, now at the university of Trento. In comparison with other famous software for Rietveld refinement like Fullprof and GSAS, I have found the problem of a correct input of data in order to start a refinement much better addressed for the point of view of a beginner like me

–Emilio Napolitano–
Application of the Diffraction Technique in Solid State Chemistry from
"ab-initio" Structure Solution to Final Structure Refinement
–Powder and Single Crystal–
Doctoral Thesis in Sciences and Chemical Technology, XXIV cycle
University of Sassari

Pag. 3

when I started. Also it was easy and intuitive for me to understand the language of the numerical approach together with that of crystallography and powder diffraction.

The next problem was that of being able to describe a relatively simple material not produced in the laboratory by using powder diffraction. This was the case for a natural material when studying a wide collection of dinosaur bones. Specifically we wanted to assess the bone microstructure evolution due to the so-called taphonomy and diagenetic effects. This work permitted to me to deal with the parameters of the data collection, as well as the structure and microstructure. The meaning of some parameters were quite straightforward to understand and refine, such as the scale factor of the phases, lattice parameters, average crystallite size, lattice strain, some others were a little obscure because an address of crystallography was necessary. Particularly, it was necessary to acquire a knowledge of structure classification in terms of the space groups, understanding the multiplicity associated to the Wyckoff sites, the special fractional atomic position parameters vs the general positions (x, y, z), the temperature factors, the atomic scattering factors. In summary, to evaluate carefully the importance of each structural parameter that was adjusted during the Rietveld refinement, the ingredients of this ability were common to the approach required when solving structure "ab-initio" using powder patterns by neutron or X-rays, The term "ab-initio" should not be confused with quantum chemistry, because it means here the ability to solve the structure of an unknown compound from scratch, on the only basis of the powder pattern from the substance supposed pure (single-phase). This knowledge however is not the only prerequisite, because one should also have a hint about the chemical composition of the substance and its stoichiometry and density. For a chemist this is a rather simple information, because the compounds are synthesized in the laboratory, starting from reactants well-known in terms of composition. Yet, the products sometimes are evolving along different paths with respect to those hypothesized after precipitation and crystallization. Nevertheless, the possibilities to assemble the atoms are "relatively easy" for me because of my education in chemistry.

When some of my colleagues working abroad proposed to us the topic of solving the structure of an unknown compound, likely an imide of Mg*, I responded with enthusiasm to such an invitation because I was convinced that was the correct way to complete my formation in the field of "structure determination of materials for energy and environment ". The benchmark given to us was the resolution of the product of decomposition of $Mg(NH_3)_2$ for which three patterns of excellent quality were supplied,

–Emilio Napolitano–
Application of the Diffraction Technique in Solid State Chemistry from
"ab-initio" Structure Solution to Final Structure Refinement
–Powder and Single Crystal–
Doctoral Thesis in Sciences and Chemical Technology, XXIV cycle
University of Sassari

Pag. 4

two of those collected at the synchrotron radiation stations of Grenoble at low and RT temperature, the other at the nearby ILL neutron facility.

Here I became in contact with the problem of indexing, and the implications involved in assigning a sequence of integers in view of the consequences for reconstructing correctly the so-called reciprocal space. The set of candidate space groups for the compound was immediately recognized in the hexagonal system, thanks to the use of programs available from the net, which encouraged me a lot. However, soon after I discovered that this important contribution was correctly reported by Juza and Roberts some thirty years ago(!) using diffraction powder patterns collected with a conventional apparatus. The experiments done by Dr. Francesco Dolci about the amide decomposition and amine evolution were suggesting the Magnesium imide formation MgNH, but no sensible step forward was reached with respect to the previous work of thirty years ago, unless to solve definitely the structure. It was surprising for me to learn that this relatively simple compound very common in many exemplary reaction was not solved yet and this made a strong challenge to pursue in this direction.

The web pages made available by Prof. Armel Le Bail in his site were rich of information and suggestions about the best way to start with the problem. After using the McMaille program of indexing, supplemented by Dicvol, Ito and Treor, and Fullprof for the space group candidates we started our efforts of structure solution, on the basis of the density measurements reported by Juza and using Endeavour, a simulated annealing program. I soon realized that the basic use of Endeavour with 36 atoms in the unit cell placed independently until to reach a match with the experimental sequence of intensity profiles was too long to be pursued. The chemistry was simply introduced and the computation time incredibly shortened by imposing the MgNH molecule with a non-linear arrangement as it might be expected on the basis of simple considerations about the bond orbitals. We also restricted our attention on the main candidate space group: P6/m was not considered by Juza and coworkers, given to the scarce availability of numerical methods at their time. Removal of such computation limitation is an easy thing today, thanks to the work of many scientists, many of them are also Italians. So, the first solution appeared quite soon and the proof was also made available in a golden plate by the neutron diffraction pattern collected by the Petten group.

The P6/m space group with 6(k) and 6(j) Wyckoff positions for Mg, N and H respectively, was solving very satisfactory our set of experimental patterns. Energy minimization approaches carried out by the Petten group eventually confirmed our solution. I was happy about this because the magnesium imide represents the first ab-initio structure

–**Emilio Napolitano**–
Application of the Diffraction Technique in Solid State Chemistry from
"ab-initio" Structure Solution to Final Structure Refinement
–**Powder and Single Crystal**–
Doctoral Thesis in Sciences and Chemical Technology, XXIV cycle
University of Sassari

Pag. 5

solution made here in Sassari. With new excitement I started to look around for new problems by my colleagues pointing to the same direction.

By chance, almost simultaneously, my colleague Dr. Claudio Pistidda supplied to me a very complex powder pattern obtained following a hydrogen reaction of magnesium boride with sodium hydride at high pressure and temperature. The initial attempts to index some extra lines recovered from a complex pattern of four known phases disappointingly failed. However, using another similar pattern of the same material collected within the context of a European project involving Claudio with Dr. Sebastiano Garroni, Dr. Christian Bonatto and Dr. Daphny Pottmaier, it was incredible to arrive at simple indexing schemes such as for tetragonal geometry where a and c appeared very similar or with the c/a ratio √2 which was calling our attention for the cubic sequence. This was the door open to the structure solution in term of a boron-rich phase.

During this period, I made a contact with Dr. Luca Lutterotti of the University of Trento who kindly accepted to guest my period of thesis reserved for conducting research in collaboration with advanced laboratories on the cultivated subject. This was a unique opportunity for me, because I had a contact with an excellent expertise that has conducted to what I think the best easy-to-use Rietveld approach program ever written (and available free-of-charge!). Working closely with the author of such program was another challenge to improve my abilities in the structure solution of patterns. The Department of Materials Engineering in Trento has several similarities with the Department of Chemistry in Sassari due to the presence of chemists very able in the synthesis of new compounds, so I quickly came to the conclusion that some work could be done also on the basis of the creative approach of my colleagues working in Sassari, even if not strictly allocated in my group of Physical Chemistry. Dr. Salvatore Baldino and Dr. Daniele Muroni quickly supply to me some powdered microcrystals and crystals. The rest is reported in the latter development of the thesis.

With Dr. Luca Lutterotti and the Head of the School of Chemistry it was planned a further period abroad, in a laboratory distinguished in terms of diffraction instrumentation from single-crystals to powder diffractometers. The CRYSTMAT unit at the Centre of Caen (Normandie, FR) suggested to me by Dr. Luca Lutterotti was presenting such simultaneity and this was another challenging period when I hope to have taken full benefit in view of my scopes. It is here that I have collected data of unsurpassed quality to solve the structure of $C_{21}H_{36}NO_3$, $C_{27}H_{37}NO_5$, $[P(Ph)_3CH_2CN]\cdot BF_4$ and other compounds. I should also say that this professional improvement was possible thanks to the exceptional profile of scientists like Prof. Daniel Chateigner and Dr. Olivier

–Emilio Napolitano–
Application of the Diffraction Technique in Solid State Chemistry from
"ab-initio" Structure Solution to Final Structure Refinement
–Powder and Single Crystal–
Doctoral Thesis in Sciences and Chemical Technology, XXIV cycle
University of Sassari

Pag. 6

Perez and the whole staff met at Caen. Without their full availability and complete reliance I could not achieve the results that I was able to report here.

A special thanks to Professor Stefano Enzo, for his precious teachings, recommendations and encouragements to me in these three years, in particular for his powerful "forza forza…".

Many thanks to Dr. Luca Lutterotti, for all his teaching about crystallography, softwares, extreme sports and for the creation of Maud-software.

I am particularly grateful to Dr. Renato Campesi and Dr. Francesco Dolci, at Petten (The Netherlands) when they prompted for this collaboration, which permitted to enucleate the core of my entire work, and to Mr. Gavino Ruggiu who created a special and powerful work station that gave to me the possibility to deal with the calculus problems in the SDPD route.

Special thanks to Prof. Suffritti, director of the Doctoral School in Science and Chemical Technology of Sassari, who supported me when I proposed to spend part of my PhD period in Trento (Italy) at the DIMTI and in Caen at the CRYSTMAT(France).

–Emilio Napolitano–
Application of the Diffraction Technique in Solid State Chemistry from
"ab-initio" Structure Solution to Final Structure Refinement
–Powder and Single Crystal–
Doctoral Thesis in Sciences and Chemical Technology, XXIV cycle
University of Sassari

Pag. 7

Acknowledgments

Many thanks to my family and my girlfriend Eleonora that supported me during all this special period and in particularly for their patience, necessary during unconventional work times.

Many thanks to all the person that believe in me.

A special thanks to S. Baldino and A. Contini for these last important days.

–Emilio Napolitano–
Application of the Diffraction Technique in Solid State Chemistry from
"ab-initio" Structure Solution to Final Structure Refinement
–Powder and Single Crystal–
Doctoral Thesis in Sciences and Chemical Technology, XXIV cycle
University of Sassari

Pag. 8

Contents

−Emilio Napolitano−
Application of the Diffraction Technique in Solid State Chemistry from
"ab-initio" Structure Solution to Final Structure Refinement
−Powder and Single Crystal−
Doctoral Thesis in Sciences and Chemical Technology, XXIV cycle
University of Sassari

Pag. 9

–Emilio Napolitano–
Application of the Diffraction Technique in Solid State Chemistry from
"ab-initio" Structure Solution to Final Structure Refinement
–Powder and Single Crystal–
Doctoral Thesis in Sciences and Chemical Technology, XXIV cycle
University of Sassari

Pag. 10

Introduction

In modern society the health progress is based on new and advanced pharmaceutical and technological materials including drugs[1], compounds for energy-environment[2-3-4-5], technological devices[6] etc. Establishing the crystal structure in solid state matter is a mandatory pre-requisite for understanding and predicting the function and applied properties of the materials.

In addition to this, the knowledge of the atomic scale geometry in solid state chemistry is a fundamental step to control and understand the synthesis pathway.

The single crystal[7] and powder[8] diffraction play a fundamental role to achieve this goal. These two methods are non-destructive analytical techniques which provide detailed information about the internal lattice of crystalline substances, unit cell dimensions, bond-lengths, bond-angles, and details of site-ordering until to define completely the crystal structure.

Historically, the diffraction by crystals occurred after the discovery of X-rays, that is that electromagnetic light having wavelength comparable with the atomic distances. Even if the discovery of Roentgen occurred in 1895[9] some thirty years after the atomic spectra lines in spectroscopy, P. P. Ewald was able to develop an elegant theory for diffraction soon after in 1912. On the other hand the theoretical understanding of the line succession in atomic spectra had to wait for the Schroendiger development of quantum mechanics.

The diffraction studies were initially conducted on single crystals. In fact, even today this approach is the most widely and routinely applied technique for determining structures. On the other hand the limitation of such technique rests on the request to obtain the specimen in a single crystal of sufficient size and quality. Unfortunately, many technologically and important industrial chemicals

–Emilio Napolitano–
Application of the Diffraction Technique in Solid State Chemistry from
"ab-initio" Structure Solution to Final Structure Refinement
–Powder and Single Crystal–
Doctoral Thesis in Sciences and Chemical Technology, XXIV cycle
University of Sassari

Pag. 11

can be synthesized only in polycrystalline form and cannot be grown as single crystals.

The applied features in solid state chemistry do not only consist in understanding the spatial distribution of the atoms inside the unit cell. Also the knowledge and control of microstructure play an important role[10]. In facts, dimension and orientation of the crystallites, imperfections, dislocations, and all kinds of disorder[11] often are responsible for interesting properties of such materials.

These kinds of investigation are possible only with polycrystalline compounds and this is the limit for the single crystal method.

Powder Diffraction is actually one of the most widely used techniques to characterize the state of the condensed inorganic/organic materials, and sometimes it is used even in biological molecules.

It is a useful tool in different fields such as: solid state chemistry, natural sciences pharmaceuticals, archaeology and cultural heritage, metallurgy etc. In all these areas most of the crystallized matter that we can investigate are in facts in polycrystalline state; each crystal has the size of a few microns or even just a few nanometers.

In principle powder diffraction, was used to identify ("fingerprinting") crystalline phases for more than half a century, based on the fact that different crystal structures give rise to distinct powder diffraction patterns when polycrystalline materials are illuminated with X-rays or neutrons, so it was exclusively limited to qualitative and semi-quantitative phase analysis until the 70's. The approach was to create a general archive of the solved structures, in order to make possible a comparison between the known succession of X-ray lines of the solved

–Emilio Napolitano–
Application of the Diffraction Technique in Solid State Chemistry from
"ab-initio" Structure Solution to Final Structure Refinement
–Powder and Single Crystal–
Doctoral Thesis in Sciences and Chemical Technology, XXIV cycle
University of Sassari

Pag. 12

compounds for polycrystalline form (fingerprint) with that collected the powder created in the laboratory using mostly a Debye-Scherrer camera (search-match approach). Scherrer is also known because he developed a simplified equation that allowed to estimate quickly the average crystallite size extension from the width of the most intense profile. This simple and rough approach is still used nowadays.

The major breakthrough of the powder diffraction as a quantitative tool in material sciences has occurred in 1969 with the introduction of the so called whole pattern fitting profile refinement approaches or, alternatively with the Rietveld method[12-13-14], a technique for crystal structure refinement which, for the first time, made use of the entire powder pattern instead of analyzing individual non-overlapped Bragg reflections.

This method permitted an extension of the diffraction technique on polycrystalline compounds, from structural refinement to quantitative structural and microstructural characterization.

In the Rietveld's approach the experimental powder diffraction data are utilized without extraction of the individual integrated intensities, and all structural microstructural and instrumental parameters are taken into account and possibly optimized by a least-squared refinement method until to carry out the best match (fit) between the experimental and calculated pattern.

Full profile refinement is computationally intense and requires a reasonable starting structural model and a good set of experimental data for the analysis success.

–Emilio Napolitano–
Application of the Diffraction Technique in Solid State Chemistry from
"ab-initio" Structure Solution to Final Structure Refinement
–Powder and Single Crystal–
Doctoral Thesis in Sciences and Chemical Technology, XXIV cycle
University of Sassari

Pag. 13

An important application of the Rietveld's method in powder material field is on multiphase samples. In the following work emphasis to this statement may be retrieved during the solution of an unknown phase occurring after an hydriding reaction of light borides under extreme conditions and in the analysis of the phases of dinosaur bones collected in Spain, where the largest European source of these fossils exists.

In the two studies mentioned above, it emerges both the fundamental importance of the knowledge of the spatial disposition of atoms and molecule inside the unit cell, as well as fraction composition of different phases present in the polycrystalline compound under investigation with the possibility to determine the microstructural information, such us average size dimension and orientation of crystallites. The knowledge of these details allow to determine technological properties of such analyzed material or to hypothesize the past processes to which likely the fossils have undergone.

The study of properties of solid magnesium amides has revealed to us how powder diffraction can be useful tool to study structural changes associated with phase transitions and chemical transformations in solids, because of the experiments can be performed in-situ. Analogously the opportunity to monitor structural-microstructural-and phases changes in a polycrystalline material in response to different conditions such as temperature, pressure, mechanical treatment or exposure to gaseous atmospheres of varying composition (such as variation of relative humidity) has determined our approach when studying TiO_2 powders.

The investigation of materials according to these lines of work finds application in many areas both academic and industrials, for example the quality control and polymorph screening[15] for drugs, cements, etc.

–Emilio Napolitano–
Application of the Diffraction Technique in Solid State Chemistry from
"ab-initio" Structure Solution to Final Structure Refinement
–Powder and Single Crystal–
Doctoral Thesis in Sciences and Chemical Technology, XXIV cycle
University of Sassari

Pag. 14

In principle the same experiments can be performed on single crystal, but phase transitions and chemical transformations monitored as a function of temperature and pressure or other environment parameters, are often associated with a reduction in crystal quality (e.g. by twinning, fracturing etc) to the point of making useless this approach.

Anyway single crystal experiments, when applicable, still remain the best choice for the determination of complex crystal structures of unknown compounds. Two chapters of the present work are exemplary in dealing with this topic.

The possibility to choose the investigation technique is limited by the chemistry itself or by the application of the compound. In fact, in general but not in each case, the desired product following a reaction is synthesized in polycrystalline state and only after this step a chemist or material scientist tries to grow a single crystal. There are difficult cases where it happens that a specific material doesn't grow with optimal dimension and crystal quality and the powder diffraction remains the only tool for material structure investigation.

For all the above mentioned reasons in the past 20th years, an interest on structure solution from powder diffraction data has proposed to the interest of crystallographers[16].

Even if such approach was sporadically used earlier, this objective represents a real challenge.

In principle all the information available in a single crystal diffraction pattern are the same stored following a powder diffraction experiment. The main difficult resides in the fact that the three dimensional information from single crystal investigation are compressed in one dimension in powder diffractogram as a function of just the diffraction angle 2θ.

–Emilio Napolitano–
Application of the Diffraction Technique in Solid State Chemistry from
"ab-initio" Structure Solution to Final Structure Refinement
–Powder and Single Crystal–
Doctoral Thesis in Sciences and Chemical Technology, XXIV cycle
University of Sassari

Pag. 15

This leads to a systematic and accidental reflections overlapping, creating strong difficult in each step towards the structure solution: indexing, intensity extraction, refinement.

Sometimes the determination of correct lattice parameters and the extraction of correct individual intensity could become impossible to overcome.

The possibility to solve a structure from powder diffraction data (SDPD) can be reached provided that basic guidelines can be followed, such as collecting an optimum set of diffraction data, for example from synchrotron or neutron sources, and to process them with new powerful algorithm. The present work is reporting exemplary features of these basic requirements.

Shortly, two methods[17] can be used to solve a structure from powder diffraction data: direct space methods [18-19] and direct methods [20].

The direct method uses procedures developed in the reciprocal space for single crystals and optimized for powder data. The efficiency of this latter technique is affected by the difficulty of extracting unambiguous values of the individual intensities, which will then be processed by means of Direct or Patterson method. The success depends on several factors like the efficiency of the full-pattern-decomposition programs, the peak overlapping, presence of preferred orientation, all summarized in high quality data.

On the other side the direct space methods, used in this thesis, do not require pattern decomposition, but need a priori chemical information (composition, molecular geometry, etc). They are based on global optimization algorithms such as: Monte Carlo (MC)[21-22] Simulated Annealing (SA)[23], Genetic Algorithm (GA)[24] etc.

–Emilio Napolitano–
Application of the Diffraction Technique in Solid State Chemistry from
"ab-initio" Structure Solution to Final Structure Refinement
–Powder and Single Crystal–
Doctoral Thesis in Sciences and Chemical Technology, XXIV cycle
University of Sassari

Pag. 16

These algorithms are able to orient and locate atoms or structural models inside the unit cell until to find a global minimum function corresponding to the best agreement between the calculated and experimental pattern.

This procedure corresponds to choose starting N parameters describing the system under investigation, called Degree of Freedom (DoF): translation and rotation for a molecule or polyhedron, and internal DoF like torsion angles, bond length and bond angles.

These parameters are randomly changed in order to explore an N-dimension hypersurface until to find the global minimum corresponding with a low R_w value.

The direct space method is a good tool to overcome the intensity overlap problem in powder diffraction.

Of course we should not forget that when the crystal structure of unknown compound is too complex to be solved from powder diffraction data, one may go back to think again about the single crystal technique is the best way for structure determination, hence the possibility to grow a single crystal of good quality.

This diffraction method of the Bragg reflections are spatially resolved into three dimensions in reciprocal space. This important feature is possible because of the single crystal exhibits a single continuous lattice throughout the entire volume sample.

The advantage to avoid overlapping reflections I_{hkl}, makes easy the indexing step, and so metric parameters are readily determined. The same advantage occurs for the choice of the right space group.

These two steps are the most critical in structure solution in powder diffraction.

–Emilio Napolitano–
Application of the Diffraction Technique in Solid State Chemistry from
"ab-initio" Structure Solution to Final Structure Refinement
–Powder and Single Crystal–
Doctoral Thesis in Sciences and Chemical Technology, XXIV cycle
University of Sassari

Pag. 17

In each intensity reflection I_{hkl} it is stored all the information about the location of the atoms inside the unit cell.

It is proportional to the square of the structure factor F_{hkl}

$$I_{hkl} \propto F^2_{hkl} \qquad \text{(eq.1)}$$

Where the F^2_{hkl} is equal to

$$F_{hkl} = \sum_{i=1}^{N} f_i e^{-2\pi i(hx_i + hy_i + hz_i)} e^{-B_i sin^2/\lambda^2} \qquad \text{(eq.2)}$$

In equation 2, f_i is the atomic scattering factor of the ith atom, which has the coordinates

(x_i, y_i, z_i), B_i is the Debye-Waller factor and λ is the wavelength used in the diffraction experiment.

The equation 2. can be transformed into

$$F_{hkl} = F_{hkl} \ e^{i\varphi_{hkl}} \qquad \text{(eq.3)}$$

Where F_{hkl} is the amplitude and φ_{hkl} is the phase reflection.

Direct and reciprocal spaces are related to one another as forward and reverse Fourier transformations

$$\rho \ x,y,z = \frac{1}{V} \ F_{hkl} e^{i\varphi_{hkl}} \qquad \text{(eq.4)}$$

$\rho \ x,y,z$ is the electron density inside the unit cell.

Unfortunately, the phase angles are lost in a diffraction experiment which is able to collect intensity values always positive that misses the amplitude sign, so the crystal structure cannot be reconstructed directly. This obstacle toward the structure solution is known as the 'phase problem'.

–Emilio Napolitano–
Application of the Diffraction Technique in Solid State Chemistry from
"ab-initio" Structure Solution to Final Structure Refinement
–Powder and Single Crystal–
Doctoral Thesis in Sciences and Chemical Technology, XXIV cycle
University of Sassari

Pag. 18

To overcame this problem various algorithms are used, such direct methods, Patterson methods, maximum entropy, charge flipping.

As we will see the two techniques show their proper advantages and disadvantages, and their application is limited by the nature of sample or other instrument factors.

Traditionally, single-crystal and powder diffractometers were placed in different laboratories and single-"crystallographers" and powder "diffractionists" had little interaction with each other generating two parallel professional careers.

The scope of this thesis of PhD is to acquire a general expertise in diffraction overcoming this false dualism. The possibility to be master in both the single-crystal and powder approaches by exploiting the advantages of the two methods is an important ability dealing with solid state chemistry.

References
1. S. Datta, D.J. W. Grant. Nature Reviews Drug Discovery 2004, 3, 42-57
2. M. Ni, M.KH. Leug, D.Y.C Leug, K. Sumathy. Renewable and Sustainable Energy Reviews. 11 (2007) 401–425.
3. U.G. Akpan, B.H Hameed. J. Hazardous Materials. 2009, 520-529.
4. O'Regan B., Grätzel M., *Nature*, 1991, 353, 737-39.
5. L. Schlapbach & A. Züttel . 2001 15 November NATURE, vol 414.
6. G. Hashmi, K. Miettunen, T. Peltola, J. Halme, I. Asghar, K. Aitola, M. Toivola, P. LundRenewable and Sustainable Energy Reviews 15 (2011) 3717–3732.

–Emilio Napolitano–
Application of the Diffraction Technique in Solid State Chemistry from
"ab-initio" Structure Solution to Final Structure Refinement
–Powder and Single Crystal–
Doctoral Thesis in Sciences and Chemical Technology, XXIV cycle
University of Sassari

Pag. 19

7. T. Warne, M. J. Serrano-Vega, J. G. Baker, R. Moukhametzianov1, P. C. Edwards, R. Henderson, A. G. W. Leslie, C. G. Tate & G. F. X. Schertler. NATURE, 2008 24 July, Vol, 454.

8. M. Poojary, A. Clearfield. Acc. Chem. Res. 1997, 30, 414-422

9. Crystal structure analysis: a primer, third ed. IuCr, J.P. Glusker, K.N. Trueblood

10. U. F. Kocks, C. N. Tomè, H. R. Wenk,.Texture an anisotropy. Preferred Orientation in Polycrystals and their Effect on Materials Properties, 1998. Cambridge University Press.

11. A. Guinier, X-ray Diffraction in Crystals, Imperfect Crystals and Amorphous Bodies. Freeman, San Francisco, 1963. Reprinted by Dover, York, 1994

12. Young, R.A.(1993), *The Rietveld Method*, Oxford: University Press. (ISBN 0 19 855577 6) Chapter 2.

13. Rietveld,H.M.(1967). *Acta Crystallogr*.,**22**,151-2.

14. Rietveld,H.M.(1969). *J. Appl. Crystallogr*.,**2**,65-71.

15. J. Bernstein, R. J. Davey, and J. Henck. Angew. Chem. Int. Ed. 1999, 38, 3440 -3461

16. A. Le Bail. (2001) Trends in structure determination by powder diffractometry, in *Advances in Structure Analysis*. Edited by R. Kuzel and J. Hasek CSCA, Praha.

17. W. I. F. David, K. Shankland, L.B. McCusker, and Ch. Baerlocher, Eds., Oxford University Press,Oxford, New York (2002).

18. W. I. F. David and K. Shankland. Structure determination from powder diffraction data. ActaCryst. A64, 52 (2008).

19. 7 R. Cerny´ and V. Favre-Nicolin, Direct space methods of structure determination from powder diffraction: principles, guidelines and perspectives. Z. Kristallogr. 222, 105 (2007).

20. C.Giacovazzo Acta Crist. (1996). A52, 331-339

–Emilio Napolitano–
**Application of the Diffraction Technique in Solid State Chemistry from
"ab-initio" Structure Solution to Final Structure Refinement
–Powder and Single Crystal–
Doctoral Thesis in Sciences and Chemical Technology, XXIV cycle
University of Sassari**

Pag. 20

21. Y.G Andreev, P. Lightfoot and P. G Bruce, J. Appl. Cryst. 1997, 30, 294

22. K. D. M Harris, M. Tremayyne, P. Lighfoot and P. G Bruce, J. Am. Chem. Soc., 1994, 116, 3543.

23. A.A. Coelho . J. Appl. Cryst. 33, 899 (2000).

24. K. D. M Harris, R. L. Johnston, Benson M. Kariuki, M, Tremayne   J. Chem. Research, 1998

–Emilio Napolitano–
Application of the Diffraction Technique in Solid State Chemistry from
"ab-initio" Structure Solution to Final Structure Refinement
–Powder and Single Crystal–
Doctoral Thesis in Sciences and Chemical Technology, XXIV cycle
University of Sassari

Pag. 21

Kinetics of structural evolution occurring in titanium dioxide nanocrystalline powders subjected to mechanical treatment

Titanium oxide is one of the most studied systems in solid state chemistry because of its huge field of application: from biocompatible[1] material for prosthetic implants to cosmetics[2], material for environment application in water splitting[3] for hydrogen generation and oxidation of organic compounds in water purification systems[4], to solar cells[5-6], etc.

All its applications are made possible because of the titanium oxide is present in nature under different polymorph systems, each one having different physical-chemical properties determined in turn by their crystal structure features.

This work specifically investigates the kinetics[7] of phase transformation processes undergone by titanium dioxide powders during the mechanical treatment.

X-ray diffraction has been employed to carry out a quantitative characterization of the powder structural evolution by using the so-called Rietveld approach.

Using a suitable modelling of transformation kinetics, the fraction of powder processed on the average at each collision was estimated. The mass of powder involved in phase transformation and microstructural refinement processes at each collision was then worked out by a systematic variation of the powder charge inside the reactor.

–Emilio Napolitano–
Application of the Diffraction Technique in Solid State Chemistry from
"ab-initio" Structure Solution to Final Structure Refinement
–Powder and Single Crystal–
Doctoral Thesis in Sciences and Chemical Technology, XXIV cycle
University of Sassari

Pag. 22

Experimental

Experiments were carried out on TiO_2 anatase commercial powders. The powders were handled inside a glove box under Ar atmosphere with nitrogen, oxygen and humidity below 5 ppm. A given powder charge m_p ranging between 1 and 12 g was sealed under Ar atmosphere in a hardened steel cylindrical reactor with a single stainless steel ball of about 12 g. The reactor was fixed on the mechanical arm of a Spex Mixer/Mill mod. 8000 and displaced at a frequency of about 14.6 Hz. The collision frequency N and the average impact energy E took the average values of 29.2 Hz and 0.103 J respectively[8-9]. The mechanical treatment of powders was carried out for selected time intervals, at the end of which the reactor was emptied and refilled with the same charge of unprocessed powders. Powders were submitted to wide-angle X-ray diffraction (XRD) analyses. XRD patterns were collected with a Bruker diffractometer equipped with Cu Kα radiation. The scattered intensity was best-fitted by a set of mathematical functions according to the Rietveld method[10-11-12].

Data analysis

After the data collection the raw data handling steps has been performed and subsequently a Rietveld refinement has been carry out until to obtain phase-microstructural and crystal structure changes information.

The identification of individual phase contributions to the diffracted intensity Fig.1 permitted quantitative information to be gained on the relative amount of the different phases and on their microstructural features. In turn, this allowed us to work out a reliable kinetics of both the phase transformation behavior and the crystallite size refinement of anatase at each selected value of total powder charge (m_p).

–Emilio Napolitano–
Application of the Diffraction Technique in Solid State Chemistry from
"ab-initio" Structure Solution to Final Structure Refinement
–Powder and Single Crystal–
Doctoral Thesis in Sciences and Chemical Technology, XXIV cycle
University of Sassari

Pag. 23
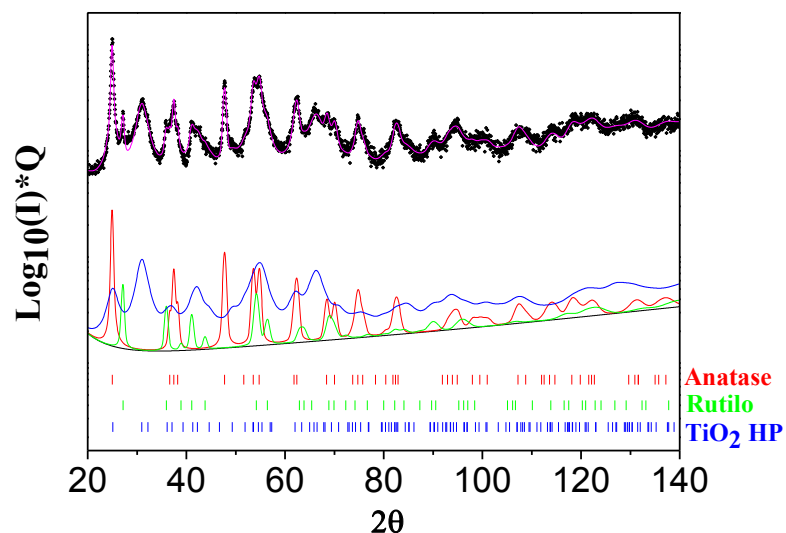
Figure 1. *The XRD pattern of TiO2 powders processed for 400 min in the case of trials performed with a total powder charge m_p in this case of 10 g the simulated contributions of the different phases are superposed to the experimental XRD pattern. For clarity, the logarithm of the scattered intensity I, log(I), has been multiplied by the scattering vector Q.*

XRD TiO$_2$ 10g
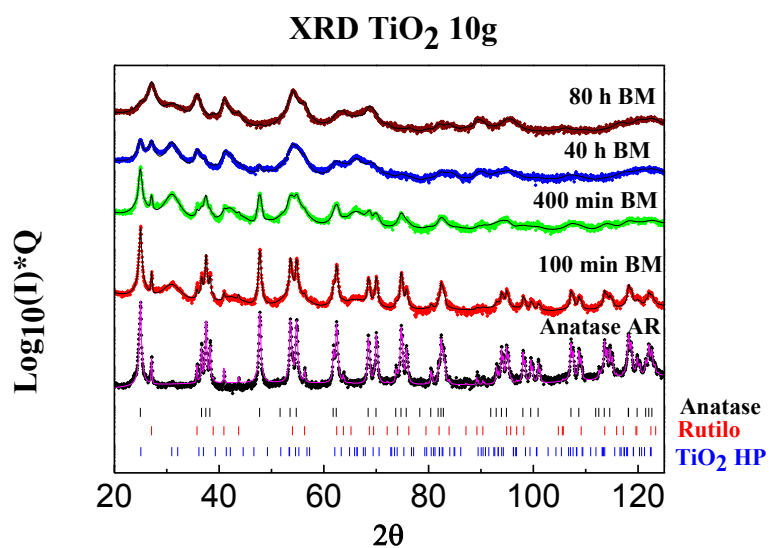
Figure 2. *A sequence of XRD patterns describing the gradual anatase-to-rutile transition for TiO$_2$ powders processed for the quoted time intervals. Data refer to the case of trials performed with a total amount of powder inside the reactor equal to 10 g. The total best-fitted Rietveld numerical profiles are also shown At longer times of mechanical treatment, a growth of the rutile reflections is observed, with a progressive disappearance of the peaks pertaining to anatase and TiO$_2$ II.*

–Emilio Napolitano–
Application of the Diffraction Technique in Solid State Chemistry from
"ab-initio" Structure Solution to Final Structure Refinement
–Powder and Single Crystal–
Doctoral Thesis in Sciences and Chemical Technology, XXIV cycle
University of Sassari

Pag. 24

In all of the investigated cases, the mechanical treatment induces a gradual transition from anatase (tetragonal a,b = 3.7855(1) Å, c= 9.5148(1) Å S.G: I41/amd) to TiO2 II high-pressure phase[13-14] (orthorhombic sri-lankite type a = 4.515(6) Å; b=5.497(5) Å; c=4.939(5) Å, SG: Pbcn) and then to rutile (tetragonal a,b=4.5954(4) Å, c= 2.9597(6)Å; S.G: P42/mnm) for extended mechanochemical treatment. A few XRD patterns are given in Fig. 2 for the sake of illustration together with best-fitted Rietveld profiles.

The Rietveld procedure indicates that the amount of rutile contained in the initial anatase powders is actually on the order of 4.0 wt.% (Table 1). At longer times of mechanical treatment, a growth of the rutile weigtht percent is observed, with a progressive disappearance of the amount phase pertaining to anatase and TiO_2 II.

The quantitative evaluation of phases as a function of the treatment shows that

$$X_{An} = A_o \cdot e^{-k1 \cdot t} \qquad\qquad eq.1$$

$$X_{HP} = A_o \cdot k_1/(k_2-k_1) \cdot [e^{-k1 \cdot t} - e^{-k2 \cdot t}] \qquad\qquad eq.2$$

$$X_{Rut} = A_o - [A_o \cdot k_2/(k_2-k_1) \cdot e^{-k1 \cdot t}] + [A_o \cdot k_1/(k_2-k_1) \cdot e^{-k2 \cdot t}] \qquad\qquad eq.3$$

the reaction proceeds with a consecutive kinetics (Fig.3).

The kinetic curves have been suitably interpolated by model curves (eq.1-2-3)[15], which allowed the rough evaluation of the apparent rate constants of the phase transformation processes from reactant powders to intermediate and then to final product.

–Emilio Napolitano–
Application of the Diffraction Technique in Solid State Chemistry from
"ab-initio" Structure Solution to Final Structure Refinement
–Powder and Single Crystal–
Doctoral Thesis in Sciences and Chemical Technology, XXIV cycle
University of Sassari

Pag. 25

BM Time/min	Anatase Wt%	TiO2-HP Wt%	Rutile Wt%
0	96	0	4
10	66	30	4
20	54	42	4
40	33	59	8
60	20	64	16
120	4	62	34
240	2	32	66
360	2	14	84
480	1	7	92

Table 1. Phase quantities (wt%) carried out by the Mechanical treatment of 1g of TiO$_2$ Anatase.
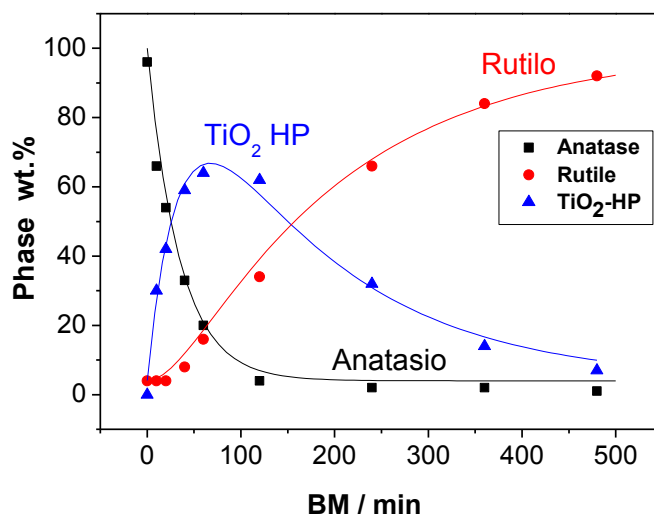
Figure 3.Weight fraction of Anatase, TiO$_2$-HP and Rutile phase, respectively as a function of the time ball milling process (BM) in this case 1g of starting TiO2 anatase.

Both anatase and rutile diffraction peaks undergo a decrease of their intensity and a broadening due to the formation of a nanometric structure and the accumulation of lattice defects. Microstructural refinement (Table 2.Fig.4) is accompanied by the appearance of new peaks, which can be attributed to the TiO$_2$ II phase.

BM Time/min	Anatase Cryst/ Å	TiO2-HP Cryst/ Å	Rutile Cryst/ Å
0	2280	0	2320
10	665	42	920
20	520	45	740
40	356	50	312
60	361	61	230
120	280	59	105
240	258	54	107
360	265	45	110
480	264	44	110

Table 2. The average crystallite size L of anatase, TiO$_2$-HP and rutile as a function of ball milling time.

–Emilio Napolitano–
Application of the Diffraction Technique in Solid State Chemistry from
"ab-initio" Structure Solution to Final Structure Refinement
–Powder and Single Crystal–
Doctoral Thesis in Sciences and Chemical Technology, XXIV cycle
University of Sassari

Pag. 26
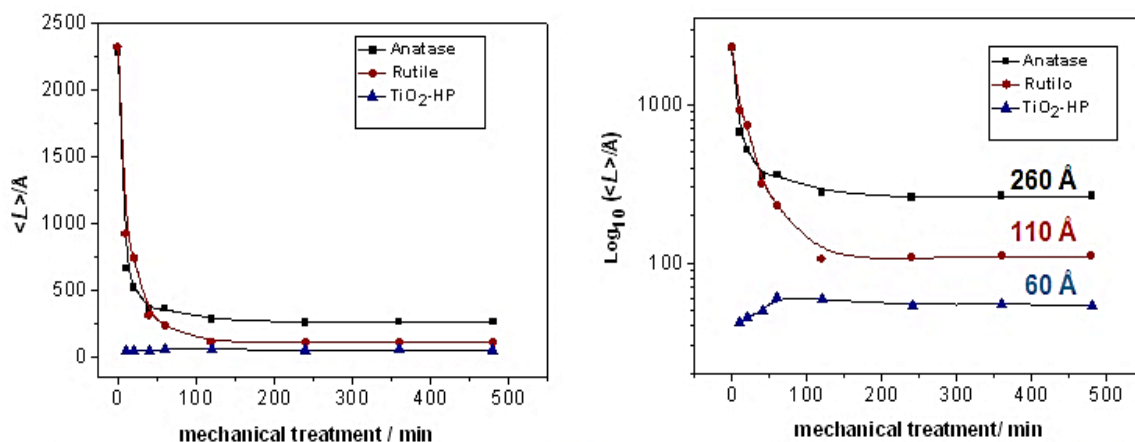
Figure 4. Graphical representation of the average crystallite size L of anatase, TiO_2-HP and rutile as a function of ball milling time(i), logarithm scale (ii).

Analyzing the mechanochemical process, it is composed by a huge number of discrete events in which structural and chemical modifications occur at each impact between the milling tools. Different processes, such as crystallite size refinement and phase transformation, take place concomitantly and the amount of powder involved in each process at the impact is determined by the complex phenomena occurring on microscopic scale under the action of compressive and shear stresses.

Using the information carried out with the Rietveld method (below mentioned) and a phenomenological model of mechanical processing developed in our laboratory (Delogu)[16] we are able to estimate the mass m* of powder that experiencing critical load condition (CLCs) during each discrete process event. This quantity stays approximately constant, irrespective of the total powder charge inside the reactor (m_p).

These values can be estimated by the slope of the plots of the apparent rate constants k_{an} and k_{ll} (obtained from the best-fitting of the kinetic curves) as a function of the reciprocal of powder charge m_p, m_p^{-1}, shown in Fig.5.

–Emilio Napolitano–
Application of the Diffraction Technique in Solid State Chemistry from
"ab-initio" Structure Solution to Final Structure Refinement
–Powder and Single Crystal–
Doctoral Thesis in Sciences and Chemical Technology, XXIV cycle
University of Sassari

Pag. 27
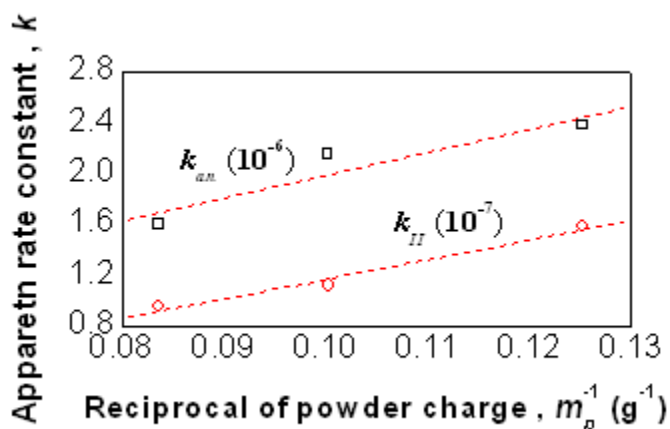
Figure 5. The rate constants k_{an} and k_{II} for the anatase-to-TiO$_2$ II phase and for the TiO$_2$ II phase-to-rutile transformations as a function of the reciprocal of powder charge m_p, m_p^{-1}. As indicated, k_{an} and k_{II} are expressed in units of $1\cdot10^{-6}$ and $1\cdot10^{-7}$ respectively. Best-fitted lines are also shown.

So the powder processed at each collision for the anatase-to-TiO$_2$-II phase and for the TiO$_2$-II phase-to-rutile transformations are respectively equal to 17.9 and 1.5 µg. These quantities powder involved in phase transformation processes is quite small if compared with the average amount ~1mg of powder trapped[16-17-18] at individual collisions. Of course, the fraction of anatase transformed into TiO$_2$-II is larger than the TiO$_2$-II one transformed into rutile.

Similar features are observed in the study of the microstructural refinement process of anatase powders. The average crystallite size L of anatase is shown in Fig. 6 as a function of the number n of collisions.

–Emilio Napolitano–
Application of the Diffraction Technique in Solid State Chemistry from
"ab-initio" Structure Solution to Final Structure Refinement
–Powder and Single Crystal–
Doctoral Thesis in Sciences and Chemical Technology, XXIV cycle
University of Sassari

Pag. 28
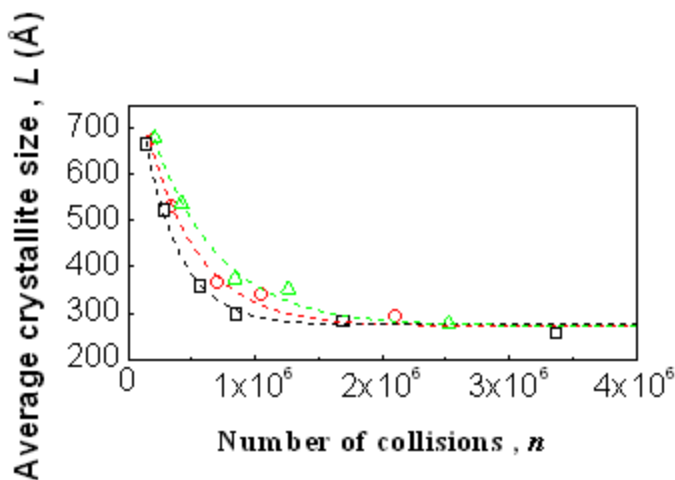
Figure 6 The average crystallite size L of anatase as a function of the number n of collisions trials performed with powder charges m_p equal to 8 ($\square$), 10 ($\bigcirc$) and 12 ($\triangle$) g. Best-fitted curves are also shown.

It can be seen that data arrange according to exponentially decreasing trends. The different values of rate constant K obtained by the best-fitting procedure are shown in (Fig. 7) as a function of the reciprocal of the total powder charge m_p, m_p^{-1}.
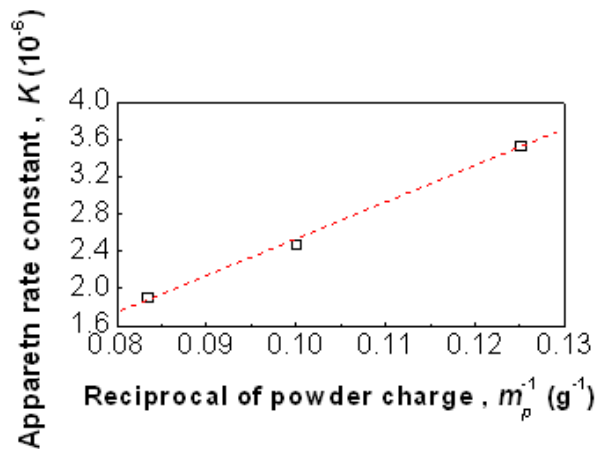
Figure 7. The apparent rate constant K for the crystallite size refinement of anatase powders as a function of the reciprocal of powder charge m_p, m_p^{-1} . The best-fitted line is also shown.

–Emilio Napolitano–
Application of the Diffraction Technique in Solid State Chemistry from
"ab-initio" Structure Solution to Final Structure Refinement
–Powder and Single Crystal–
Doctoral Thesis in Sciences and Chemical Technology, XXIV cycle
University of Sassari

Pag. 29

Also in this case, a linear relationship between the apparent rate constant K and m_p^{-1} is observed. In analogy with the cases of anatase-to-TiO_2 II and TiO_2 II-to-rutile phase transformations, the linear plot in Fig. 7 allows an estimate of the mass m_L^* of anatase powder that, on average, undergoes CLCs for the crystallite size refinement at each collisions. The m_L^* value obtained is roughly equal to 40.3 µg. Therefore, about 40.3 µg of anatase experiences CLCs at each collision and undergoes a reduction of their crystallite size.

Conclusion

The present work is based on X-ray investigation and Rietveld refinement on TiO_2 ball milled powder material.

The mechanical treatment induced the gradual transformation of the initial anatase into the intermediate TiO_2-II phase and of this latter into the final rutile, the quantitative evaluation of phases as a function of the treatment shows that the reaction proceeds with a consecutive kinetics.

At the same time, anatase was converted into a nanostructured phase by a progressive reduction of its crystallite size L. The microstructural refinement of anatase powders proceeds at rates significantly higher than the ones observed in the case of phase transformations. It follows that inducing a reduction of crystallite size is relatively easier than promoting a phase transformation.

–Emilio Napolitano–
Application of the Diffraction Technique in Solid State Chemistry from
"ab-initio" Structure Solution to Final Structure Refinement
–Powder and Single Crystal–
Doctoral Thesis in Sciences and Chemical Technology, XXIV cycle
University of Sassari

Pag. 30

References

1. M.P. Casaletto, G.M. Ingo, S. Kaciulis, G. Mattogno, L. Pandol®, G. Scavia. Applied Surface Science 172 (2001) 167-177.
2. Zu, Y.; Lei, Y.; Yu, X. *New Mater. Chem. Technol.* **1998**, *6*, 26
3. M. Ni, M.KH. Leug, D.Y.C Leug, K. Sumathy. Renewable and Sustainable Energy Reviews. 11 (2007) 401–425.
4. U.G. Akpan, B.H Hameed. J. Hazardous Materials. (2009) 520-529.
5. O'Regan B., Grätzel M., *Nature*, 1991, 353, 737-39.
6. Michael Gräetzel d, Hwan Kyu Kim. Dyes and Pigments 91 (2011) 192e198
7. Delogu F., Cocco G., *J. Of Materials Synthesis and Processing,* 2000, 8, 271-77
8. Delogu F, Mulas G, Schiffini L, Cocco G. Mater. Sci. Eng. A 2004; 382: 280.
9. Delogu F, Cocco G. J. Alloys Compd. 2007; 436: 233.
10. Young, R.A.(1993), *The Rietveld Method*, Oxford: University Press. (ISBN 0 19 855577 6) Chapter 2.
11. Rietveld,H.M.(1967). *Acta Crystallogr*.,**22**,151-2.
12. Rietveld,H.M.(1969). *J. Appl. Crystallogr*.,**2**,65-71.
13. Filatov S. K., Bendeliani N. A., *Doklady Physics,* 2007, 52, 195-99.
14. Gerward L., Staun Olen J., *J. Appl. Cryst*., 1997, 30, 259-64
15. M.J.Pelling, P. W. Seakings. (1995) Reaction Kinetics, Oxford University Press. (ISBN 0 19 855527 X) Chapter 8.
16. Delogu F, Mulas G, Schiffini L, Cocco G. Mater. Sci. Eng. A 2004; 382: 280.
17. Delogu F. Acta Mater. 2008; 56: 905
18. Manai G, Delogu F, Rustici M. Chaos 2001; 12: 601.

–Emilio Napolitano–
Application of the Diffraction Technique in Solid State Chemistry from
"ab-initio" Structure Solution to Final Structure Refinement
–Powder and Single Crystal–
Doctoral Thesis in Sciences and Chemical Technology, XXIV cycle
University of Sassari

Pag. 31

A multi-technique approach by XRD, XRF, FT-IR to characterize the diagenesis of dinosaur bones from Spain.

A combined investigation by X-ray fluorescence (XRF), Fourier Transform Infrared spectroscopy (FT-IR), Raman spectroscopy and powder X-ray Diffraction (XRD), supplemented with the Rietveld analysis, was conducted on sixty Spanish dinosaur bone specimens from Upper Jurassic/Lower Cretaceous to Upper Cretaceous age to investigate taphonomy and diagenetic processes. The diffraction approach assessed in all specimens the presence of fluorapatite at various levels of percentage as the mineral phase constituting the fossil bone. In addition to fluorapatite, calcite and quartz were also found as main secondary phases in many specimens. The infrared spectra of fossil bones show significant changes in the phosphate and carbonate band intensity with respect to a non-fossil bone. Conversely, the X-ray fluorescence spectra turned out to be mainly dominated by the presence of Ca, obviously accompanied by phosphorus. Simultaneously, other elements accompanying Ca, such as Fe and Sr were found at significant concentration levels.

A considerable amount of Fe and Sr ions were incorporated in the structure of fluorapatite, but when their concentration was found elevated in the fluorescence spectrum, the diffraction data revealed the presence of goethite (FeOOH) and celestite ($SrSO_4$) phases. While the X-ray diffraction phase analysis also revealed the presence of kaolinite, dolomite, barite and gypsum, in some fluorescence spectra further elements like Y, As, Pb, Ti, Mn, Cr, Cu, Zn were present in concentration at trace level. The introduction/substitution of new elements with the infiltration of new phases due to diagenesis is also affecting to various extent the Raman and FT-IR spectra with modification of some bands and/or the appearance of new bands. Impurities may affect drastically the quality of the Raman spectra.

–Emilio Napolitano–
Application of the Diffraction Technique in Solid State Chemistry from
"ab-initio" Structure Solution to Final Structure Refinement
–Powder and Single Crystal–
Doctoral Thesis in Sciences and Chemical Technology, XXIV cycle
University of Sassari

Pag. 32

The average crystallite size of the "apatitic" constituent phase was found to vary from a minimum of ca. 183(±10) Å to an upper level of 2100 (±200) Å. No systematic relation between apatite crystallite size and age of the dinosaur bones was found that suggests a high variability of diagenetic processes affecting the growth of bone crystallites even in the same site.

Introduction

The study about chemical and mineralogical composition of fossil animal and human bones may be a precious source of information about the past. However, a large fraction of these studies have focused on archaeological samples and biomaterials and only to a little extent on dinosaur fossils [1-9]. Changes involving the structure and chemical composition of bones may occur in two different periods, i.e., first during the animal's life, and second during the fossilization process. The time scale of these two stages may be incommensurable and a distinction is made between biostratinomy and fossildiagenesis. During the biostratinomic stage, micro-organisms and other biotic processes can attack the organic and inorganic content of bones, degrading mineral bone phases[10, 11]. In addition, abiotic factors can degrade the bones both before or after burial [12]. If the bones are not subjected to microbial or biotic erosion or the processes are affected by drastic physical or chemical changes, fossilization may occur soon after burial [10, 13, 14].

Some processes may occur to preserve rather than degrading fossils, particularly the incorporation of new ions into the crystal structure and/or recrystallisation of skeletal apatite,[14,15-18]. These processes are mainly controlled by abiotic, physical and chemical environmental soil conditions, particularly groundwater chemistry around the buried bone material [9, 10, 18]. The bioapatite of animal and

–Emilio Napolitano–
Application of the Diffraction Technique in Solid State Chemistry from
"ab-initio" Structure Solution to Final Structure Refinement
–Powder and Single Crystal–
Doctoral Thesis in Sciences and Chemical Technology, XXIV cycle
University of Sassari

Pag. 33

human bones turns out to be very similar at an atomic level and the structure is generally approximated using the stoichiometric mineral hydroxylapatite $Ca_5(PO_4)_3OH$.

Wopenka and Pasteris [19] have recently discussed the limitations of such an inorganic phase as a model of bones especially in view of several types of ionic substitutions in the apatite lattice that may change the mineral characteristics. Of course, *post-mortem* taphonomic and diagenetic changes are expected to add further complexity to the structure and microstructure of fossil bones, not only due to new ionic substitutions but also in terms of new biogenic or authigenic phases that form in the fossilizing bone. Wopenka and Pasteris [19] locate the natural bioapatite inside an hyper-phase diagram with end-members of apatite minerals such as hydroxylapatite, fluorapatite, A-type carbonated apatite, B-type carbonated fluorapatite (old mineral name francolite), B-type carbonated hydroxylapatite (old mineral name dahllite). A good knowledge of the chemical and mineralogical composition of fossil bones as the result of a whole host of physical, chemical and biological processes can be obtained directly from fluorescence and powder diffraction of X-rays [20]. For the study of molecular features in bones, the above techniques have been recently supplemented by Infrared and Raman spectroscopy [21,22]. It should be considered that the fluorescence technique gives direct information on the elemental composition that can be usefully compared with the quantitative phase evaluation from X-ray diffraction and with information about the molecular groups as derived from Raman and Infrared spectroscopy. The recent numerical development of powder X-ray Diffraction technique according to the Rietveld method has supplied a new approach to reveal the structure details of natural apatites, as we have recently verified in archaeological and geological contexts [23].

–Emilio Napolitano–
Application of the Diffraction Technique in Solid State Chemistry from
"ab-initio" Structure Solution to Final Structure Refinement
–Powder and Single Crystal–
Doctoral Thesis in Sciences and Chemical Technology, XXIV cycle
University of Sassari

Pag. 34

Chipera and Bish [24], Zocco and Schwartz [3], Dumont et al. [7] have analysed the effect of crystallite size and strain in the apatite lattice, which is a way to evaluate the crystallinity index CI [25, 26].

Conversely, Elorza et al. [15] measured the apatite crystallinity from the width of the (002) peak of dinosaur bones and found it to be significantly higher than for modern bone. They also reported X-ray diffraction (XRD) patterns of bones according to which the replacement of biogenic hydroxylapatite by francolite is related to diagenetic changes.

A multiple-technique approach combining XRD, XRF, FT-IR and Raman analysis proved to be useful to better characterize the mineralogical and chemical composition of fossil bones. This information enables a better understanding of bone fossilization processes but knowledge of the phase composition is also important in order to choose the appropriate treatment and chemical products for optimal conservation and preservation of the fossils [27].

Material and Methods

Bone samples

Table I reports the list of sixty dinosaur bone specimens examined in this work, their geological period and formation, taxa and provenance locations.

–Emilio Napolitano–
Application of the Diffraction Technique in Solid State Chemistry from
"ab-initio" Structure Solution to Final Structure Refinement
–Powder and Single Crystal–
Doctoral Thesis in Sciences and Chemical Technology, XXIV cycle
University of Sassari

Pag. 35

TABLE I

Sample code	Classification	Series Epoch and System Period	Formation and Basin	Location
Patiras	Dinosauria (unclassified)	Lower Cretaceous (Barremian)	Arcillas de Morella Maestrat Basin	Todolella (Castellón)
CL	Dinosauria (Ornithopoda)	Lower Cretaceous (Barremian)	Cantaperdius Maestrat Basin	Portell (Castellón)
CL 42	Dinosauria (Ornithopoda)	Lower Cretaceous (Barremian)	Cantaperdius Maestrat Basin	Portell (Castellón)
CL 56	Dinosauria (Ornithopoda)	Lower Cretaceous (Barremian)	Cantaperdius Maestrat Basin	Portell (Castellón)
La Cuba	Dinosauria (unclassified)	Lower Cretaceous (Barremian)	Cantaperdius Maestrat Basin	Portell (Castellón)
La Fita	Dinosauria (Ornithopoda)	Lower Cretaceous (Barremian)	Arcillas de Morella Maestrat Basin	Cinctorres (Castellón)
La Fita balsa	Dinosauria (Ornithopoda)	Lower Cretaceous (Barremian)	Arcillas de Morella Maestrat Basin	Cinctorres (Castellón)
Qurolles III	Dinosauria (Ornithopoda)	Lower Cretaceous (Aptian)	Cantaperdius Maestrat Basin	Portell (Castellón)
Qurolles M	Dinosauria (Ornithopoda)	Lower Cretaceous (Aptian)	Cantaperdius Maestrat Basin	Portell (Castellón)
MC1-5	Dinosauria (Ornithopoda)	Lower Cretaceous (Aptian)	Cantaperdius Maestrat Basin	Portell (Castellón)
SAV-39	Dinosauria (Eusauropoda)	Lower Cretaceous (Aptian)	Arcillas de Morella Maestrat Basin	Morella (Castellón)
SAV-67	Dinosauria (Eusauropoda)	Lower Cretaceous (Aptian)	Arcillas de Morella Maestrat Basin	Morella (Castellón)
Povet	Dinosauria (Ornithopoda)	Lower Cretaceous (Aptian)	Arcillas de Morella Maestrat Basin	Morella (Castellón)

–Emilio Napolitano–
Application of the Diffraction Technique in Solid State Chemistry from
"ab-initio" Structure Solution to Final Structure Refinement
–Powder and Single Crystal–
Doctoral Thesis in Sciences and Chemical Technology, XXIV cycle
University of Sassari

Pag. 36

Camino	Dinosauria (unclassified)	Lower Cretaceous (Aptian)	Arcillas de Morella Maestrat Basin	Morella (Castellón)
EAP 38	Dinosauria (unclassified)	Lower Cretaceous (Aptian)	Arcillas de Morella Maestrat Basin	Morella (Castellón)
EAP 40-39	Dinosauria (unclassified)	Lower Cretaceous (Aptian)	Arcillas de Morella Maestrat Basin	Morella (Castellón)
EAP 43	Dinosauria (unclassified)	Lower Cretaceous (Aptian)	Arcillas de Morella Maestrat Basin	Morella (Castellón)
Comptadors A1	Dinosauria (unclassified)	Lower Cretaceous (Aptian)	Arcillas de Morella Maestrat Basin	Cinctorres (Castellón)
Todolella 1	Dinosauria (unclassified)	Lower Cretaceous (Aptian)	Arcillas de Morella Maestrat Basin	Todolella (Castellón)
Torre Julian	Dinosauria (unclassified)	Lower Cretaceous (Aptian)	Arcillas de Morella Maestrat Basin	Todolella (Castellón)
A 10	Dinosauria (Teropoda)	Lower Cretaceous	Arcillas de Morella Maestrat Basin	Cinctorres (Castellón)
A 13	Dinosauria (unclassified)	Lower Cretaceous	Arcillas de Morella Maestrat Basin	Cinctorres (Castellón)
2ANA12	Dinosauria (Ornithopoda)	Lower Cretaceous	Arcillas de Morella Maestrat Basin	Cinctorres (Castellón)
2ANA61	Dinosauria (Ornithopoda)	Lower Cretaceous	Arcillas de Morella Maestrat Basin	Cinctorres (Castellón)
2ANA77	Dinosauria (Ornithopoda)	Lower Cretaceous	Arcillas de Morella Maestrat Basin	Cinctorres (Castellón)
3ANA58	Dinosauria (Ornithopoda)	Lower Cretaceous	Arcillas de Morella Maestrat Basin	Cinctorres (Castellón)

–Emilio Napolitano–
Application of the Diffraction Technique in Solid State Chemistry from "ab-initio" Structure Solution to Final Structure Refinement –Powder and Single Crystal– Doctoral Thesis in Sciences and Chemical Technology, XXIV cycle University of Sassari

Pag. 37

4ANA3	Dinosauria (unclassified)	Lower Cretaceous	Arcillas de Morella Maestrat Basin	Cinctorres (Castellón)
4ANA75	Dinosauria (unclassified)	Lower Cretaceous	Arcillas de Morella Maestrat Basin	Cinctorres (Castellón)
Escápula-ANA	Dinosauria (Ornithopoda)	Lower Cretaceous	Arcillas de Morella Maestrat Basin	Cinctorres (Castellón)
Mas Roig	Dinosauria (unclassified)	Lower Cretaceous	Arcillas de Morella Maestrat Basin	Cinctorres (Castellón)
El Maset	Dinosauria (unclassified)	Lower Cretaceous	Arcillas de Morella Maestrat Basin	Cinctorres (Castellón)
Manzanera	Dinosauria (unclassified)	Lower Cretaceous	Cantaperdius Maestrat Basin	La Mata (Castellón)
Mas de Rafael-2	Dinosauria (unclassified)	Lower Cretaceous	Arcillas de Morella Maestrat Basin	Todolella (Castellón)
Psm-Mila	Dinosauria (unclassified)	Limit upper Jurassic – Lower Cretaceous	Fm. Villar del Arzobispo; Southwestern Iberian Basin	Puebla de San Miguel (Valencia)
Psm-Maite	Dinosauria (unclassified)	Limit upper Jurassic – Lower Cretaceous	Fm. Villar del Arzobispo; Southwestern Iberian Basin	Puebla de San Miguel (Valencia)
Psm-Andres	Dinosauria (unclassified)	Limit upper Jurassic – Lower Cretaceous	Fm. Villar del Arzobispo; Southwestern Iberian Basin	Puebla de San Miguel (Valencia)
Psm-Carles	Dinosauria (unclassified)	Limit upper Jurassic – Lower Cretaceous	Fm. Villar del Arzobispo; Southwestern Iberian Basin	Puebla de San Miguel (Valencia)
CerroTadon	Dinosauria (unclassified)	Limit upper Jurassic – Lower Cretaceous	Fm. Villar del Arzobispo; Southwestern Iberian Basin	Alpuente (Valencia)
HTCO4-3	Dinosauria (unclassified)	Limit upper Jurassic – Lower Cretaceous	Fm. Villar del Arzobispo; Southwestern Iberian Basin	Alpuente (Valencia)
Rascaña	Dinosauria	Limit upper	Fm. Villar del	Alpuente

–Emilio Napolitano–
Application of the Diffraction Technique in Solid State Chemistry from
"ab-initio" Structure Solution to Final Structure Refinement
–Powder and Single Crystal–
Doctoral Thesis in Sciences and Chemical Technology, XXIV cycle
University of Sassari

Pag. 38

	(unclassified)	Jurassic – Lower Cretaceous	Arzobispo; Southwestern Iberian Basin	(Valencia)
Yac-David	Dinosauria (unclassified)	Limit upper Jurassic – Lower Cretaceous	Fm. Villar del Arzobispo; Southwestern Iberian Basin	Alpuente (Valencia)
Corral de Marin	Dinosauria (unclassified)	Limit Upper Jurassic – lower Cretaceous	Fm. Villar del Arzobispo; Southwestern Iberian Basin	Alpuente (Valencia)
229	Dinosauria (unclassified)	Limit Upper Jurassic – Lower Cretaceous	Fm. Villar del Arzobispo; Southwestern Iberian Basin	Alpuente (Valencia)
Losilla	Dinosauria (Eusauropoda)	Limit Upper Jurassic-Lower Cretaceous	Fm. Villar del Arzobispo; Southwestern Iberian Basin	Alpuente (Valencia)
Aras de Alpuente	Dinosauria (Eusauropoda)	Limit Upper Jurassic-Lower Cretaceous	Fm. Villar del Arzobispo; Southwestern Iberian Basin	Alpuente (Valencia)
La Ventura	Dinosauria (Eusauropoda)	Limit Upper Jurassic-Lower Cretaceous	Fm. Villar del Arzobispo; Southwestern Iberian Basin	Alpuente (Valencia)
El Collado	Dinosauria (unclassified)	Limit Upper Jurassic-Lower Cretaceous	Fm. Villar del Arzobispo; Southwestern Iberian Basin	La Cuevarruz (Valencia)
El Collado 1	Dinosauria (unclassified)	Limit Upper Jurassic-Lower Cretaceous	Fm. Villar del Arzobispo; Southwestern Iberian Basin	La Cuevarruz (Valencia)
Serrat del Corb	Dinosauria (Hadrosauria)	Upper Cretaceous	Tremp Tremp Basin	Isona (Lleida)
Serrat-R2	Dinosauria (Hadrosauria)	Upper Cretaceous	Tremp Tremp Basin	Isona (Lleida)
Molí del Baró	Dinosauria (unclassified)	Upper Cretaceous	Tremp Tremp Basin	Isona (Lleida)
La Penella	Dinosauria (unclassified)	Upper Cretaceous	Tremp Tremp Basin	Peramola (Lleida)
Lo Bas	Dinosauria (unclassified)	Upper Cretaceous	Tremp Tremp Basin	Abella de la Conca (Lleida)
La Llau de Bas	Dinosauria (unclassified)	Upper Cretaceous	Tremp Tremp Basin	Abella de la Conca (Lleida)
Nerets	Dinosauria (unclassified)	Upper Cretaceous	Tremp Tremp Basin	Villamitjana (Lleida)
Pous	Dinosauria	Upper	Tremp	Basturs

–Emilio Napolitano–
Application of the Diffraction Technique in Solid State Chemistry from
"ab-initio" Structure Solution to Final Structure Refinement
–Powder and Single Crystal–
Doctoral Thesis in Sciences and Chemical Technology, XXIV cycle
University of Sassari

Pag. 39

	(Hadrosauria)	Cretaceous	Tremp Basin	(Lleida)
Basturs Poble	Dinosauria (Hadrosauria)	Upper Cretaceous	Tremp Tremp Basin	Basturs (Lleida)
Basturs Poble-07	Dinosauria (Hadrosauria)	Upper Cretaceous	Tremp Tremp Basin	Basturs (Lleida)
Boiga	Dinosauria (unclassified)	Upper Cretaceous	Tremp Tremp Basin	Conques (Lleida)
Peguera 1-Figols	Dinosauria (Hadrosauria)	Upper Cretaceous	Tremp Fígols-Vallcebre Basin	Figols (Barcelona)

Table1: List of the Spanish dinosaur bones with taxa, geological period and provenance location.

All the fossil bone samples are Upper Jurassic/Lower Cretaceous to Upper Cretaceous (~ 150 to 65 Ma) in age and belong to large dinosaurs of different taxa (Table 1) from three regional deposits, described in the following:

1) The Upper Jurassic and Lower Cretaceous deposits of the southwestern Iberian Basin at Alpuente are formed by deltaic siliciclastic sediments deposited in fluvial, estuarine, beach and shallow-marine environments, controlled by eustatic sea level changes. These sediments belong to "*Villar del Arzobispo*" Formation, consisting of limestone, sandstone and clay minerals, "*Huérguina*" Formation (limestones) and "*Collado*" Formation (sandstones and clays), respectively.

2) The Cretaceous deposits are well distributed from middle to east of the Iberian Peninsula. The "*Cantaperdius*" Formation (composed by fluvial and lacustrine sediments) and the "*Morella*" Formation (Lower Cretaceous, clay stones, formed by deltaic sediments deposited in fluvial, estuarine, beach and shallow-marine environments) crop out in the Maestrat Basin, that is located in the eastern part of the Iberian rift system (Iberian Chain) with Mesozoic sediments up to 5.8 km thickness[28, 29]. This important geological structure formed during the Mesozoic rift stage[30].

–Emilio Napolitano–
Application of the Diffraction Technique in Solid State Chemistry from
"ab-initio" Structure Solution to Final Structure Refinement
–Powder and Single Crystal–
Doctoral Thesis in Sciences and Chemical Technology, XXIV cycle
University of Sassari

Pag. 40

3) The Upper Cretaceous deposits of the northwestern Iberian Peninsula at Tremp Basin are formed by terrestrial sediments with up to 1000 m in thickness. The Tremp Formation has an Upper Campanian to Lower Eocene age and is formed by grey clays with lignite at the base and predominantly red clays with sandstones and fluvial conglomerates or non-marine limestone intercalations [31].

The vertebrate material was mechanically separated from the sediment with an engraver drill. Subsequently the bones were washed with distilled water. For all specimens, the bone was sampled in the innermost part of the bone cortex (compacta) of the cortical tissue.

All the sixty fossil dinosaur bone samples were kindly made available from: Colección Museográfica de Cinctorres (Castellón), Museu de la Conca Dellà (Lleida), Universidad de Valencia and Institut Català de Paleontologia, Sabadell (Barcelona).

For comparison to the fossil dinosaur bone samples a fresh animal bone as well as synthetic hydroxylapatite was also analyzed using the same techniques. A recent rhesus monkey bone was used for this purpose but any other recent animal or human bone would have been suitable as the phase composition of bone similar and not taxon-specific.

The fresh bone of a rhesus monkey was made available by Teesside University (Middlesbrough, UK); synthetic powder hydroxylapatite was synthesized by Aldrich chemistry®.

–Emilio Napolitano–
Application of the Diffraction Technique in Solid State Chemistry from
"ab-initio" Structure Solution to Final Structure Refinement
–Powder and Single Crystal–
Doctoral Thesis in Sciences and Chemical Technology, XXIV cycle
University of Sassari

Pag. 41

METHODS

XRD analysis

0.5 g of each dinosaur bone was ball milled in a agate jar for one-minute using a SPEX mixer-mill model 8000. Our sample holder for XRD analysis is a circular cavity of 25 mm in diameter and 3 mm in depth. It contains about 420 mg of bone.

The XRD patterns were recorded overnight using Bruker D8, Philips PW-1050 and Siemens D-500 diffractometers in the Bragg–Brentano geometry with CuKα radiation (λ = 1.54178 Å). The X-ray generator worked at a power of 40 kV and 30 mA and the resolution of the instruments (divergent and antiscatter slits of 0.5°) was determined using α-SiO_2 and α-Al_2O_3 standards free from the effect of reduced crystallite size and lattice defects [32].

The goniometer was equipped with a graphite monochromator in the diffracted beam and the patterns were collected with 0.05° of step size which turned out to be adequate for the range of crystallite size in apatite phases here investigated. The powder patterns were collected in the angular range 10°-140° in 2θ, with counting time of 40 s per point. This strategy is suitable also for other phases such as quartz, which has crystallites normally extended in size more than one thousand Å, i.e., above the upper resolution limit of the instrument. Digitized diagrams were analyzed according to the Rietveld method[33], using the programme MAUD[34]. This is an efficient approach that evaluates quantitatively the structure-microstructure parameters and amount of mineralogical phases, taking also into account the instrumental parameters. For inorganic phase mixtures of medium complexity (3-4 phases) the detection limit of the technique is thought to be 1-2 wt%. One important advantage of the Rietveld method is that no standard is required for quantitative evaluation of phases, thus minimizing the

–Emilio Napolitano–
Application of the Diffraction Technique in Solid State Chemistry from
"ab-initio" Structure Solution to Final Structure Refinement
–Powder and Single Crystal–
Doctoral Thesis in Sciences and Chemical Technology, XXIV cycle
University of Sassari

Pag. 42

work on sample preparation. Moreover, one merit of the MAUD program is that the numerical evaluation of the whole pattern is accomplished using all recognized phases with a parametric peak shape function convoluting the instrument function with simultaneous broadening due to size and strain effects.

While XRF supplies the element composition of osseous materials, the powder diffraction technique inspects the phase composition. In addition to this, the line broadening analysis of XRD patterns may be applied for a simple evaluation of crystallinity in hydroxylapatite (HA), which is the main biomineral phase of bones. Note that the term crystallinity is instinctively intended as degree of organization of the bone HA phase on an atomic scale.

Rather than referring to the crystallinity of HA, a valid and more correct approach is to evaluate the X-ray peak sharpening of HA bones in terms of the average size of coherently diffracting domains (otherwise referred to as crystallites) and/or average imperfection density, also called lattice disorder or microstrain[1, 35]. These parameters supply a means to define numerically the organization of bones in an atomic scale. In any case, the quantitative evaluation of phases, their lattice parameters and their average coherent diffraction domain size may be obtained by applying the Rietveld method as it was suggested by Michel et al.[36].

XRF analysis

XRF measurements have been carried out by using a portable equipment composed of an X-ray tube (molybdenum anode, Oxford Instruments) working at 25 kV and 0.1 mA. We have pressed about 200 mg of powdered bone tissue to form a pellet with diameter of 10 mm and 1 mm thick.

An aluminium collimator 1 cm long and with an internal hole of 1 mm in diameter permits to irradiate an area of about 0.2 cm^2 of the object to be analysed, at a distance tube window-sample of about 2 cm. A Si-PIN detector from AMPTEK

–Emilio Napolitano–
Application of the Diffraction Technique in Solid State Chemistry from
"ab-initio" Structure Solution to Final Structure Refinement
–Powder and Single Crystal–
Doctoral Thesis in Sciences and Chemical Technology, XXIV cycle
University of Sassari

Pag. 43

was employed with a thickness of about 300 μm and characterized by an energy resolution of about 200 eV at 5.9 keV.

FT-IR analysis

FT-IR spectra were collected with a Bruker Vertex 70V spectrometer in terms of absorbance vs wavenumber ν in the range 400-4500 cm^{-1}. About 3 mg bone were hand-grinded and mixed with KBr in the weight ratio 1:100 respectively, to make pellets suitable for beam irradiation.

It should be considered that bands of the infrared spectrum of recent and fossil bones are relevant to obtain molecular information concerning the phosphate/carbonate group ratio. Additional bands may also be evaluable due to minerals other than those related to the apatite-like structure.

Raman analysis

The Raman spectra were collected with by a Bruker Senterra confocal Raman microscope working with a laser excitation wavelength of 785 nm at 100 mW of power and a beam diameter of 1.2 microns. In the confocal mode the 20x objective was selected, an array of 60 x 78 points was defined to cover a sample area of 90 x 117 microns with a step of 1.5 microns and each spectrum of the map was obtained by averaging 5 acquisitions of 2 seconds.

RESULTS

In order to describe appropriately the experimental work performed it seems suitable to apply a cross comparison of the techniques employed to evaluate in

–Emilio Napolitano–
Application of the Diffraction Technique in Solid State Chemistry from
"ab-initio" Structure Solution to Final Structure Refinement
–Powder and Single Crystal–
Doctoral Thesis in Sciences and Chemical Technology, XXIV cycle
University of Sassari

Pag. 44

selected cases how they can help our understanding of processes involved in the fossilization of the dinosaur bones.

Multi techniques comparison of single phase specimens
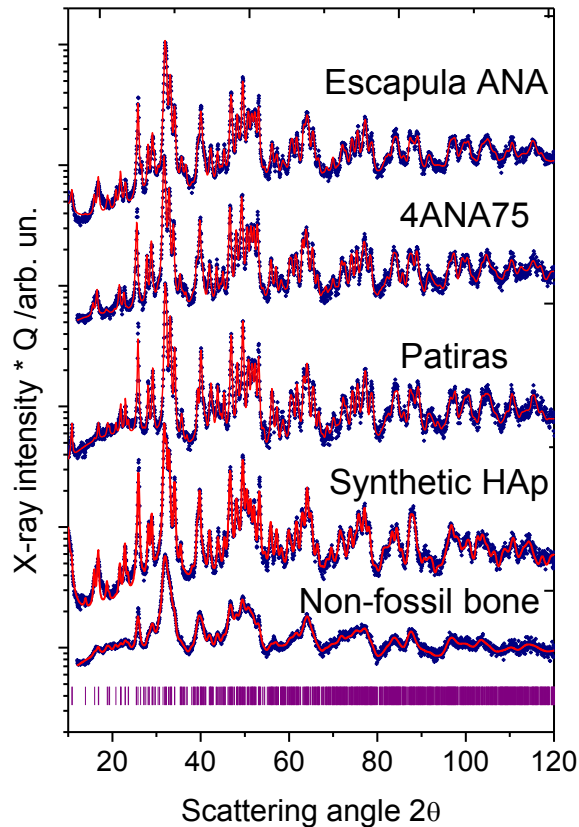
Figure 1, displays the XRD experimental patterns (data points) and the Rietveld fit (full lines) of three fossil specimens compared with a fresh bone and with the hydroxylapatite mineral synthesized chemically in the laboratory. The patterns of

−Emilio Napolitano−
**Application of the Diffraction Technique in Solid State Chemistry from
"ab-initio" Structure Solution to Final Structure Refinement
−Powder and Single Crystal−
Doctoral Thesis in Sciences and Chemical Technology, XXIV cycle
University of Sassari**

Pag. 45

these specimens, namely *Escapula Ana*, *4ANA75* and *Patiras* are single phase because satisfactorily described using the structure factor of monoclinic apatite, precisely fluorapatite. Following Elliot et al.[37] we have adopted a monoclinic description of the unit cell (Space Group $P2_1/c$, 4 molecular units) rather than the usual hexagonal cell of S. G. $P6_3/m$ with two molecules of hydroxylapatite because this appears to be more stable from an energetic point of view. As a matter of fact, the lattice parameter of the monoclinic phase a_M ($_M$ refers to monoclinic) coincides with that of the hexagonal phase a_H ($_H$ stands for hexagonal), but b_M is about $2 \times a_H$, $c_M = c_H$ and $\beta_M \approx 120°$ [38]. Thus, the monoclinic unit cell volume V_M is about twice that of V_H.

Figure 2 shows the XRF spectra of the same specimens reported in Figure 1.

−Emilio Napolitano−
Application of the Diffraction Technique in Solid State Chemistry from
"ab-initio" Structure Solution to Final Structure Refinement
−Powder and Single Crystal−
Doctoral Thesis in Sciences and Chemical Technology, XXIV cycle
University of Sassari

Pag. 46

The spectrum of the *Patiras* specimen closely resembles the results reported for a dinosaur bone by PIXE analysis[39] both in terms of accessed energy range and of relative peak intensities. This similarity suggests that the elemental information from the emissions detected after irradiating the bones with particles rather than electrons is actually very close.

In all spectra of figure 2, we easily recognize the Ca doublet and the P peak at lower energies. In addition to these common features there are differences in terms of elemental composition among the modern bone (rhesus monkey), the synthetic hydroxylapatite and the three single-phase fluorapatite fossil bone specimens, on account of the taphonomic and diagenetic processes to which the fossil was subjected.

The multi-technique approach here used may lead to sensible results from the physical point of view using just useful qualitative hints about the composition of elements. In fact, the single-phase character evidenced by the XRD investigation reported in Figure 1 for the three specimens here considered suggests that Ca atoms found by XRF are divalent cations in the apatite lattice that may be substituted by Sr, Cu and Fe during dissolution-reprecipitation processes like evidenced by Kolodny et al.[40]. Of course also monovalent K cations may be involved in partial replacement of Ca, as well as the other elements that were detected with low concentration like Cr, Mn, Rb and Y.

In figure 2 the peaks of *4ANA75* fossil attributed to Fe and Y are stronger than in the *Patiras* specimen. Furthermore, the presence of weak but appreciable emissions due to Zn, As and Pb respectively, have also been inferred from the curve calculated for best-fit. The case of *Escapula ANA* evidences an even more intense contribution of the Fe and Sr ions that, of course, must replace divalent Ca ions in the structure of fluorapatite at a considerable level since it appeared as a single phase from the diffraction inspection (Figure 1).

–Emilio Napolitano–
Application of the Diffraction Technique in Solid State Chemistry from
"ab-initio" Structure Solution to Final Structure Refinement
–Powder and Single Crystal–
Doctoral Thesis in Sciences and Chemical Technology, XXIV cycle
University of Sassari

Pag. 47

A comparison of FT-IR spectra of these specimens, shown in Figure 3, supplies further interesting information about the chemistry of the fossils.
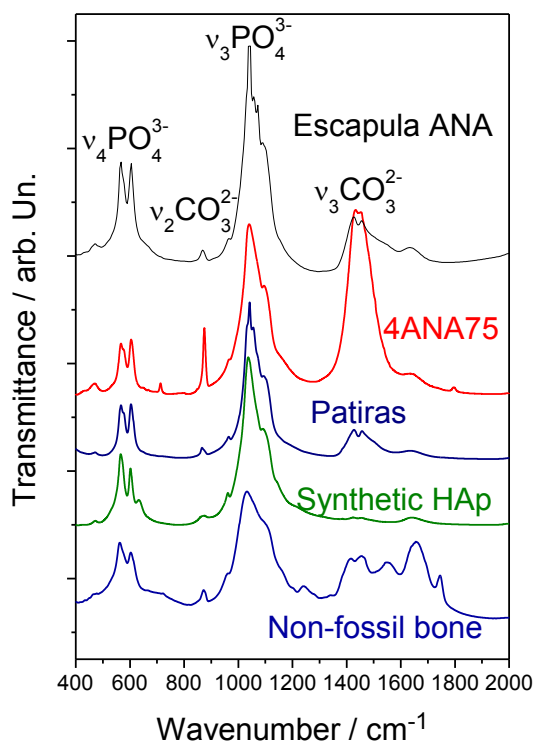
The fresh bone of the rhesus monkey (bottom spectrum) shows the typical ν_4 PO_4^{3-} and ν_3 PO_4^{3-} IR vibrations of phosphates belonging to apatite in the range from 530-650 cm^{-1} and 900-1200 cm^{-1} respectively[41,42]. In addition to the phosphate groups, we can see in the range from 1300 to 1800 cm^{-1} a multitude of bands that may be related to the organic material and water incorporated in the fresh bone[43, 44].

With respect to the non-fossil bone, the spectrum of synthetic hydroxylapatite (second curve from the bottom of Figure 3) shows actually an increase of the ν_4

−Emilio Napolitano−
Application of the Diffraction Technique in Solid State Chemistry from
"ab-initio" Structure Solution to Final Structure Refinement
−Powder and Single Crystal−
Doctoral Thesis in Sciences and Chemical Technology, XXIV cycle
University of Sassari

Pag. 48

PO_4^{3-} splitting factor, which is supplemented by the appearance of a shoulder at 633 cm^{-1}. In addition to this, for synthetic hydroxylapatite no important peak envelope but only weak features indicative of residual carbonate and humidity are observed in the range 1300-1800 cm^{-1} on account of absence of organic matter and water.

Conversely, the spectrum of *Patiras* sample shows the ν_4 PO_4^{3-} and ν_3 PO_4^{3-} contribution from phosphates groups plus a broad feature in the range 1350-1550 cm^{-1} that can be attributed to the presence of CO_3^{2-} groups in the fluorapatite structure. In particular, the ratio of the absorbance of the ν_3 CO_3^{2-} band at 1415 cm^{-1} to that of the ν_4 PO_4^{3-} band at 575 cm^{-1} is reported to be linearly related to the carbonate content of the apatite.

A large amount of carbonate groups may be inferred from the spectrum of specimen *4ANA75* where a very intense ν_3 CO_3^{2-} band is observed. The appearance of this band is related to the narrow ν_2 band at 875 cm^{-1} also ascribed to carbonates (ν_2 CO_3^{2-}). Actually, it is from such comparison that this specimen may be inferred as francolite.

The infrared spectrum of *Escapula ANA* specimen shows a more conventional profile intensity of vibrational activities of the ν_2 CO_3^{2-} and ν_3 CO_3^{2-} bands, with apparently sharper ν_4 PO_4^{3-} and ν_3 PO_4^{3-} bands that are difficult to relate to the relatively low average crystallite size extent reported from XRD in Table II.

It is worth to note that the ν_4 PO_4^{3-} cluster of bands in *Patiras*, *4ANA75* and *Escapula ANA* specimens are different with respect to synthetic apatite and modern bone, and this may be related either to fluorination of bones or ionic substitution by Fe and Sr for the Ca sites in the apatite lattice. The Figure 4 is a more detailed view of the ν_4 PO_4^{3-} bands of six specimens (modern bone, synthetic hydroxylapatite, *Patiras*, *La Fita*, *La Cuba*, *A10*) in the range 500-700 cm^{-1}.

–Emilio Napolitano–
Application of the Diffraction Technique in Solid State Chemistry from
"ab-initio" Structure Solution to Final Structure Refinement
–Powder and Single Crystal–
Doctoral Thesis in Sciences and Chemical Technology, XXIV cycle
University of Sassari

Pag. 49
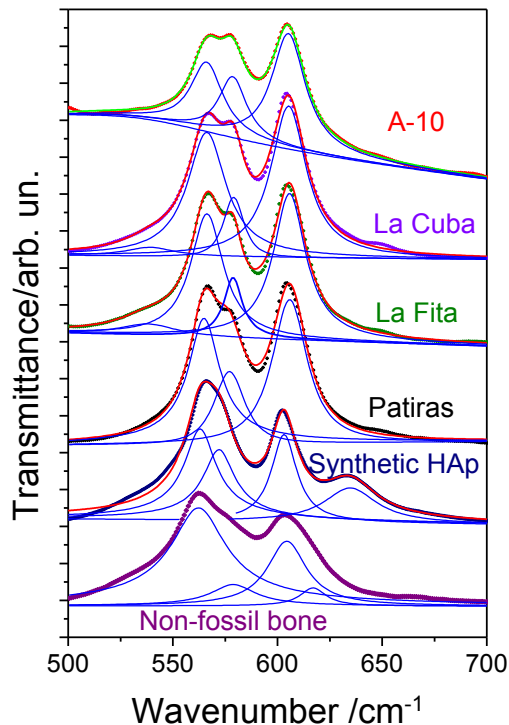
FIGURE 4. THE ν_4 PHOSPHATE BAND ENVELOPE OF FT-IR SPECTRA FOR SELECTED DINOSAUR BONES SPECIMENS, IN COMPARISON WITH MODERN BONE AND SYNTHETIC HYDROXYAPATITE (HA). WITH RESPECT TO THE FEATURES COMMON TO MODERN BONE AND SYNTHETIC HYDROXYAPATITE, THE FIT OF EACH BAND EVIDENCE HOW FOSSILIZATION INVOLVES A BAND SHARPENING, A DECREASE OF THE TWO INTENSITY BANDS AROUND 570 CM^{-1} AND THE ABSENCE OF ANY BAND AT 635 CM^{-1}, PROBABLY ON ACCOUNT OF THE OH GROUP DISAPPEARANCE FOLLOWING FLUORITIZATION.

The experimental data points of the envelope were fitted using symmetric Pearson VII functions and the individual behaviour for each component adjusted at the end of the best fit is reported in correspondence of the maxima and shoulders. One can see that that for non-fossil bone the envelope may be actually described by four partially overlapping bands whose total broadening is related to the crystallinity index throughout the splitting factor SF[45, 46].

The splitting factor envelope is sharper in the synthetic sample, with emergence of one band shifted at 630 cm^{-1}. However, in the case of fossils we clearly see that the band at 630 cm^{-1} is hidden and that the envelope, though sharp, admit just three bands. Michel et al.[36] have attributed the phosphate band at 630 cm^{-1}

–Emilio Napolitano–
Application of the Diffraction Technique in Solid State Chemistry from
"ab-initio" Structure Solution to Final Structure Refinement
–Powder and Single Crystal–
Doctoral Thesis in Sciences and Chemical Technology, XXIV cycle
University of Sassari

Pag. 50

to the P-O-H mode, so we can infer that the fluorination have completely removed the hydroxyl group in our specimens. Conversely, the IR spectra of enamel fossils of Michel et al.[35] did show four modes of absorption.

In complex substituted apatites it is customary to complement the vibrational activity of the IR spectra with that from Raman[22] since some modes may be both IR and Raman active but others may be only IR or Raman active[47].

The micro-Raman spectra of the set of specimens previously discussed are reported in figure 5 as raw data and turn out to be very different in term of the signal-to-background ratio.
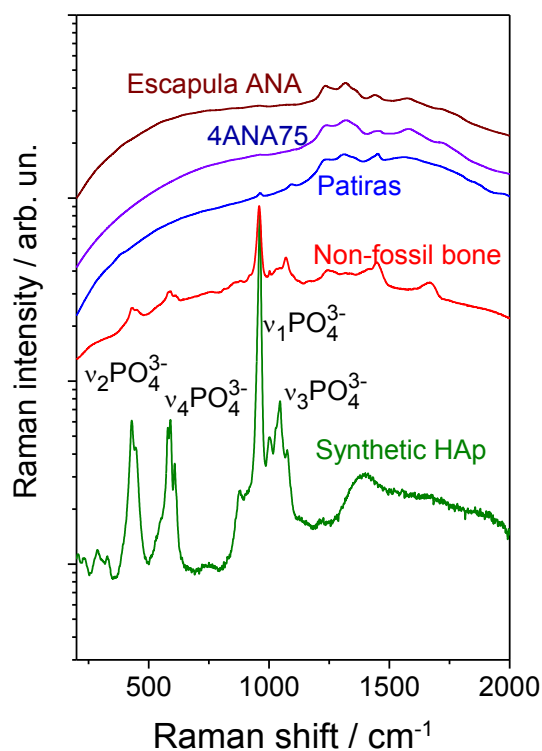
FIGURE 5. THE RAMAN SPECTRA OF THE SPECIMENS STUDIED BY XRD, XRF AND FT-IR. SYNTHETIC HYDROXYAPATITE SHOWS THE BEST SIGNAL-TO-BACKGROUND RATIO, WHILE THE FOSSILS APPEAR COMPLETELY COMPROMISED BY A STRONG FLUORESCENCE BURYING THE MODES OF FLUORAPATITE. VERY LIKELY THE BACKGROUND OF THE NON-FOSSIL MODERN BONE IS DUE TO ORGANIC PROTEIN AND WATER CONTENT.

–Emilio Napolitano–
Application of the Diffraction Technique in Solid State Chemistry from
"ab-initio" Structure Solution to Final Structure Refinement
–Powder and Single Crystal–
Doctoral Thesis in Sciences and Chemical Technology, XXIV cycle
University of Sassari

Pag. 51

It is known that Raman spectroscopy investigations are usually difficult because of fluorescence problems caused from impurities of a contaminated sample or from the matrix surrounding an inclusion. Indeed, the best visibility of the hydroxylapatite bands occur in the synthetic sample, while the fresh bone appears to be partially obscured by a background one order of magnitude more intense[48]. Yet, the main bands belonging to biogenic hydroxylapatite are still recognized as well as additional bands that we can attribute to the presence of collagen and water, in agreement with the IR observation. These bands are totally lost in a more intense background in the case of the three fossils which have incorporated fluorine, as indicated by the unit cell volume data from XRD. It can be seen that new broad features are emerging in the range 1200-1900 cm^{-1} maintaining a certain degree of similarity. However, they are of difficult assignment in view of the extended ion exchange suffered by the specimens as demonstrated by the XRF spectra of figure 2, to the point of making useless any choice of the incident wavelength in order to minimize the background contribution.

3.2. Multi techniques comparison of specific multiphase specimens

Despite the care used in the fossil unearthing procedure, cleaning and sampling the compact part of the bone, the possibility of the incorporation of clay minerals in the internal pore space of buried fossil bones is always very likely, as demonstrated the results of the *Povet* specimen reported in figure 6.

–Emilio Napolitano–
Application of the Diffraction Technique in Solid State Chemistry from
"ab-initio" Structure Solution to Final Structure Refinement
–Powder and Single Crystal–
Doctoral Thesis in Sciences and Chemical Technology, XXIV cycle
University of Sassari

Pag. 52
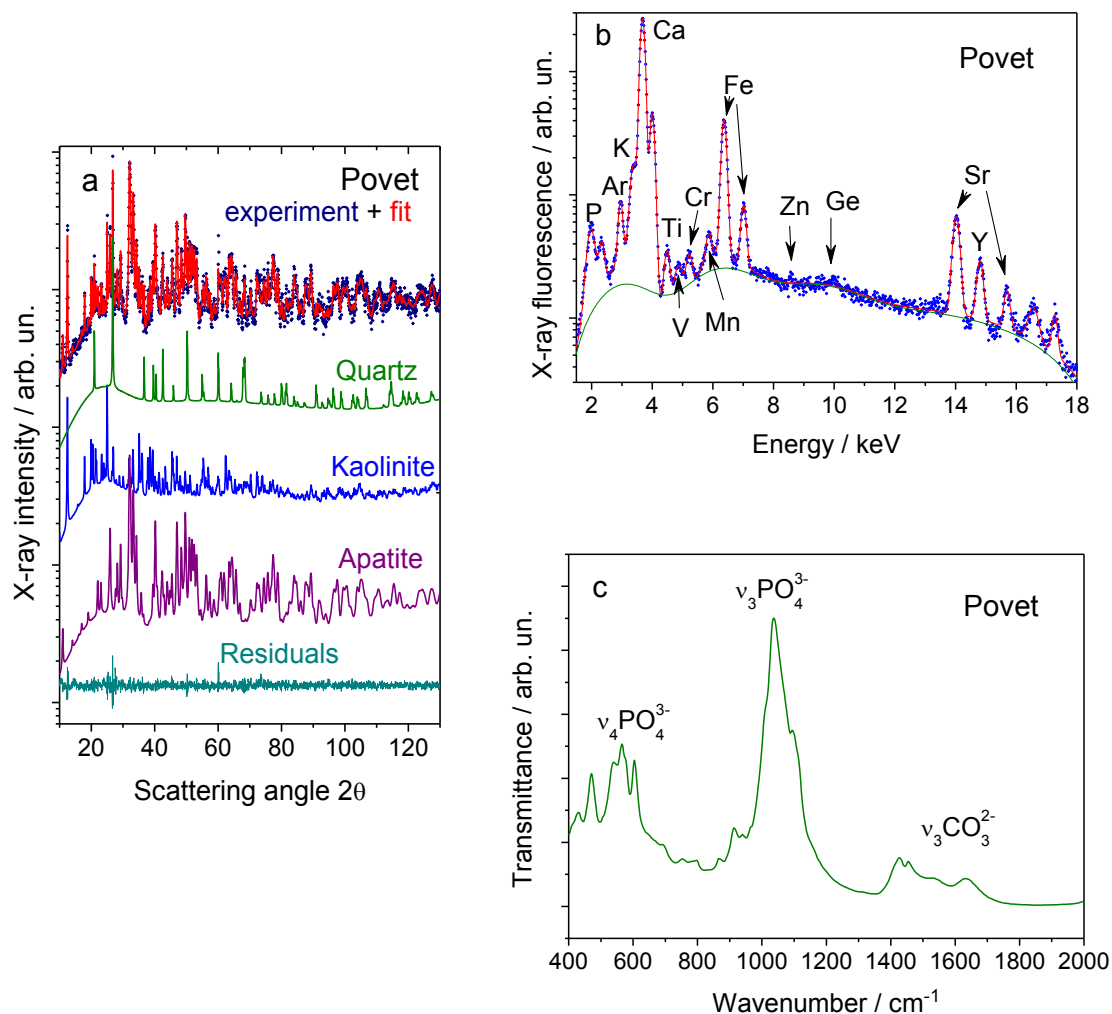
FIGURE 6. THE XRD, XRF AND FT-IR RESULTS OF THE POVET SPECIMEN. (A) THE BONE IS NOT ANYMORE SINGLE PHASE APATITE AS THE XRD PATTERN DISPLAYS EVALUABLE CONTRIBUTIONS FROM KAOLINITE AND QUARTZ INFILTRATED FROM THE NEARBY SEDIMENT. (B) IN ADDITION TO CALCIUM AND PHOSPHORUS FROM APATITE, THE CORRESPONDENT XRF SPECTRUM HIGHLIGHTS THE PRESENCE OF IRON, STRONTIUM AND YTTRIUM PLUS THE WEAK CONTRIBUTION OF FIRST SERIES TRANSITION ELEMENTS. (C) WITH RESPECT TO SINGLE-PHASE APATITE, THE FT-IR SPECTRUM IS ONLY SLIGHTLY AFFECTED BY THE SI-O MODES OF QUARTZ AND KAOLINITE MAINLY AT FREQUENCIES LOWER THAN 600 CM^{-1}.

The XRD pattern is described in terms hydroxylapatite component, accompanied by a large fraction of kaolinite and some quartz. For the sake of completeness we have also reported at the bottom of figure 6a the band of residuals, i.e., the

–Emilio Napolitano–
Application of the Diffraction Technique in Solid State Chemistry from
"ab-initio" Structure Solution to Final Structure Refinement
–Powder and Single Crystal–
Doctoral Thesis in Sciences and Chemical Technology, XXIV cycle
University of Sassari

Pag. 53

difference between experiment and calculation at each data point. Of course both kaolinite and quartz can be ascribed to the most common minerals of embedding sediment and were likely incorporated into the bone pore space.

The fluorescence spectrum in figure 6b shows that even this sample contains Fe ions, as well as appreciable quantities of Sr and Y.

In addition to carbonate and phosphate bands of hydroxylapatite, the FT-IR spectrum of *Povet* fossil (see Figure 6c) shows new bands at low frequencies (470 and 540 cm^{-1}). We note that the principal absorption frequencies of crystalline silica are reported to occur at 1126, 809, and 452 cm^{-1}, respectively. Thus, only the latter band appears to be appreciable since relatively unaffected by nearby peak overlapping. Very likely the shoulder at 540 cm^{-1} can be attributed to frequencies from kaolinite[49].

Another interesting case is represented by *Molì del Barò* specimen. Despite the complexity of the data, the pattern was resolved by the Rietveld method in a satisfactory fashion as it can be seen from the best fit of figure 7a, which this time reports the bar sequence of peaks for each contributing phase rather than the structure factor optimized after the fit.

–Emilio Napolitano–
Application of the Diffraction Technique in Solid State Chemistry from
"ab-initio" Structure Solution to Final Structure Refinement
–Powder and Single Crystal–
Doctoral Thesis in Sciences and Chemical Technology, XXIV cycle
University of Sassari

Pag. 54
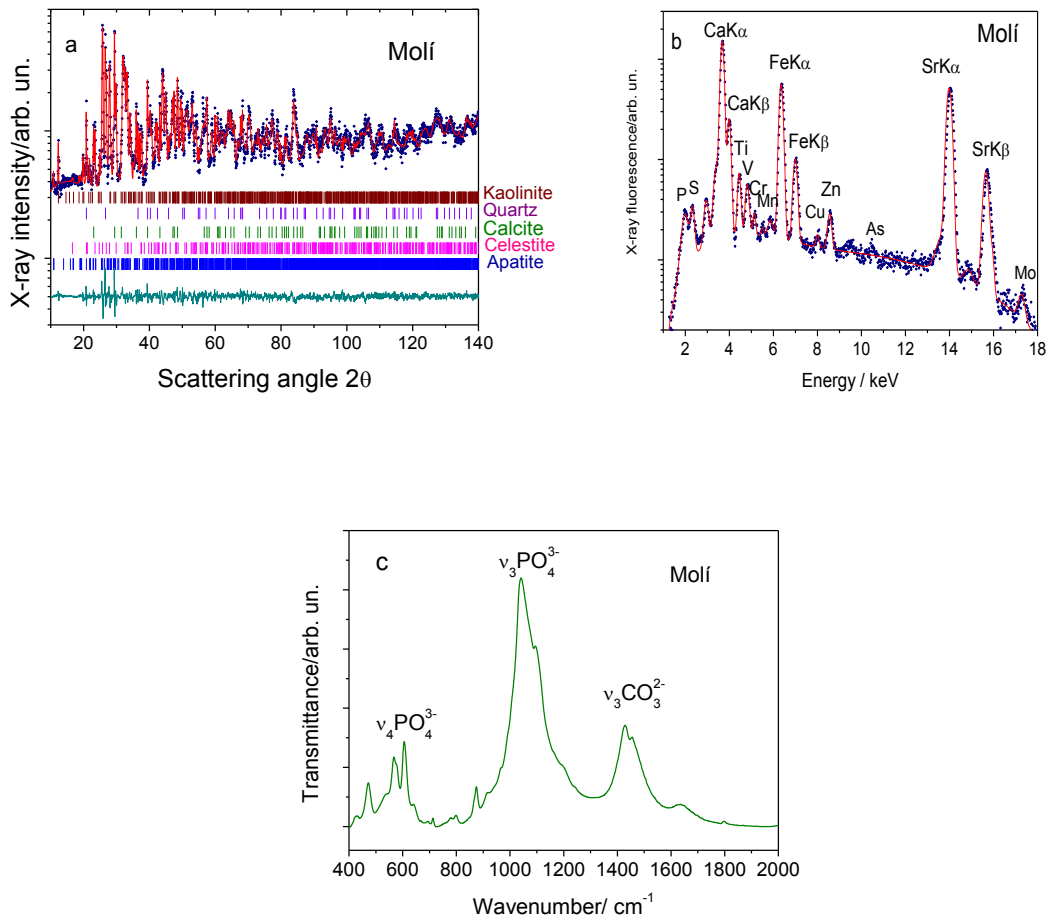
FIGURE 7. MULTI-TECHNIQUE ANALYSIS CARRIED OUT ON A COMPLEX DINOSAUR BONE SPECIMEN CONTAINING SEVERAL MINERAL PHASES. (A) THE XRD PATTERN OF MOLÌ DEL BARÒ WAS RESOLVED WITH THE CONTRIBUTION OF FIVE PHASES, AMONG THOSE THE CELESTITE APPEARS EXOTIC. THE CORRESPONDING XRF SPECTRUM (B) SHOWS NOTABLE PRESENCE OF STRONTIUM IN ADDITION TO THE USUAL ELEMENT DISTRIBUTION EXPECTED FOR BONE FOSSILS. (C) THE FT-IR SPECTRUM.

Beyond the "apatitic" phase, which is ca. 48 wt.% of the specimen, we have evaluated numerically the presence of celestite phase at a 25 wt.% level, together with calcite, quartz and ca. 4 wt.% of kaolinite.

−Emilio Napolitano−
Application of the Diffraction Technique in Solid State Chemistry from
"ab-initio" Structure Solution to Final Structure Refinement
−Powder and Single Crystal−
Doctoral Thesis in Sciences and Chemical Technology, XXIV cycle
University of Sassari

Pag. 55

The presence of calcite, quartz and kaolinite is ascribable to the limestone and clay minerals typical for the sediment of the Tremp basin, while the abundant presence of celestite is unusual compared to other dinosaur bones.

As expected after XRD evaluation, the XRF spectrum of Molí del Baró (see figure 7b) shows a strong contribution from the Sr Kα and Kβ lines, and a weak signal of sulphur. Both elements are to be related to celestite $SrSO_4$. The strong contributions due to Fe atoms are not mirrored in the XRD pattern by any oxide-hydroxides Fe-based phases such as goethite and hematite.

In the XRF spectrum of Figure 7b, we can appreciate and possibly quantify the presence of transitional elements such as Ti, V, Cr, Mn, Cu, Zn, As. These elements are likely hosted in the lattices of the apatite-like and kaolinite-like phases detected by XRD.

Despite the complexity of phase and elemental constitution assessed by XRD and XRF, the FT-IR spectrum of the *Molí del Baró* specimen looks rather "simple" again highlighting phosphate and carbonate bands typical of francolite.

Of course, when using FT-IR investigations, the carbonate band can be also ascribed to calcite because the technique is molecular rather than structure sensitive to the point that there is no sensible numerical way to separate these chemically distinct contributions from the envelope.

On the other hand the principal ranges of observed frequencies for sulphates occur at 1030~1180 cm^{-1} (strong bands) and at 580-670 cm^{-1} (weaker bands) respectively (see figure 7c).

It may be deduced that the FT-IR technique is not able to resolve properly also the bands of sulphate groups from those of phosphates.

As it is documented in the XRD pattern of Figure 8a, gypsum was found in appreciable quantity together with some calcite in the *HTCO4-3* specimen, which

–Emilio Napolitano–
Application of the Diffraction Technique in Solid State Chemistry from
"ab-initio" Structure Solution to Final Structure Refinement
–Powder and Single Crystal–
Doctoral Thesis in Sciences and Chemical Technology, XXIV cycle
University of Sassari

Pag. 56

was extracted from a basin at least partially affected by shallow-marine environment.
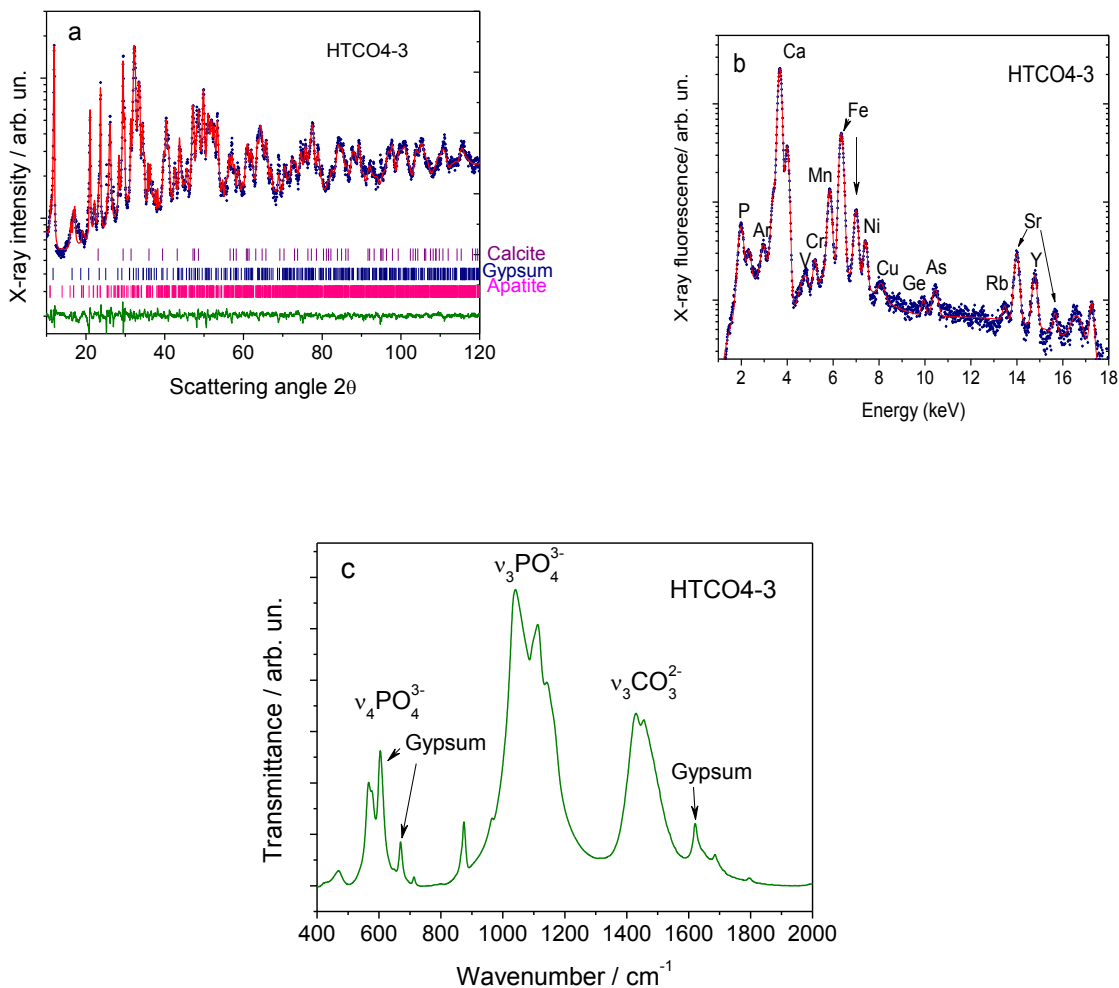
FIGURE 8. (A) THE XRD PATTERN OF HTCO4-3 SPECIMEN SHOWING IN ADDITION TO FRANCOLITE A CONSIDERABLE AMOUNT OF GYPSUM AND SOME CALCITE. (B) THE XRF PATTERN SHOWS THE PRESENCE OF IRON SPECIES TOGETHER WITH MANGANESE, STRONTIUM AND YTTRIUM PLUS OTHER ELEMENTS IN LOWER QUANTITY. (C) THE FT-IR ABSORPTION BANDS OF GYPSUM ARE EASILY RECOGNIZABLE AS INDICATED BY ARROWS AND MAY AFFECT THE ν_4 PHOSPHATE BAND.

The XRF spectrum of this specimen (see figure 8b) shows, as customary for this bone fossil collection, the appreciable presence of Fe, accompanied by Mn, Sr, Y and to a lesser extent by V, Cr, Cu, Ge and Rb.

–Emilio Napolitano–
Application of the Diffraction Technique in Solid State Chemistry from
"ab-initio" Structure Solution to Final Structure Refinement
–Powder and Single Crystal–
Doctoral Thesis in Sciences and Chemical Technology, XXIV cycle
University of Sassari

Pag. 57

Of course the divalent cation of these elements can substitute for Ca in the lattice structures inferred from the Rietveld refinement of XRD patterns.

A further consideration deserves the FT-IR spectrum reported in Figure 8c. As noted before, the symmetry of sulphate groups makes their vibrational bands to occur close to those of the phosphate, creating overlapping to the ν_4 PO_4^{3-} band at lower frequencies as indicated in the figure.

The combined XRF, XRD and FT-IR inspection of the *Qurolles M* specimen supplies new appealing aspects.
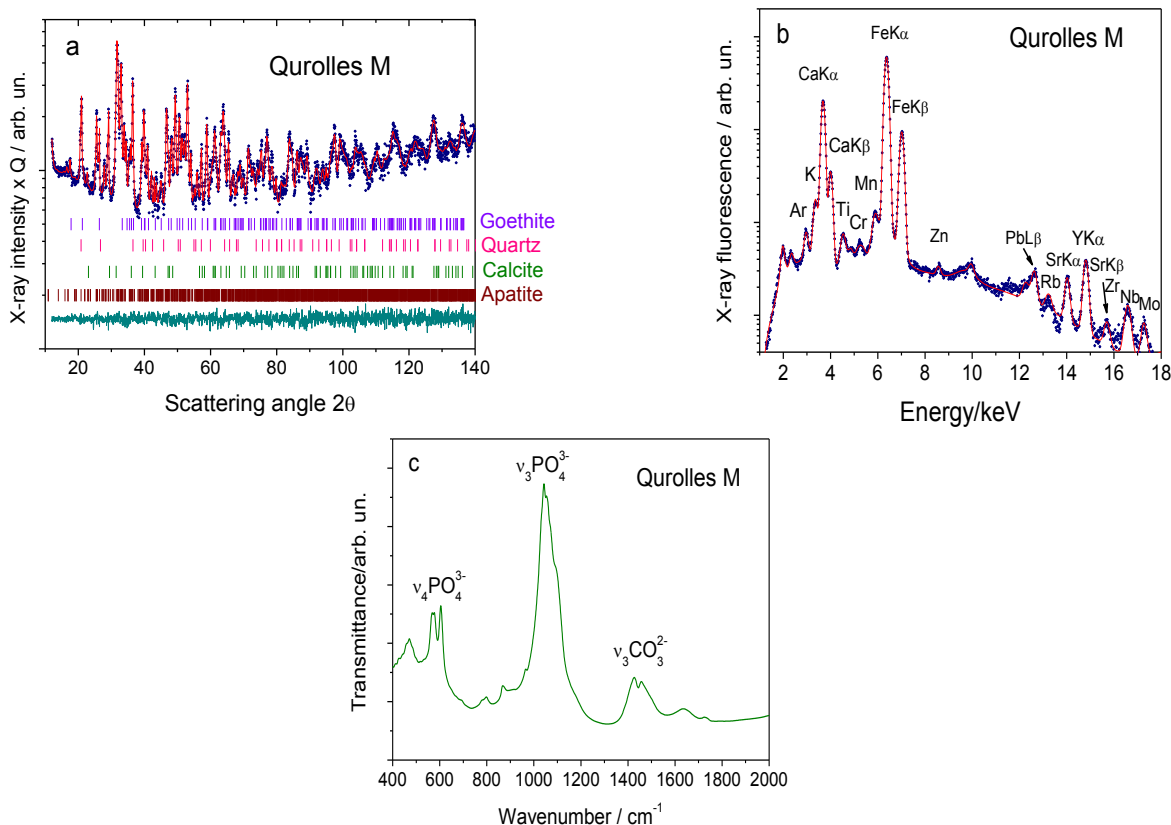
FIGURE 9. (A) THE XRD PATTERN OF THE QUROLLES M SPECIMEN WITH THE CONTRIBUTION OF THE GOETHITE PHASE. (B) THE XRF SPECTRUM SHOWS A CONTRIBUTION FROM THE IRON LINES STRONGER THAN THOSE OF CALCIUM DUE TO THE HIGH CONTENT OF GOETHITE (24%). (C) THE FT-IR SPECTRUM DISPLAYS THE HIGHER INTENSITIES OF MOLECULAR CARBONATE GROUPS OF FRANCOLITE WHILE THE CONTRIBUTIONS OF OTHER MOLECULES IS DIFFICULT TO EXTRACT.

The XRD pattern refinement reported in figure 9a shows that also in this case the bone specimen is not single-phase. The fluorapatite-like phase (francolite) is the

−Emilio Napolitano−
Application of the Diffraction Technique in Solid State Chemistry from
"ab-initio" Structure Solution to Final Structure Refinement
−Powder and Single Crystal−
Doctoral Thesis in Sciences and Chemical Technology, XXIV cycle
University of Sassari

Pag. 58

most abundant, but is accompanied by ca. 24 wt% of goethite and small quantities of calcite and quartz. The XRF spectrum in figure 9b displays a strong contribution from Fe which appears even more intense than Ca. The presence of a high level of Fe inferred from XRF is in good agreement with the considerable fraction of goethite detected by XRD.

The FT-IR contribution in the frequency range reported in figure 9c is limited to point out the occurrence of relatively weak carbonate bands on account of the 4 wt% amount of calcite assessed by XRD, while the signals of goethite are not appreciable here.

An important issue concerns the variability of phase and chemical composition of bone specimens from the same geological setting. This comparison is reported in figure 10a, which shows the XRD pattern of specimens *Camino* and *EAP 40-39*.
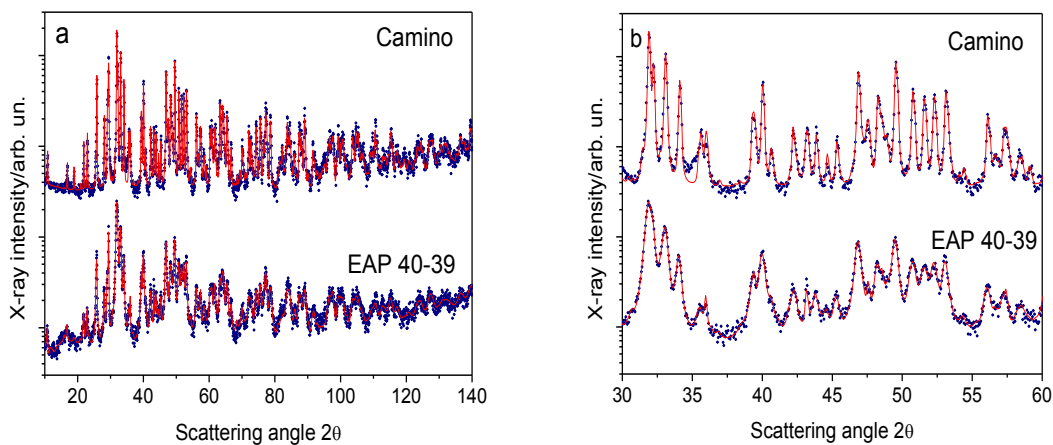
–Emilio Napolitano–
Application of the Diffraction Technique in Solid State Chemistry from
"ab-initio" Structure Solution to Final Structure Refinement
–Powder and Single Crystal–
Doctoral Thesis in Sciences and Chemical Technology, XXIV cycle
University of Sassari

Pag. 59
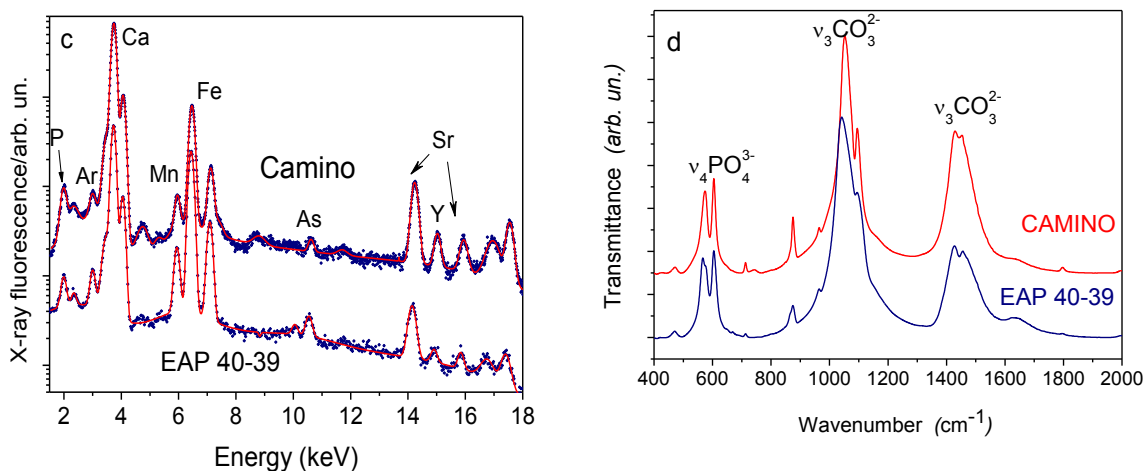
FIGURE 10. (A) THE XRD PATTERNS OF TWO BONES FROM DIFFERENT DINOSAURS SAMPLED FROM THE SAME GEOLOGICAL UNIT ("MORELLA" FORMATION). THE UPPER PATTERN OF THE CAMINO SPECIMEN SHOWS LINE PROFILES FROM THE FLUORAPATITE SHARPER THAN IN THE EAP 40-39 SPECIMEN AT THE BOTTOM, REFLECTING MARKEDLY DIFFERENT AVERAGE CRYSTALLITE SIZE OF 2107 Å AND 382 Å, RESPECTIVELY (TABLE II). (B) THIS COMPARISON MAY BE BETTER EVALUATED ACROSS A NARROWER ANGULAR RANGE AS REPORTED IN THE RIGHT HAND SIDE PLOT. (C) THE XRF PATTERNS SHOW A SIMILAR ELEMENTAL DISTRIBUTION, WITH NOTABLE PRESENCE OF IRON AND STRONTIUM IN BOTH SPECIMENS; (D) THE CORRESPONDING FT-IR SPECTRA SHOW THE PRESENCE OF CARBONATE BANDS IN THE RANGE 1350-1550 CM[-1] AT DIFFERENT LEVEL OF CONCENTRATION THAT CAN BE CORRELATED WITH THE CALCITE CONTENT FROM XRD QUANTITATIVE PHASE ANALYSIS.

The upper pattern referred to the *Camino* specimen shows line profiles from the fluorapatite sharper than in the *EAP 40-39* specimen at the bottom, reflecting a markedly different average crystallite size. This comparison may be better evaluated across a narrower angular 2θ range (30°-60°) as reported in the plot of Figure 10b.

The XRF graphs (see Figure 10c) show a similar elemental distribution, with notable presence of Fe and Sr. The corresponding FT-IR spectra (Figure 10d) show the presence of carbonate bands in the range 1350-1550 cm^{-1} at different level of concentration that can be correlated with the calcite content from XRD quantitative phase analysis.

Finally, we like to show the micro-Raman spectra obtained by closing the confocal hole and defining a smaller collection volume in order to spatially locate and appropriately distinguish the secondary mineral infilling in fossil bones. In particular, we have surface mapped a portion of the *Torre Julian* sample.

–Emilio Napolitano–
Application of the Diffraction Technique in Solid State Chemistry from
"ab-initio" Structure Solution to Final Structure Refinement
–Powder and Single Crystal–
Doctoral Thesis in Sciences and Chemical Technology, XXIV cycle
University of Sassari

Pag. 60
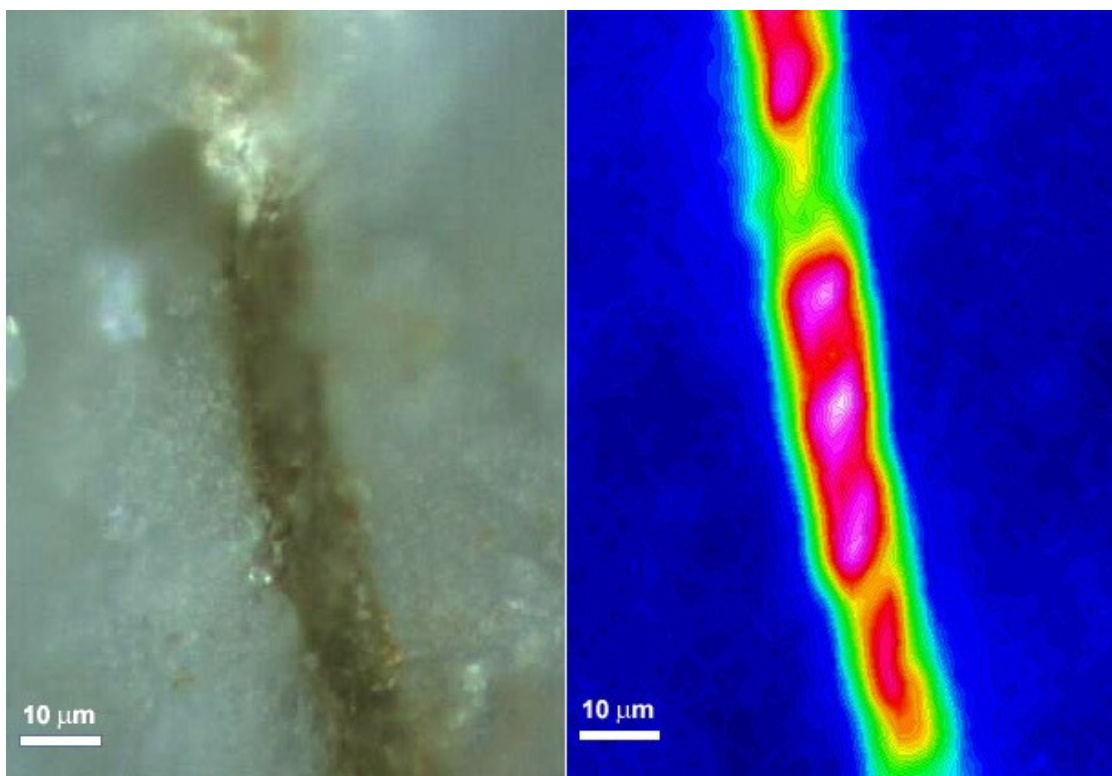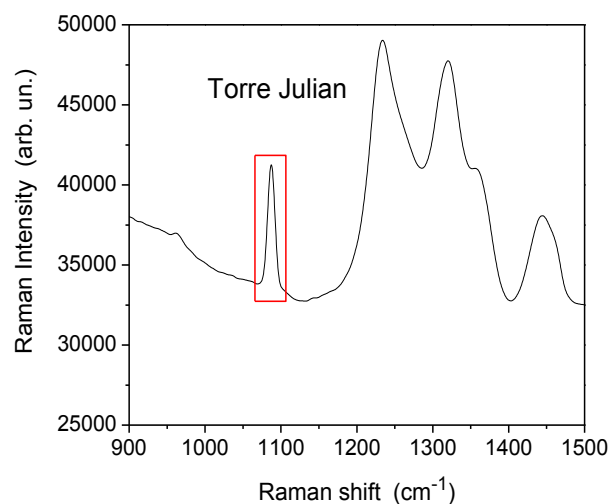
FIGURE 11. THE RAMAN CONFOCAL INVESTIGATION FOR THE CALCITE PRESUMED ON THE BASIS OF CO_3^{2-} MODES OF THE SPECTRUM IN THE RANGE 1072-1100 CM^{-1} AS IN (A). IT WAS CARRIED OUT CONSIDERING THE AREA ENCOMPASSING AN HAVERSIAN CANAL (B). THE RAMAN IMAGE (C) TELLS US THAT THE SUPPOSED CALCITE FORMS AN INNER SURFACE CRUST AROUND THE HAVERSIAN CANAL. THE VIOLET-WHITE AREAS OF THE RAMAN IMAGE, CORRESPONDING TO THE MAXIMUM VALUE OF THE PEAK INTEGRAL, INDICATE THE PRESENCE OF THE MAXIMUM AMOUNT OF CALCITE. CONVERSELY, THE BLUE COLOUR CORRESPONDING TO THE ZERO VALUE, INDICATES THE TOTAL ABSENCE OF CALCITE, WHILE ALL OTHER COLOURS CORRESPOND TO INTERMEDIATE AMOUNTS OF CALCITE.

–Emilio Napolitano–
**Application of the Diffraction Technique in Solid State Chemistry from
"ab-initio" Structure Solution to Final Structure Refinement
–Powder and Single Crystal–
Doctoral Thesis in Sciences and Chemical Technology, XXIV cycle
University of Sassari**

Pag. 61

The peak of the Raman spectrum in the range 1072-1101 cm^{-1} reported in figure 11 (a) was integrated from the visible image of the selected sample area in figure 11 (b) thus allowing to define the Raman microscopic image shown in figure 11 (c). Indeed, the integration peak originate from carbonate modes belonging to calcite, as it was also confirmed by the Rietveld analysis carried out in the *Torre Julian* specimen.

Raman imaging of the selected area suggests that the calcite phase precipitates just as a surface crust around the haversian canals of the bone.

DISCUSSION

Quantitative evaluation of phases

Table II collects the main phases of dinosaur bones found by the XRD investigation with their quantitative estimate according to the Rietveld method, the cell volume of the supposed "apatitic" phase, its average crystallite size as well as major and minor elements detected by XRF.

Sample code	Phase %	Average crystallite size (Å)	$V_c/2$	Elements with strong XRF peaks	Elements with medium XRF peaks	Elements with weak XRF peaks
Patiras	Apatite 100%	420	524.1	Ca	P,Fe,Sr	Y,Cu,Cr,Mn
CL	Apatite 90% Calcite 10%	439	524.0	Ca,Fe	P,Sr,Y	V,Cr,Mn,Ge,Br
CL 42	Apatite 26% Calcite 72% Quartz 2%	576	524.5	Ca,Fe	P	Cr,Mn,Sr,Y
CL 56	Apatite 89% Calcite 11%	406	523.9	Ca	Y,P,Fe,Sr	Ti,V,Cr,Mn
La Cuba	Apatite 80% Calcite 19% Quartz 1%	398	523.9	Ca	P,Fe,Sr	Ti,V,Cr,Mn,Cu,Y
La Fita	Apatite 72% Calcite 28% Quartz 1%	415	525.3	Ca,Fe	P,Sr	Mn,Pb,Y
La Fita balsa	Apatite 81% Calcite 18% Quartz 1%	399	523.7	Ca,Fe	P,Sr	Mn,Pb,Cu,Y
Qurolles III	Apatite 84%	383	521.9	Ca,Fe	P,Sr,Y	Cr,Mn,Pb

–Emilio Napolitano–
Application of the Diffraction Technique in Solid State Chemistry from "ab-initio" Structure Solution to Final Structure Refinement –Powder and Single Crystal– Doctoral Thesis in Sciences and Chemical Technology, XXIV cycle University of Sassari

Pag. 62

	Dolomite 15%, quartz+Calcite (traces)					
Qurolles M	Apatite 70% Goethite 24% Calcite 4% Quartz 2%	349	521.9	Ca,Fe	Y	P,Ti,Cr,Mn,Zn,Pb,Rb,Sr
MC1-5	Apatite 85% Calcite 15% Quartz (traces)	411	523.0	Ca,Fe	P,Sr	Ti,V,Cr,Mn,Pb,Y
SAV-39	Apatite 96% Quartz 4%	399	524.8	Ca,Fe	P,Y,Sr	V,Cr,Mn,Cu,Pb,Zn
SAV-67	Apatite 85% Quartz 7% Berlinite 1% Kaolinite 7%	457	525.3	Ca,Fe	P,Mn,Sr	Ti,Cr,Zn,Pb,Y
Povet	Apatite 67% Kaolinite 25% Quartz 8%	437	524.0	Ca,Fe	P,Sr,Y	Ti,V,Cr,Mn,Zn,Ge
Camino	Apatite 80% Calcite 20%	2107	524.7	Ca,Fe	Sr,Mn,P	Y,Ti,As,Zn
EAP 38	Apatite 94% Calcite 1% Goethite 4% Quartz 1%	352	523.8	Ca,Fe	P,Mn	Ti,Zn,Pb,As,Y
EAP 40-39	Apatite 88% Calcite 12%	382	523.9	Ca,Fe	Sr,Mn,P	As,Y
EAP 43	Apatite 93% Calcite 3% Quartz 3% Goethite 1%	485	524.3	Ca,Fe	P,Mn,Sr	V,Cu,Pb,Y
Comptadors A1	Apatite 66% Calcite 24% Quartz 8% Kaolinite 2%	432	525.7	Fe,Ca	Mn	Ti,P,Sr,Rb
Todolella 1	Apatite 98% Calcite 1% Quartz 1%	436	525.4	Ca,Fe	P,Mn,Zn,Sr	Ti,Ga
Torre Julian	Apatite 52% Calcite 47 % Quartz 1%	411	524.3	Ca	Fe,P,Sr	Mn,Zn,Ni,Y
A 10	Apatite 68% Quartz 4% Goethite 28%	226	522.6	Ca,Fe	P,Mn,Sr	S,V,Cr,Zn,Pb,Y
A 13	Apatite 96% Quartz 2% Goethite 2%	255	522.5	Ca,Fe,Sr	P	Mn,Cu,Zn,As,Br,Y
2ANA12	Apatite 96% Calcite 4%	282	523.5	Ca,Fe	P,Sr,Mn	Cr,Pb,Y
2ANA61	Apatite 82% Quartz 14% Goethite 4%	310	524.5	Ca,Fe	P,Sr	Mn,Cu,Zn,As,Br,Y

–Emilio Napolitano–
Application of the Diffraction Technique in Solid State Chemistry from
"ab-initio" Structure Solution to Final Structure Refinement
–Powder and Single Crystal–
Doctoral Thesis in Sciences and Chemical Technology, XXIV cycle
University of Sassari

Pag. 63

2ANA77	Apatite 92% Calcite 4% Goethite 3% Quartz 1%	298	524.1	Ca,Fe	P,Sr	Mn,Cu,Zn,As,Br,Y
3ANA58	Apatite 88% Calcite 5% Goethite 4% Quartz 3%	274	524.0	Ca,Fe	P,Sr	Mn,Cu,Zn,As,Br,Y
4ANA3	Apatite 68% Quartz 22% Goethite 8%	183	523.4	Ca,Fe	P,Sr	Mn,Cu,Zn,As,Br,Y
4ANA75	Apatite 100%	312	522.9	Ca,Fe	P,Sr	V,Cr,Mn,Zn,Y
Escápula-ANA	Apatite 99% Calcite 1%	278	525.6	Ca,Fe,Sr	P	V,Zn,Y
Mas Roig	Apatite 75% Calcite 3% Kaolinite 22%	347	524.7	Ca,Fe	P,Sr,Y	Ti,V,Cr,Mn,Zn,Ge
El Maset	Apatite 87% Calcite 13%	312	523.1	Ca,Fe	P,Sr,Y	Ti,V,Cr,Mn,Cu
Manzanera	Apatite 82% Calcite 18%	391	524.4	Fe,Ca	Y,Sr	P,Pb,As,Cu,Zn
Mas de Rafael-2	Apatite 91 % Calcite 9%	311	523.2	Ca	P,Mn,Fe,Sr	Ti,Cu,Hf
Psm-Maite	Apatite 92% Calcite 8% Quartz (traces)	335	525.1	Ca	P,Fe,Sr	Ti,Mn,Y,Rb,Cu,Ni
Psm-Mila	Apatite 82% Calcite 18%	308	523.8	Ca	P,Fe,Sr	Ti,Mn,Y,Rb,Cu,Ni
Psm-Andres	Apatite 92% Calcite 8%	311	524.3	Ca	P,Fe,Sr	Ti,Mn,Y,Rb,Cu
Psm-Carles	Apatite 78% Calcite 21% Quartz 1%	361	524.5	Ca	P,Fe,Sr	Ti,Mn,Y,Rb,Cu,Ni
CerroTadon	Apatite 94% Gypsum 4% Quartz 1% Calcite 1%	333	524.3	Ca,Fe	P,Mn	Cr,Cu,As,Sr,Y
HTCO4-3	Apatite 61% Gypsum 35% Calcite 4%	306	524.6	Ca,Fe	P,Mn	Cr,V,Cu,As,Sr,Y
Rascaña	Apatite 81% Calcite 19%	347	524.9	Ca,Fe	P,Y,Sr	V,Cr,Mn,Cu,Pb,Zn
Yac-David	Apatite 88% Dolomite 11% Calcite 1%	300	523.9	Ca,Fe	P,Sr,Y	Cr,Mn,Pb
Corral de Marin	Apatite 79% Calcite 21%	299	524.2	Ca	P,Fe,Sr	Ti,V,Cr,Mn,Cu,Y
229	Apatite 93% Calcite 7%	328	524.7	Ca,Fe	P,Sr	Ti,V,Cr,Mn,Y
Losilla	Apatite 40% Calcite 33% Quartz 19%	592	523.2	Ca,Fe,Cu	P	Ti,Mn,Sr,Y,Pb

–Emilio Napolitano–
Application of the Diffraction Technique in Solid State Chemistry from
"ab-initio" Structure Solution to Final Structure Refinement
–Powder and Single Crystal–
Doctoral Thesis in Sciences and Chemical Technology, XXIV cycle
University of Sassari

Pag. 64

	Kaolinite 8%					
Aras de Alpuente	Apatite 58% Calcite 42%	554	524.3	Ca,Fe	P,Cu,Sr	Mn,Y,Rb,As
La Ventura	Apatite 62% Calcite 29% Quartz 9%	453	523.8	Ca	P,Fe	Ti,Cr,Mn,Pb,Cu,Sr,Y
El Collado	Apatite 75% Calcite 25%	522	523.7	Ca	Fe	Ti,V,Cr,Mn,Cu,Sr,Y,P
El Collado 1	Apatite 92% Calcite 7% Quartz 1%	346	525.2	Ca,Fe	P,Sr	V,Cr,Mn,Ge,Br,Y
Serrat del Corb	Apatite 55% Calcite 44% Quartz 1%	575	523.9	Fe,Ca	--	P,Ti,V,Mn,Pb,Sr,Y
Serrat-R2	Apatite 36% Calcite 59% Quartz 5%	633	522.8	Ca	Fe,P,Sr	Mn,Ni,Cu,Zn
Molí del Baró	Apatite 48% Calcite 15% Quartz 8% Celestite 25% Kaolinite 4%	740	521.8	Ca,Fe,Sr	P	S,Ti,V,Mn,Cu,Zn,As
La Penella	Apatite 96% Calcite 3% Quartz 1%	367	523.0	Ca,Fe	P,Sr	Ti,V,Cr,Mn,Zn,As,Nb
Lo Bas	Apatite 68% Calcite 30 % Quartz 2%	330	522.1	Ca,Fe	P,Sr	Ti,V,Cr,Mn,Cu,Zn,As,Y
La Llau de Bas	Apatite 81% Calcite 12% Goethite 7%	559	524.0	Ca,Fe	Sr,P	Ti,Mn,Cu,,Pb,Y
Nerets	Apatite 80% Calcite 19% Quartz 1%	581	524.0	Ca	P,Fe,Sr	Ti,Mn,Y,Rb,Cu,Ni
Pous	Apatite 59% Calcite 37% Quartz 4%	449	523.2	Ca,Fe	P,Sr	Ti,V,Cr,Mn,Y,Ni
Basturs Poble	Apatite 55% Calcite 35% Quartz 10%	612	523.1	Ca,Fe	P,Sr	Ti,Mn,Cu,Pb,Y
Basturs Poble-07	Apatite 76% Calcite 24%	326	520.9	Ca,Fe	P,Sr	Ti,V,Cr,Mn,Cu,Zn,Ge,As,Y
Boiga	Apatite 67% Calcite 32% Quartz 1%	326	523.2	Ca,Fe	P,Sr	Ti,Cr,Mn,Cu,Zn,Y
Peguera 1-Figols	Apatite 74% Calcite 14% Quartz 7% Kaolinite 5%	600	524.1	Ca,Fe	P,Sr	Ti,V,Mn,Pb,Y

Table 2: List of the XRD phases analysis complemented with average crystallite size, cell volume of monoclinic apatite structure data and major and minor elements detected by XRF.

–Emilio Napolitano–
Application of the Diffraction Technique in Solid State Chemistry from
"ab-initio" Structure Solution to Final Structure Refinement
–Powder and Single Crystal–
Doctoral Thesis in Sciences and Chemical Technology, XXIV cycle
University of Sassari

Pag. 65

Concerning the phases constituting the fossil bones, a high variability can be pointed out among the various samples. The most frequent phases in the samples studied are mostly fluorapatite, quartz and calcite. The *Molì del Barò* specimen represents the maximum complexity in terms of five minerals detected simultaneously by XRD.

The apatite phase content in the various specimens varies because of the number and amount of the other secondary mineral phases present, ranging from a minimum of 26 wt% for the sample *CL 42 ,* up to 100 wt% in the case of the samples *Escapula Ana*, *4ANA75* and *Patiras*. These specimens were found in the same sedimentary basin and geological formation made up by clay sediments so it may be suggested that clay minerals constitute an alkaline environment equally suitable as limestone for the best conservation of bone as a single apatite phase, apart from the quick degradation of the organic phase and the well-established fluorine exchange reaction.

However, the presence of clays does not preserve the single-phase property of all fossils necessarily, as it follows from the mineralogical phase constitution for the other specimens of the same basin.

Quartz normally derives from the embedding sediment and rarely is an authigenic mineral. Conversely, the presence of calcite as an authigenic mineral is common in many fossil sites[1, 50] and may infill in bone voids or deposit at the surface as a thin and white crust. Our evidence at a micro-scale level from confocal Raman shows that calcite occupies the haversian canals.

In the further specimens here investigated we have also determined several other phases such as kaolinite (25 wt % $Al_2Si_2O_5(OH)_4$, *Povet* specimen), 24 wt% goethite (FeOOH, *Qurolles M* specimen), 25 wt% celestite $SrSO_4$ (*Molì del Barò* specimen), 35 wt% gypsum ($CaSO_4·2(H_2O)$ *HT-CO4-3* specimen), 15 wt%. dolomite ($CaMg(CO_3)_2$, *Qurolles III* specimen*)* and 1 wt% berlinite ($AlPO_4$, *Sav 67* specimen).

–Emilio Napolitano–
Application of the Diffraction Technique in Solid State Chemistry from
"ab-initio" Structure Solution to Final Structure Refinement
–Powder and Single Crystal–
Doctoral Thesis in Sciences and Chemical Technology, XXIV cycle
University of Sassari

Pag. 66

It is clear that also the presence of these phases may be ascribed to the mineralogic features of the sediment. Particularly, the *Molì del Baro* site is different from the other in terms of deposition environment. Its Formation consist of fossiliferous black mudstones, rich in plant remains (including leaves and remains of charred wood) and thin layers of micro-conglomerates. It represents a deposition in an abandoned meander. The presence of the plants, the dark-gray or black color indicates conditions of lack of oxygen in bottom waters, typical of stagnant water bodies. The dinosaur remains, especially hadrosaur bones, are not frequent but they are very well preserved[51]. Thus, celestite phase may form in sedimentary settings through evaporation of brackish water.

The molar volume $V_M/2$ of each monoclinic cell of the apatite-like phase is varying from a lower value of 520.9 $Å^3$ (*BP 07* sample) to an upper value of 525.7 $Å^3$ (*Comptadors-A1* specimen). This is consistent with the literature data referred to fluorapatite that supply several unit cell volume values ranging from 522.18 $Å^3$ to 528.41 $Å^3$, respectively[52, 53].

Even the literature values of francolite range from a minimum of 518.73 $Å^3$ to a maximum of 523.81 $Å^3$ [54,55] and scatter around the values reported for fluorapatite. We have recently estimated that fluorination of bone apatite is taking place in about 4-5 Ma after examining the unit cell volume change of biogenic apatite vs. geological age.[23]

Crystallite size vs. age

The average crystallite size values obtained from the peak sharpening of the apatite-like phase [24, 25, 26] in the XRD diagrams (see Table II) were obtained after correction for the instrument function and after separation of the broadening fraction due to lattice strain. The patterns of the three single-phase fossil bones given in figure 1 look similar to the commercial hydroxylapatite synthesized in the

–Emilio Napolitano–
Application of the Diffraction Technique in Solid State Chemistry from
"ab-initio" Structure Solution to Final Structure Refinement
–Powder and Single Crystal–
Doctoral Thesis in Sciences and Chemical Technology, XXIV cycle
University of Sassari

Pag. 67

laboratory as they appear to have an increased average of the crystallite size (from 280 to 420 Å - see data of Table II) larger than the average value of ca. 170 ± 10 Å normally found in non-fossil human and animal bones (curve of the rhesus monkey at the bottom of figure 1)[56]. These values are found coherent with the observed change in the Splitting Factor of the v_4 PO_4^{3-} band of the correspondent FT-IR spectra even though the fluorination of apatite modifies the shape of this band envelope to a certain extent.

However, we have previously observed[23] that the recrystallization process brought about by fossilization does not occur homogeneously across the geological times. For example, for the *Camino* and *EAP 40-39* specimens, we have pointed out an evident difference in the peak broadening of the two patterns, on account of average crystallite size of 2100 Å (± 200 Å) and 382 Å(± 20), respectively. Also, out of the three fossils consisting of single phase apatite examined in figure 1, the larger average crystallite size (ca. 410 ± 20 Å) is observed in sample with the most recent stratigraphic age.
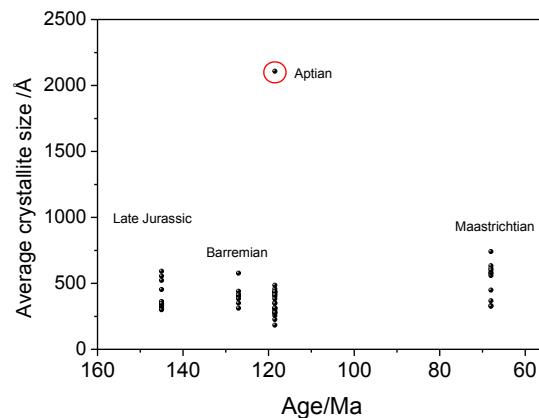
Figure 12: plot of average crystallite size vs. Age/Ma of our dinosaur collection showing the absence of correlation between average crystallite size and age. It can be argued that the recrystallization process brought about by fossilization does not occur progressively across the times, but it can also be overlapped by specific effects typical of local geological environment.

−Emilio Napolitano−
Application of the Diffraction Technique in Solid State Chemistry from
"ab-initio" Structure Solution to Final Structure Refinement
−Powder and Single Crystal−
Doctoral Thesis in Sciences and Chemical Technology, XXIV cycle
University of Sassari

Pag. 68

In Figure 12 we report the average crystallite size for apatite microcrystals of our samples as a function of age in the range 150-65 Ma, ordered according to their Epoch-Geological stages and Formations, showing the absence of correlation between average crystallite size and age.

The unpredictable change of the average crystallite size values and SFs suggest that correlation between crystallisation indices and bone age has to be regarded with obvious caution, as it was suggested by Person et al.[26, 57] and Farlow and Argast[14].

In our previous study[23], we have observed a undeniable correlation in another set of fossils distributed more homogeneously in a wider age range. From the present data it seems that the crystallization induced by just the time is overlapped by other factors depending on the geological Formation that may inhibit (e.g., *4ANA3* sample) or enhance the process.

The behaviour of the *Camino* specimen stands out of any general trend is an outlier since we do not observe apatite crystallize size that exceed 740 Å (*Molì del Barò* specimen) for all other specimens. Beyond diagenesis a value for the crystallite size above 2000 Å can be explained only by a fire exposure to which this dinosaur bone was subjected. In fact, similar values for the average crystallite size of apatite are reported only in human bones incinerated in a temperature range of 900-1000 °C[56, 58, 59].

Element distribution and solid solutions

It should be pointed out that, apart from the Ca ions, XRF invariably shows the presence of Fe ions in the fossils, even if this is not always mirrored in the corresponding XRD diagrams by evident Fe-based phases.

For example, the Escapula ANA spectrum reported in figure 2 (top pattern) shows a large amount of Fe but appears to be single-phase francolite in the

–Emilio Napolitano–
Application of the Diffraction Technique in Solid State Chemistry from
"ab-initio" Structure Solution to Final Structure Refinement
–Powder and Single Crystal–
Doctoral Thesis in Sciences and Chemical Technology, XXIV cycle
University of Sassari

Pag. 69

corresponding diagram of figure 1. This suggests that the mere element distribution from XRF fluorescence analysis alone may not be helpful for a precise account of the fossil diagenesis involved even applying microscale investigations. After this comparison, the strong presence of Fe may be ascribed to a substitution of this element for Ca in the francolite structure. In analogy, for the Povet specimen (see figure 7), the presence of Fe assessed by XRF and the absence of any Fe-based phase indicated by the XRD investigation can be compatible with substitution either for Ca by Fe ions in the apatite lattice or for Al in the kaolinite phase.

Of course the correlation between Fe found by XRF and goethite phase is immediate in cases like that shown in figure 9. Goethite is the only Fe-based phase observed by XRD in our collection of samples (precisely in 8 specimens) and was also reported previously in other dinosaur bones, though not evaluated quantitatively[15]. Its presence was attributed to a hydromorphic process because of seasonal variations of the ground water level. It is also possible that the specimens showing high amount of Fe in the XRF spectra but any Fe-based phase in the correspondent XRD pattern may actually contain limonite, i.e., amorphous FeOOH, that cannot be detected by diffraction unless an approximate presence larger than 25 wt%.

Presence of goethite and calcite together occurs just for *2ANA77*, *3ANA58* and *La Llau de Bas* specimens and is thought to be possible only under oxidising conditions, whereas the precipitation of pyrite and calcite under reducing conditions and the later oxidation of pyrite to hematite is more common [18, 60]. In several studies, the presence of hematite and other Fe-oxides in the samples were interpreted as the result of weathering of pyrite [e.g.18]. Two further ways of Fe oxide formation in fossil bones are suggested by Pfretzschner[60]. The first mechanism is likely restricted to early diagenesis and occurs after the oxidation from ferrous to ferric Fe, preserving the histologic structures without replacement

−Emilio Napolitano–
Application of the Diffraction Technique in Solid State Chemistry from
"ab-initio" Structure Solution to Final Structure Refinement
–Powder and Single Crystal–
Doctoral Thesis in Sciences and Chemical Technology, XXIV cycle
University of Sassari

Pag. 70

of adjacent bone by the Fe oxides. The second possibility occurs via precipitation due to OH change. This is restricted to later diagenesis and a considerable replacement of bone matrix by Fe-oxides and/or hydroxy-oxides is expected as in the case of pyrite oxidation.

High concentration of exogenous Sr both in single phase apatite and multiphase samples suggest an intrinsic difficulty in inferring the palaeo diet based on the Sr/Ca ratio even when using successfully chemical methods for selective extraction of Sr from biogenic hydroxylapatite [61, 62, 63]. The extraction turns out to be inestricably biased by the ion exchange processes leading to precipitation of celestite and to substitution of Ca ions in the apatite lattice.

CONCLUSION

The precise understanding of diagenetic and taphonomic processes to which dinosaur bones were subjected requires a multidisciplinary approach, taking into account the potentialities and limitations of each analytical technique employed. Particularly, we have used XRD, XRF and FT-IR methods supplemented by confocal microscopic Raman images to investigate a collection of Spanish dinosaur bone specimens being 65 to 150 millions of years old to characterize the fossilization in terms of chemical and mineralogical composition, crystallite size, precipitation and infiltration, exchange reactions involving atomic and molecular ion species.

The analysis of diffraction data of dinosaur bones according to the Rietveld method using the MAUD software is unrivalled in these type of study and has shed light on numerous questions pending about the palaeological history of these extinct animals.

–Emilio Napolitano–
Application of the Diffraction Technique in Solid State Chemistry from
"ab-initio" Structure Solution to Final Structure Refinement
–Powder and Single Crystal–
Doctoral Thesis in Sciences and Chemical Technology, XXIV cycle
University of Sassari

Pag. 71

From the crystal lattice parameters of the apatite phase determined by powder XRD, it emerged that these fossil bones invariably underwent a *post-mortem* transformation from bioapatite (hydroxylapatite) to authigenic francolite (fluorapatite) structure. The XRF spectra collected in the energy range from 1.5 to 18 keV supplied analysis profile spectra with the expected presence of Ca and P as major elements. In addition, the presence of carbonate groups substituting for the phosphates in the hydroxylapatite-like structure was definitely assessed for the single-phase specimens by FT-IR spectroscopy. For a large number of specimens the presence of secondary quartz and calcite phases were frequently observed while dolomite was found in just one specimen. The average crystallite size of the apatite-like phase ranges from 183 Å to 2100 Å and varies unpredictably in the analysed specimens, inhibiting a correlation with fossil age. In all the fossils examined, varying levels of Fe were detected by XRF that may be present in the goethite phase FeOOH. However, no presence of other Fe-bearing phases such as pyrite, hematite or magnetite was observed. For the specimens that displayed considerable amount of Fe but absence of any Fe-bearing phase in the XRD spectra, the analysis suggested that Fe divalent cations may have substituted for divalent Ca cations in the francolite structure even at a considerable concentration level (up to 12 %) and without significant changes in the unit cell volume. Frequently the major elements Ca and P were also accompanied by varying amounts of transitional elements such as Ti, V, Mn, Cu, As, Rb, Y, Sr and Nb, to list the most frequently encountered. In particular, the level of Sr was occasionally found in relatively elevated concentrations. Likewise Fe ions, in the absence of specific Sr-based phase it is possible that a considerable amount of Sr substitutes for Ca ions in the structure of francolite. However, in selected cases we have documented remarkable presence of the Sr sulphate (celestite) phase. These two highly different cases of Sr present as sulphate phase in alternative to an apatitic solid solution suggest that special

–Emilio Napolitano–
**Application of the Diffraction Technique in Solid State Chemistry from
"ab-initio" Structure Solution to Final Structure Refinement
–Powder and Single Crystal–
Doctoral Thesis in Sciences and Chemical Technology, XXIV cycle
University of Sassari**

Pag. 72

care must be exercised in palaeontology if using Sr of fossil bones in order to infer a possible animal diet.

It was surmised that the presence of celestite may form in sedimentary settings through evaporation. of brackish water.

REFERENCES

1. Hubert, J.F., Panish, P.T., Chure, D.J., Prostak, K.S., 1996. Chemistry, microstructure, petrology, and diagenetic model of Jurassic dinosaur bones, Dinosaur National Monument, Utah. Journal of Sedimentary Research 66, 531–547.

2. Bocherens, H., 1997. Chemical composition of dinosaur fossils. In: Padian, K., Currie, P.J. (Eds.), The Dinosaur Encyclopedia. University of California Press, Berkeley, CA, pp 111–117

3. Zocco, T.G., Schwartz, H.L., 1994. Microstructural analysis of bone of the sauropod dinosaur *Seismosaurus* by transmission electron microscopy. Palaeontology 37, 493–503.

4. Trueman, C.N.G., Chenery, C., Eberth, D.A., Spiro, B., 2003. Diagenetic effects on the oxygen isotope composition of bones of dinosaurs and other vertebrates recovered from terrestrial and marine sediments. Journal of the Geological Society 160, 895–901.

5. Tütken, T., Pfretzschner, H.-U., Vennemann, T.W., Sun, G., Wang, Y.D., 2004. Paleobiology and Skeletochronology of Jurassic Dinosaurs: Implications from the histology and oxygen isotope compositions of bones. Palaeogeography, Palaeoclimatology, Palaeoecology 206, 217–238.

6. Fricke, H.C., Rogers, R.R., Backlund, R., Dwyer, C.N., Echt, S., 2008. Preservation of primary stable isotope signals in dinosaur remains, and

–Emilio Napolitano–
Application of the Diffraction Technique in Solid State Chemistry from
"ab-initio" Structure Solution to Final Structure Refinement
–Powder and Single Crystal–
Doctoral Thesis in Sciences and Chemical Technology, XXIV cycle
University of Sassari

Pag. 73

environmental gradients of the Late Cretaceous of Montana and Alberta. Palaeogeography, Palaeoclimatology, Palaeoecology 266, 13–27.

7. Dumont, M., A. Pyzalla, A. Kostka, Borbély A., 2011. Characterization of sauropod bone structure. In: N. Klein, K. Remes, C. T. Gee, and P. M. Sander, eds. Biology of the Sauropod Dinosaurs: Understanding the Life of Giants. Life of the Past. Indiana University Press, Bloomington, pp. 150-170.

8. Pfretzschner, H.-U., Tütken, T. 2011. Rolling bones - Taphonomy of Jurassic dinosaur bones inferred from diagenetic microcracks and mineral infillings. Palaeogeography, Palaeoclimatology, Palaeoecology 10.1016/j.palaeo.2011.01.026

9. Tütken, T., Vennemann, T.W., Pfretzschner, H.-U., 2008. Early diagenesis of bone and tooth apatite in fluvial and marine settings: Constraints from combined oxygen isotope, nitrogen and REE analysis. Palaeogeography, Palaeoclimatology, Palaeoecology 266, 254-268.

10. Trueman, C.N.G., Martill, D.M., 2002. The long-term preservation of bone: the role of bioerosion. Archaeometry 44, 371–382.

11. Jans, M.M.E., Nielsen-Marsh, C.M., Smith, C.I., Collins, M.J., Kars, H., 2004. Characterisation of microbial attack on archaeological bone. Journal of Archaeological Science 31, 87-95.

12. Denys, C., 2002. Taphonomy and experimentation. Archaeometry 4, 469–484.

13. Pfretzschner, H.-U., 2004. Fossilization of Haversian bone in aquatic environments. Comptes Rendus Palevol 3, 605-616.

14. Farlow, J.O., Argast A., 2006. Preservation of Fossil Bone from the Pipe Creek Sinkhole (Late Neogene, Grant County, Indiana U.S.A.), Journal of the Paleontological Society of Korea 22, 51–75.

–Emilio Napolitano–
Application of the Diffraction Technique in Solid State Chemistry from
"ab-initio" Structure Solution to Final Structure Refinement
–Powder and Single Crystal–
Doctoral Thesis in Sciences and Chemical Technology, XXIV cycle
University of Sassari

Pag. 74

15. Elorza, J., Astibia, H., Murelaga, X., Pereda-Suberbiola, X., 1999. Francolite as a diagenetic mineral in dinosaur and other Upper Cretaceous reptile bones (Laño, Iberian Peninsula): microstructural, petrological and geochemical features. Cretaceous Research 20, 169–187.

16. Hedges, R.E.M., 2002. Bone diagenesis: an overview of processes. Archaeometry 44, 319–328.

17. Trueman, C.N.G., Tuross, N., 2002. Trace elements in recent and fossil bone apatite. In: Kohn, M.J., Rakovan, J., Hughes, J.M. (eds.), Phosphates: Geochemical, Geobiological and Materials Importance. Mineralogical Society of America. Reviews in Mineralogy and Geochemistry 48, 489–521.

18. Wings, O., 2004. Authigenic minerals in fossil bones from the Mesozoic of England: poor correlation with depositional environments. Palaeogeography, Palaeoclimatology, Palaeoecology 204, 15–32.

19. Wopenka, B., Pasteris, J.D., *2005*. A mineralogical perspective on the apatite in *bone*. Materials Science and Engineering C25, 131–143.

20. Bradley, D.A., Muthuvelu, P., Ellis, R.E., Green, E.M., Attenburrow, D., Barrett, R., Arkill, K., Colridge, D.B., Winlove, C.P., 2007. Characterisation of mineralisation of bone and cartilage: X-ray diffraction and Ca and Sr Ka X-ray fluorescence microscopy. Nuclear Instruments and Methods in Physics Research B 263, 1–6.

21. Pucéat, E., Reynard, B., Lécuyer, C., 2004. Can crystallinity be used to determine the degree of chemical alteration of biogenic apatites? Chemical Geology 205, 83–89.

22. Thomas, D.B., Fordyce, R.E., Frew, R.D., Gordon, K.C., 2007. A rapid, non-destructive method of detecting diagenetic alteration in fossil bone using Raman spectroscopy. Journal of Raman Spectrometry 38, 1533–

–Emilio Napolitano–
Application of the Diffraction Technique in Solid State Chemistry from
"ab-initio" Structure Solution to Final Structure Refinement
–Powder and Single Crystal–
Doctoral Thesis in Sciences and Chemical Technology, XXIV cycle
University of Sassari

Pag. 75

1537. Daniel B. Thomas, Cushla M. McGoverin, R. Ewan Fordyce, Russell D. Frew, Keith C. Gordon, (2011) Raman spectroscopy of fossil bioapatite — A proxy for diagenetic alteration of the oxygen isotope composition, Palaeogeography, Palaeoclimatology, Palaeoecology 310, *62-70*

23. Piga, G., Santos-Cubedo, A., Moya Solà, S., Brunetti, A., Malgosa, A., Enzo, S., 2009. An X-Ray Diffraction (XRD) and X-Ray Fluorescence (XRF) investigation in human and animal fossil bones from Holocene to Middle Triassic. Journal of Archaeological Science 36, 1857–1868.

24. Chipera, S.J., Bish, D.L., 1991. Applications of X-ray diffraction crystallite size/strain analysis to *Seismosaurus* dinosaur bone. Advances in X-Ray Analysis 34, 473–482.

25. Bartsiokas, A., Middleton, A.P., 1992. Characterisation and dating of recent and fossil bone by X-ray diffraction. Journal of Archaeological Science 19, 63–72.

26. Person, A., Bocherens, H., Saliege, J.F., Paris, F., Zeitoun, V., Gerard, M., 1995. Early diagenetic evolution of bone phosphate: an X-ray diffractometry analysis. Journal of Archaeological Science 22, 211–221.

27. Suñer, M., Santisteban, C., Santos-Cubedo, A., Galobart, A., 2007. Dinosaur fossils in marine facies from ANA locality, Arcillas de Morella Formation (Aptian, Lower Cretaceous, Cinctorres, Spain). 55th Symposium of Vertebrate Palaeontology and Comparative Anatomy and the 16th Symposium of Palaeontological preparation and conservation. Glasgow, 43.

28. Salas, R., Martín-Closas, C., Querol, X., Guimerà, J., Roca, E. 1995. Evoluciòn tectonosedimentaria de las Cuencas del Maestragzo y Aliaga-Penyagolosa durante el cretacico inferior. In: Publicacions de la Universitat de Barcelona, Guía de campo de las excursiones científicas realizadas durante el III Coloquio del Cretácico de España, 11–94.

–Emilio Napolitano–
**Application of the Diffraction Technique in Solid State Chemistry from
"ab-initio" Structure Solution to Final Structure Refinement
–Powder and Single Crystal–
Doctoral Thesis in Sciences and Chemical Technology, XXIV cycle
University of Sassari**

Pag. 76

29. Salas, R., Guimerà, J., Mas, R., Martín-Closas., C., Meléndez, A., Alonso, A., 2001. Evolution of the Mesozoic Central Iberian rift system and its Cainozoic inversion (Iberian chain). 145–185 in: Ziegler, P.A., Cavazza, W., Robertson, A.H.F., Crasquin-Soleau, S. (eds), Peri-Tethys Memoir 6: Peri-Tethyan Rift/Wrench Basins and passive margins. Memoires du Museum National d'Histoire Naturelle 186, 1–762.

30. Caja, M.A., Salas, R., Marfil, R., Lago, M., 2005. Heavy mineral composition and geochemistry of the Weald facies from the Maestrat Basin (Spain): Provenance implications for Late Jurassic-Early Cretaceous rifting stage. Geogaceta 38, 11–14.

31. Riera, V., Oms, O., Gaete, R., Galobart, A., 2009. The end-Cretaceous dinosaur succession in Europe: The Tremp Basin record (Spain). Palaeogeography, Palaeoclimatology, Palaeoecology 283, 160–71.

32. Enzo, S., Fagherazzi, G., Benedetti, A., Polizzi, S., 1988. A profile-fitting procedure for analysis of broadened X-ray diffraction peaks. I Methodology. Journal of Applied Crystallography 21, 536–542.

33. Rietveld, H.M., 1967. Line profiles of neutron powder-diffraction peaks for structure refinement. Acta Crystallographica 22, 151–152.

34. Lutterotti, L., Ceccato, R., Dal Maschio, R., Pagani, E., 1998. Quantitative analysis of silicate glass in ceramic materials by the Rietveld Method. Materials Science Forum 2, 87–92.

35. Michel, V., Ildefonse, Ph., Morin, G., 1996. Assessment of archaeological bone and dentine preservation from Lazaret Cave (Middle Pleistocene). Palaeogeography, Palaeoclimatology, Palaeoecology 126, 109–119.

36. Michel, V., Ildefonse, Ph., Morin, G., 1995. Chemical and structural changes in *Cervus elaphus* tooth enamel during fossilization (Lazaret cave): a combined IR and XRD Rietveld analysis. Applied Geochemistry 10, 145–159.

–Emilio Napolitano–
Application of the Diffraction Technique in Solid State Chemistry from
"ab-initio" Structure Solution to Final Structure Refinement
–Powder and Single Crystal–
Doctoral Thesis in Sciences and Chemical Technology, XXIV cycle
University of Sassari

Pag. 77

37. Elliott, J.C., Mackie, P.E., Young, R.A., 1973. Monoclinic Hydroxyapatite. Science 180, 1055–1057.

38. Ikoma, T., Yamazakai, A., Nakamura, S., Akao, M., 1999. Preparation and structure refinement of monoclinic hydroxyapatite. Journal of Solid State Chemistry 144, 272–276.

39. Goodwin, M.B., Grant, P.G., Bench, G., Holroyd, P.A., 2007. Elemental composition and diagenetic alteration of dinosaur bone: Distinguishing micron-scale spatial and compositional heterogeneity using PIXE. Palaeogeography, Palaeoclimatology, Palaeoecology 253, 458–476.

40. Kolodny, Y., Luz, B., Sander, M., Clemens, W.A., 1996. Dinosaur bones: fossils or pseudomorphs? The pitfalls of physiology reconstruction from apatitic fossils. Palaeogeography, Palaeoclimatology, Palaeoecology 126, 161–171.

41. Lebon, M., Reiche, I., Fröhlich, F., Bahain, J.-J., Falguères, C., 2008. Characterization of archaeological burnt bones: contribution of a new analytical protocol based on derivative FTIR spectroscopy and curve fitting of the v_1v_3 PO_4 domain. Analytical Bioanalytical Chemistry 392, 1479–1488

42. Lebon, M., Reiche, I., Bahain, J.-J., Chadefaux, C., Moigne, A.M., Fröhlich, F., Sémah, F., Schwarcz, H.P., Falguères, C., 2010. New parameters for the characterization of diagenetic alterations and heat-induced changes of fossil bone mineral using Fourier transform infrared spectrometry. Journal of Archaeological Science 37, 2265–2276

43. Tadic, D., Epple, M., 2004. A thorough physicochemical characterization of 14 Ca phosphate-based bone substitution materials in comparison to natural bone. Biomaterials 25, 987–994.

–Emilio Napolitano–
Application of the Diffraction Technique in Solid State Chemistry from
"ab-initio" Structure Solution to Final Structure Refinement
–Powder and Single Crystal–
Doctoral Thesis in Sciences and Chemical Technology, XXIV cycle
University of Sassari

Pag. 78

44. Stathopoulou, E.T., Psycharis, V., Chryssikos, G.D., 2008. Bone diagenesis: new data from Infrared spectroscopy and X-Ray Diffraction. Palaeogeography, Palaeoclimatology, Palaeoecology 266, 168–174.

45. Stiner, M.C., Kuhn, S.L., Weiner, S., Bar-Yosef, O., 1995. Differential burning, recrystallization, and fragmentation of archaeological bone. Journal of Archaeological Science 22, 223–237.

46. Thompson, T.J.U., Gauthier, M., Islam, M., 2009. The application of a new method of Fourier Transform Infrared Spectroscopy to the analysis of burned bone. Journal of Archaeological Science 36, 910–914.

47. Penel, G., Leroy, G., Rey, C., Bres, E., 1998. MicroRaman spectral study of the PO_4 and CO_3 vibrational modes in synthetic and biological apatites. Calcified Tissue International 63, 475–481.

48. Antonakos, A., Liarokapisa, E., Leventouri, T., 2007. Micro-Raman and FTIR studies of synthetic and natural apatites. Biomaterials 28, 3043–3054.

49. Balan, E., Saitta, A.M., Mauri, F., Calas, G., 2001. First-principles modeling of the infrared spectrum of kaolinite. American Mineralogist 86, 1321–1330.

50. Astibia, H., Payros, A., Suberbiola, X., Berreteaga, A., Elorza, J., Extebarria, N., Tosquella, J., 2005. Sedimentology and taphonomy of sirenian remains from the Middle Eocene of the Pamplona Basin (Navarre, western Pyrenees). Facies 50, 463–475.

51. O. Oms, J. Dinarès-Turell, E. Vicens, R. Estrada, B. Vila, À. Galobart, A.M. Bravo *2007*, Integrated stratigraphy from the Vallcebre Basin (southeastern Pyrenees, Spain): New insights on the continental Cretaceous−Tertiary transition in southwest Europe, Palaeogeography, Palaeoclimatology, Palaeoecology, 255, 35-47.

–Emilio Napolitano–
Application of the Diffraction Technique in Solid State Chemistry from
"ab-initio" Structure Solution to Final Structure Refinement
–Powder and Single Crystal–
Doctoral Thesis in Sciences and Chemical Technology, XXIV cycle
University of Sassari

Pag. 79

52. McConnell, D., 1973. Apatite – its crystal chemistry, mineralogy, utilization, and geologic and biologic occurrences. Wien, Heidelberg, Springer. New York.

53. Hughes, J.M., Cameron, M., Crowley, K.D., 1989. Structural variations in natural F, OH, and Cl apatites. American Mineralogist 74, 870–876.

54. Sudarsanan, K., Mackie, P.E., Young, R.A., 1972. Comparison of synthetic and mineral fluorapatite, $Ca_5(PO_4)_3F$, in crystallographic detail. Materials Research Bulletin 7, 1331–1338.

55. Sudarsanan, K., Young, R.A., 1978. Structural interactions of F, Cl and OH in apatites. Acta Crystallographica B34, 1401–1407.

56. Piga, G., Malgosa, A., Thompson, T.J.U, Enzo, S., 2008. A new calibration of the XRD technique for the study of archaeological burnt remains. Journal of Archaeological Science 35, 2171–2178.

57. Person, A., Bocherens, H., Mariotti, A., Renard, M., 1996. Diagenetic evolution and experimental heating of bone phosphate. Palaeogeography, Palaeoclimatology, Palaeoecology 126, 135–149.

58. Piga, G., Guirguis, M., Bartoloni, P., Malgosa, A., Enzo, S., 2010. A funerary rite study in the Phoenician-Punic Necropolis of Mount Sirai (Carbonia-Sardinia-Italy). International Journal of Osteoarchaeology 20, 144–157.

59. Piga, G., Hernández-Gasch J.H., Malgosa, A., Ganadu, M.L., Enzo, S., 2010. Cremation practices coexisting at the *S'Illot des Porros* Necropolis during the Second Iron Age in the Balearic Islands (Spain). Homo 61, 440–452.

60. Pfretzschner, H.-U., 2001. Iron oxides in fossil bone. Neues Jahrbuch für Geologie und Paläontologie Abhandlungen 220, 417–429.

61. Bruce K Nelson, Michael J Deniro, Margaret J Schoeninger, Donald J De Paolo, P.E Hare Effects of diagenesis on strontium, carbon, nitrogen and

–Emilio Napolitano–
Application of the Diffraction Technique in Solid State Chemistry from
"ab-initio" Structure Solution to Final Structure Refinement
–Powder and Single Crystal–
Doctoral Thesis in Sciences and Chemical Technology, XXIV cycle
University of Sassari

Pag. 80

oxygen concentration and isotopic composition of bone (1986), Geochimica et Cosmochimica Acta 50: 1941-1949

62. A. Sillen, J C Sealy (1995) Diagenesis of Strontium in Fossil Bone: A Reconsideration of Nelson et al. (1986) Journal of Archaeological Science 22, 313-320

63. Safont, S., Malgosa, A., Subirà, M.E., Gibert, J., 1998. Can Trace Elements in Fossils Provide

–Emilio Napolitano–
Application of the Diffraction Technique in Solid State Chemistry from
"ab-initio" Structure Solution to Final Structure Refinement
–Powder and Single Crystal–
Doctoral Thesis in Sciences and Chemical Technology, XXIV cycle
University of Sassari

Pag. 81

Magnesium Imide (MgND) structure solution.

The magnesium imide, MgNH has been synthetized for the first time by H. Jacobs and R. Juza in 1969[1-2]. A hexagonal geometry was found with lattice parameters a = 11.58 and c = 3.677 Å was found, but the crystal structure remained unsolved, given the difficulties to recognize the correct space group.

In recent years, related materials like Alkali amide MNH_2 and alkaline earth analogues $M_0(NH_2)_2$ (M: alkali metal, M_0: alkaline earth metal) have been subjected to an intense research because of potential materials for hydrogen storage[3].

Working on such topic, the magnesium imide, MgNH, has been re-synthetized by thermal decomposition of magnesium amide, $Mg(NH_2)_2$.

The process was monitored with an in-situ neutron diffraction of the deuterated compound. Synthesis and diffraction data were gently supplied by Dr. Francesco Dolci from JRC Institute-Petten (Holland)[4].

Data collection

The structure solution has been performed using the three sets of powder patterns collected in Grenoble with neutron and synchrotron sources (France).

Neutron diffraction was performed on the 2-axis diffractometer D20[5], at the high flux reactor of the Institut Laue-Langevin, Grenoble, (France) equipped with a curved linear position sensitive detector (PSD) resulting in rapid and simultaneous data acquisition over an angular range from 5 to 140 (2θ). The used wavelength was 1.868 Å from its (115) reflection, a d-spacing range of 1-21 Å is covered with a time-resolution of 2 min.

–Emilio Napolitano–
Application of the Diffraction Technique in Solid State Chemistry from
"ab-initio" Structure Solution to Final Structure Refinement
–Powder and Single Crystal–
Doctoral Thesis in Sciences and Chemical Technology, XXIV cycle
University of Sassari

Pag. 82

Synchrotron patterns have been collected on the ID31[6], the high resolution powder diffraction beam line, mounting a multi-detector with 9 channels, ensuring an high resolution over the analyzed range from 1° to 110° (2θ) using a wavelength of 0.39994 Å, covering the d-space range 0.8-18.8 Å.

The instrument function for each diffractometer has been determined using the NIST powder standard 640a, silicon, and a pseudo-Voigt peak-shape function for the fitting.

D20: The sample of deuterated magnesium amide has been loaded in a can of ASI-316 L steel connected to a homemade high pressure rig. The thermal decomposition pathway was tracked collecting diffraction patters until the formation of the magnesium imide phase.

ID31: The same deuterated sample with the magnesium imide phase has been loaded in a borosilicate capillary of 1.0 mm diameter. The diffraction experiment was performed in Debye-Scherrer geometry, the capillary was spun and the patterns were collected both at room temperature (298 K) and 100K.

Plotting the powder diffraction diffractograms in Q-scale, no phase transition has been monitored analyzing the patterns collected at 100K and 298K.

–Emilio Napolitano–
Application of the Diffraction Technique in Solid State Chemistry from
"ab-initio" Structure Solution to Final Structure Refinement
–Powder and Single Crystal–
Doctoral Thesis in Sciences and Chemical Technology, XXIV cycle
University of Sassari

Pag. 83
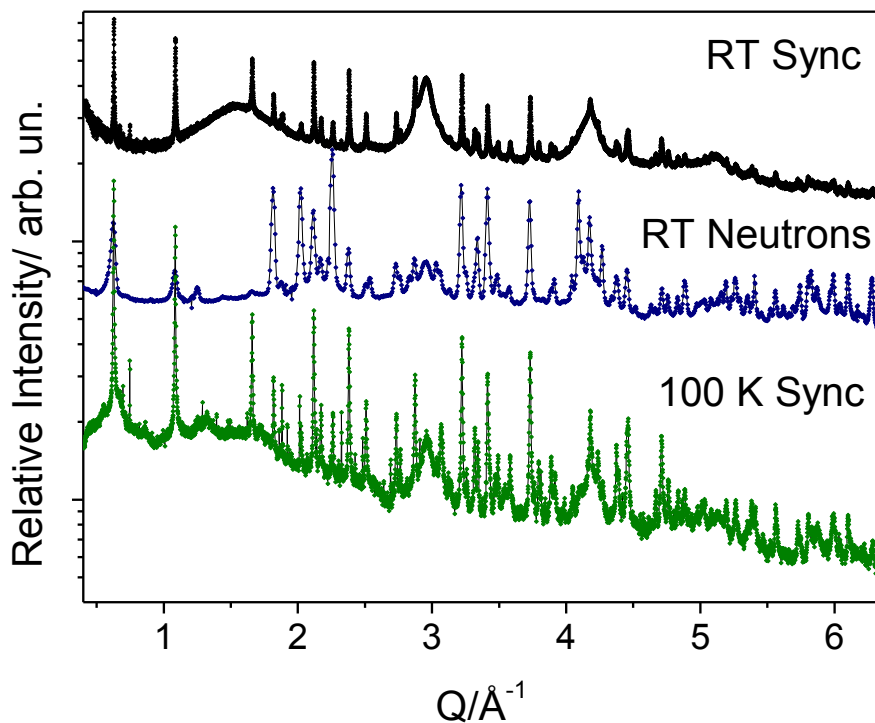
Figure 1. Neutron and Synchrotron powder patterns plotted in Q-space. There are obvious technical differences among the three patterns due to the difference scattering power of elements in the case of the two radiation employed. Note also that the RT pattern is affected by wide features due to the amorphous capillary and by the presence of a Mg(O,N) oxide phase.

Data analysis

Before to start the indexing step, search match analysis was performed for the three sets of data, to identify reagents or secondary products of known phases.

The sample showed two different sets of peaks.

An amorphous component was present in the synchrotron patterns around 1.5 $\mathring{A}^{-1}$ because of the glass capillary used for the data collection. Two other broad features at 2.9 and 4.3 $\mathring{A}^{-1}$ respectively have been attributed to cubic phase

–Emilio Napolitano–
Application of the Diffraction Technique in Solid State Chemistry from
"ab-initio" Structure Solution to Final Structure Refinement
–Powder and Single Crystal–
Doctoral Thesis in Sciences and Chemical Technology, XXIV cycle
University of Sassari

Pag. 84

periclase, Mg(O,N). The remaining sharp peaks were attributed to the imide unknown phase

The ID31 synchrotron pattern collected at 100K has been used for the indexing step, because of its better resolution in d-space, its better signal-to-background ratio and less intense peaks of the periclase-like structure.

The first 20 reflections have been inputted in different softwares, McMaille[7], Treor[8], Ito-15[9], N-Treor[10], Dicvol06[11]

All the outputs converged to the same result with high figure of merit.

Software	IN	FoM M_{20}	Vol	a	b	c	α	β	γ	Symmetry
McMaille	20	296	426.836	11.5698	11.5698	3.6819	90.00	90.00	120.00	Hex
Treor 90	20	280	426.650	11.5677	11.5677	3.6817	90.00	90.00	120.00	Hex
N-Treor	20	212	426.860	11.5695	11.5695	3.6824	90.00	90.00	120.00	Hex
Dicvol06	20	280	425.850	11.5617	11.5617	3.6785	90.00	90.00	120.00	Hex
ITO-15	20	22.4	425.800	11.5618	11.5618	3.6785	90.00	90.00	120.00	Hex
mean-val			426.399	11.5661	11.5661	3.6816	90.00	90.00	120.00	Hex

Table 1. Indexing results in hexagonal system.

These results confirmed a hexagonal cell of magnesium imide indexed also by Jacobs and Juza with lattice parameters a=11.574 Å and c = 3.681 Å.

The other solutions were discarded for the low FoM and for the incompatibility with a picnometer density measurement performed by J.and J, 1.837 g/cm^3.

In particular, the cell volume is in agreement with a number of asymmetric unit Z=12, i. e., 12 MgND molecules, for a calculated density 1.835 g/cm^3.

After identification of the powder Laue class P/6mmm, at this step a cell-constrained whole pattern decomposition has been performed with the primitive space group, refining cell parameters and intensity values through a least

–Emilio Napolitano–
Application of the Diffraction Technique in Solid State Chemistry from
"ab-initio" Structure Solution to Final Structure Refinement
–Powder and Single Crystal–
Doctoral Thesis in Sciences and Chemical Technology, XXIV cycle
University of Sassari

Pag. 85

squares procedure (Le Bail *et al.*, 1988)[12]. In this passage the peak positions have been controlled by the crystal metric parameters.

Analyzing systematic absences (*000l : l=2+1*) to find the space-group symmetry of unknown phase, twelve probable space groups were identified and submitted to a Le Bail fit calculations.

No.	Space Group	Wss	Rw_b	R_b	hkl
1	P6	21318.605	5.0007	3.6502	715
2	P63	21335.314	5.0026	3.6539	712
3	P$\bar{6}$	21285.045	4.9968	3.6455	715
4	**P6/m**	21285.048	4.9962	3.6451	715
5	P622	21250.730	4.9927	3.6395	423
6	P6$_3$22				
7	P6mm	21250.730	4.9927	3.6395	423
8	P$\bar{6}$m2	21250.730	4.9927	3.6395	423
9	P$\bar{6}$2m	21250.730	4.9927	3.6395	423
10	P6/mmm	21250.730	4.9927	3.6395	423
11	P6$_3$22				
12	P6$_3$/m	21335.313	5.0023	3.6539	712

Table 2. Le Bail fit with the choose space groups.

In powder diffraction the space groups P6, P-6, P6/m, P622, P6mm, P-6m2, P-62m and P6/mmm, follow the same extinction rules and this make them indistinguishable, but the same rules are followed by P3, P-3, P312, P321,P3m1, P31m, P-31m, P-3m1 in the trigonal system so doubling the difficulty to detect the right one.

This analysis (Table 2) demonstrates how complicate was to attribute the space-group, infact all the Le Bail fits showed very close weighted sum of squared values (Wss).

–Emilio Napolitano–
Application of the Diffraction Technique in Solid State Chemistry from
"ab-initio" Structure Solution to Final Structure Refinement
–Powder and Single Crystal–
Doctoral Thesis in Sciences and Chemical Technology, XXIV cycle
University of Sassari

Pag. 86

For overcoming this trouble, the structure solution was performed with all space groups and the symmetry determination was performed after this step.

Working on neutron data, the so called "direct-space methods"[13] was used to find the right distribution of atoms inside the unit cell, the computation has been performed using Endeavour[14] software.

This approach is based on the uses of global optimization algorithms to orient and locate the (hypothetical) starting structural model (or atoms) within the unit cell until to find a global minimum.

Endeavour[15] uses a Monte Carlo global optimization procedure called "simulated annealing"[16] and combines the global minimization of Rwp and the potential energy of the system into a cost function.

A priori chemical information, in form of fragment, was used allowing a reduction of the variables system number, from 108 (x, y, z for each atom inside the cell) to 76 (x, y, z positional and θ, φ, ψ orientational degree of freedom) of the rigid body. In this manner processing rate was improved.

Element	x (rel.)	y(rel.)	z(rel.)
N	0.61570	0.68030	0.21950
Mg	0.65610	0.56110	0.37680
H	0.52890	0.67860	0.37680

	Length Å	angle
N-H	1.0546	
Mg-N	1.7602	
Mg-N-H	--------	120

Table 3. Rigid body relative coordinate, bond length and angle

Figure 2. MgNH fragment

−Emilio Napolitano–
Application of the Diffraction Technique in Solid State Chemistry from
"ab-initio" Structure Solution to Final Structure Refinement
–Powder and Single Crystal–
Doctoral Thesis in Sciences and Chemical Technology, XXIV cycle
University of Sassari

Pag. 87
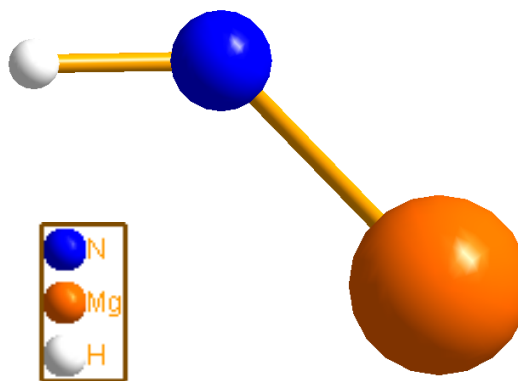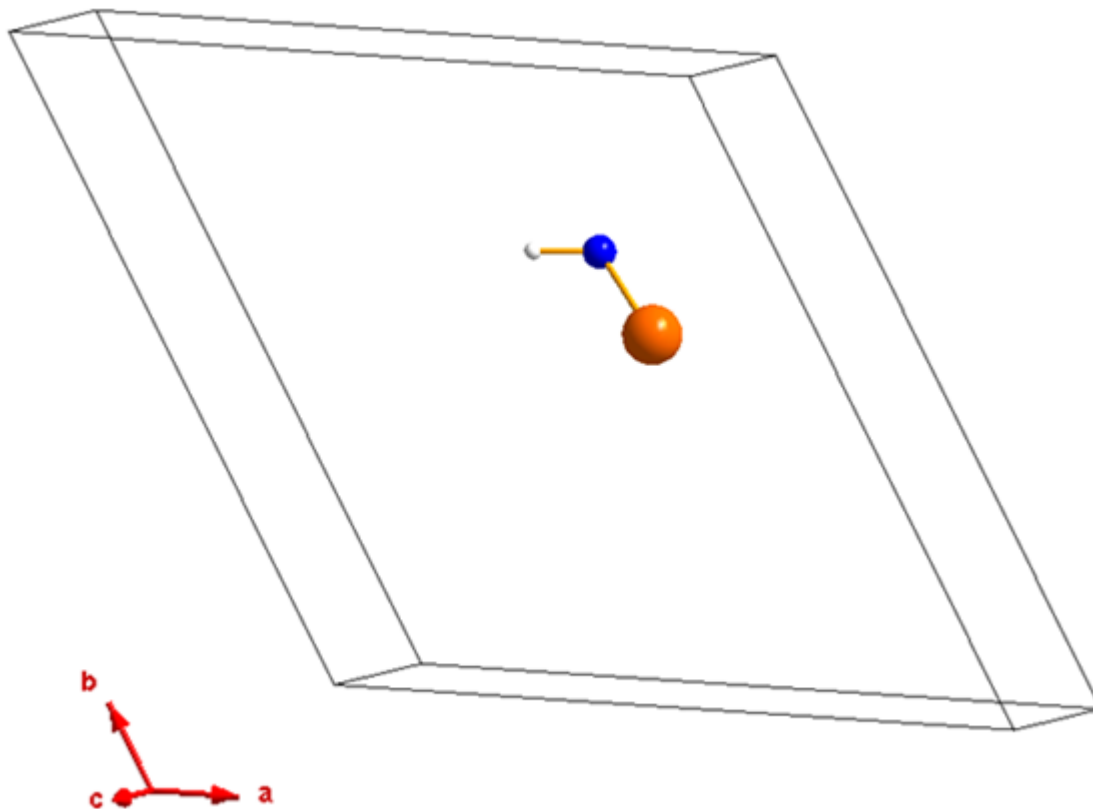
Figure 3. Fragment inside the hexagonal cell.

Integrated intensity values vs Bragg peak positions and cell constants have been imputed in Endeavour, kept them fixed and equal to the values obtained through the previous profile analysis. Starting from P1 and then for each Space Group the simulated annealing runs were carried out, defining as optimizable parameters the corresponding six positional-orientational degrees of freedom (x, y, z and θ, φ, ψ) of the molecular fragment and the intensity scale parameter. The calculus has been performed using a simple repulsion potential.

Starting from a random configuration of the rigid body inside the cell, the SA algorithm was able to calculate a powder diffraction columnar profile and to compare it with the experimental one.

−Emilio Napolitano–
Application of the Diffraction Technique in Solid State Chemistry from
"ab-initio" Structure Solution to Final Structure Refinement
−Powder and Single Crystal–
Doctoral Thesis in Sciences and Chemical Technology, XXIV cycle
University of Sassari

Pag. 88

The first structure optimization run in P1 symmetry slowly converged in a structure solution in P6/m space-group with an interesting figure of merit.

For overcoming the difficulty to attribute the correct symmetry to the unknown material and so to be sure of the goodness of the structure model, all the successive SA runs have been performed inputting the interested one, in this manner the processing rate increase drastically and all the possible solution have been explored.

The profile weighted index R-factor% and the Cost-Function showed which structure solutions were interesting and which were rather to reject.

Space Group	R-factor %	Cost function	CF-balance	seed
P6	35.73	1.10201	0.5	5
P$\bar{6}$	58.44	2.32585	0.5	2
P6/m	**34.28**	**0.99367**	**0.5**	**2**
P6/m ref.	**20.22**	**0.66075**	**0.5**	
P622	46.32	1.23	0.5	4
P6$_3$22	33.60	1.26182	0.5	2
P6$_3$22_ref	33.06	1.24197	0.5	
P6mm	40.72	1.50469	0.5	4
P$\bar{6}$m2	62.08	2.52262	0.5	2
P$\bar{6}$2m	69.03	2.49613	0.5	3
P6/mmm	59.53	4.94632	0.5	5
P6$_3$/m	60.38	2.25045	0.5	6
P63	32.97	1.09950	0.5	2

Table 4.Rwp e Cost-function of structure optimization in hexagonal crystal system.

–Emilio Napolitano–
Application of the Diffraction Technique in Solid State Chemistry from
"ab-initio" Structure Solution to Final Structure Refinement
–Powder and Single Crystal–
Doctoral Thesis in Sciences and Chemical Technology, XXIV cycle
University of Sassari

Pag. 89

Space Group	R-factor %	Cost function	CF-balance	seed
P3	28.47	0.96716	0.5	5
P3_ref	27.00	0.96716	0.5	
P$\bar{3}$	27.43	0.83364	0.5	2
P$\bar{3}$_ref	26.39	0.7937	0.5	
P312	37.91	1.22006	0.5	4
P321	36.95	1.23738	0.5	5
P3m1	37.95	1.26024	0.5	5
P31m	39.60	1.34615	0.5	5
P$\bar{3}$1m	48.68	1.44263	0.5	1
P$\bar{3}$m1	39.77	1.53191	0.5	1

Table 5. Rwp e Cost-function of structure optimization in trigonal crystal system.

The best solution was the first performed starting from a P1 space group and finishing with P6/m one. Other interesting results came out from the trigonal crystallographic system, with symmetry P3 and P-3. All the three best results have been refined and the solution in P6/m was confirmed the best one.

The Rietveld refinement has been performed using Maud software.
Starting from the previously determined back-ground and profile parameters, microstructural, structural and iso-displacement atomic parameters have been refined up to the convergence.

For the refinement of the structure with the two X-ray synchrotron patterns, D atom positions have been fixed and their B-factors with a constant value of 3.0 $Å^2$.

The structure solution of the Imide has been confirmed as a hexagonal crystal system, with space group P6/m, with 12 MgNH units inside the unit cell (Fig. 4).

–Emilio Napolitano–
Application of the Diffraction Technique in Solid State Chemistry from
"ab-initio" Structure Solution to Final Structure Refinement
–Powder and Single Crystal–
Doctoral Thesis in Sciences and Chemical Technology, XXIV cycle
University of Sassari

Pag. 90

No polymorph transition has been observed between the sample cooled up to 100K and the same at room temperature.
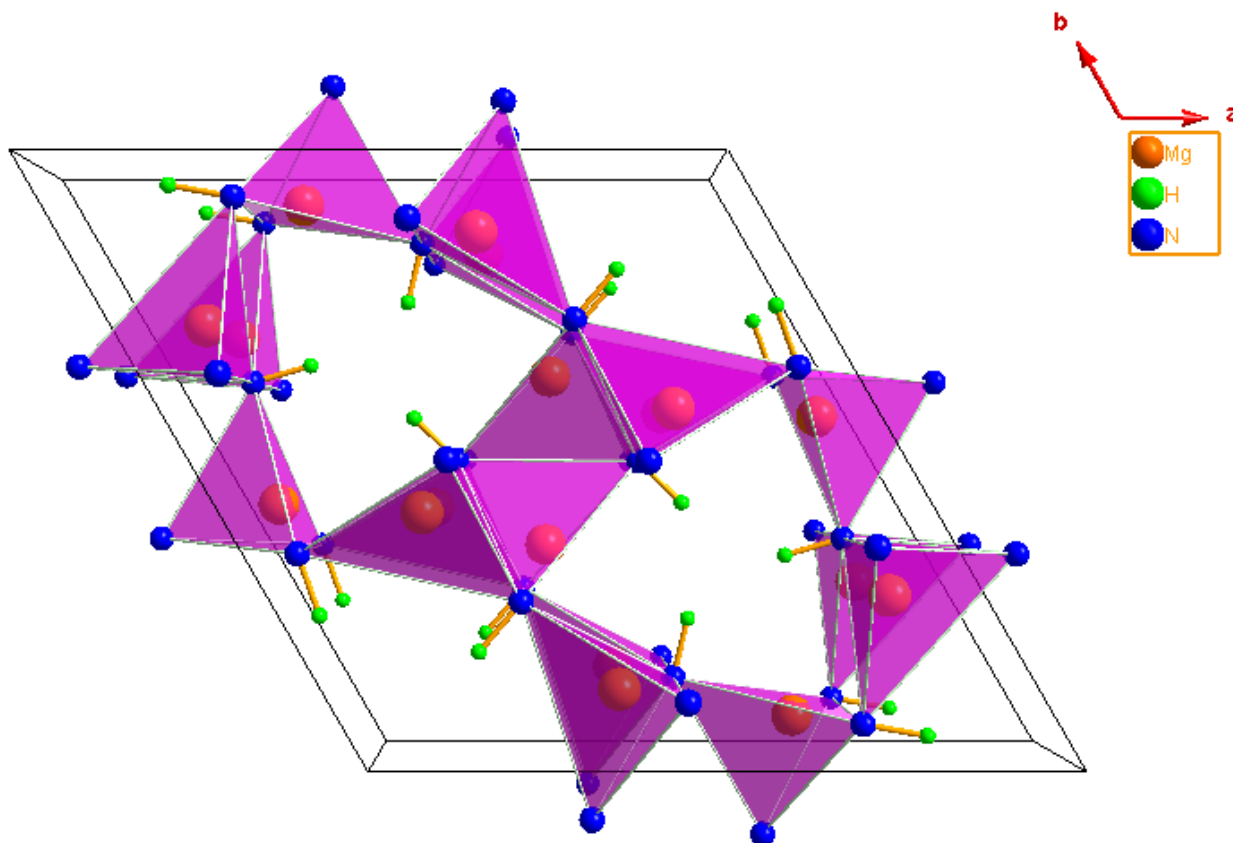
Figure 4 . Imide unit cell content view.

Light difference on bond length, angles and lattice parameters have been found, caused of course for the different temperature and for the two different sources used, synchrotron and neutron (Table 7)

−Emilio Napolitano–
Application of the Diffraction Technique in Solid State Chemistry from
"ab-initio" Structure Solution to Final Structure Refinement
−Powder and Single Crystal–
Doctoral Thesis in Sciences and Chemical Technology, XXIV cycle
University of Sassari

Pag. 91

Pattern	Rwp%	Rp	GoF	a	b	c	d/gcm^{-1}
Neutron_RT	3.0084	2.1049	2.3120	11.5807(8)	11.5807(8)	3.6814(1)	1.8324
Syncr_RT	1.9962	1.5107	2.0708	11.5709(1)	11.5709(1)	3.6803(8)	1.8360
Syncr_100K	5.6159	4.2414	1.8033	11.5685(2)	11.5685(2)	3.6799(4)	1.8370

Table 6. Rietveld values refinement, cell constant parameters show a decreasing trend to room temperature up to 100K, in opposite direction the density values.

The structure appears borden-line between meso and macro porous, hexagonal cavities with N-N diameter distance around 7.34(5) Å and triangular one N-N distance around 5.86(8) Å (Figure.1) are persent. The deuterium atoms are located inside these channels pointing to the center.
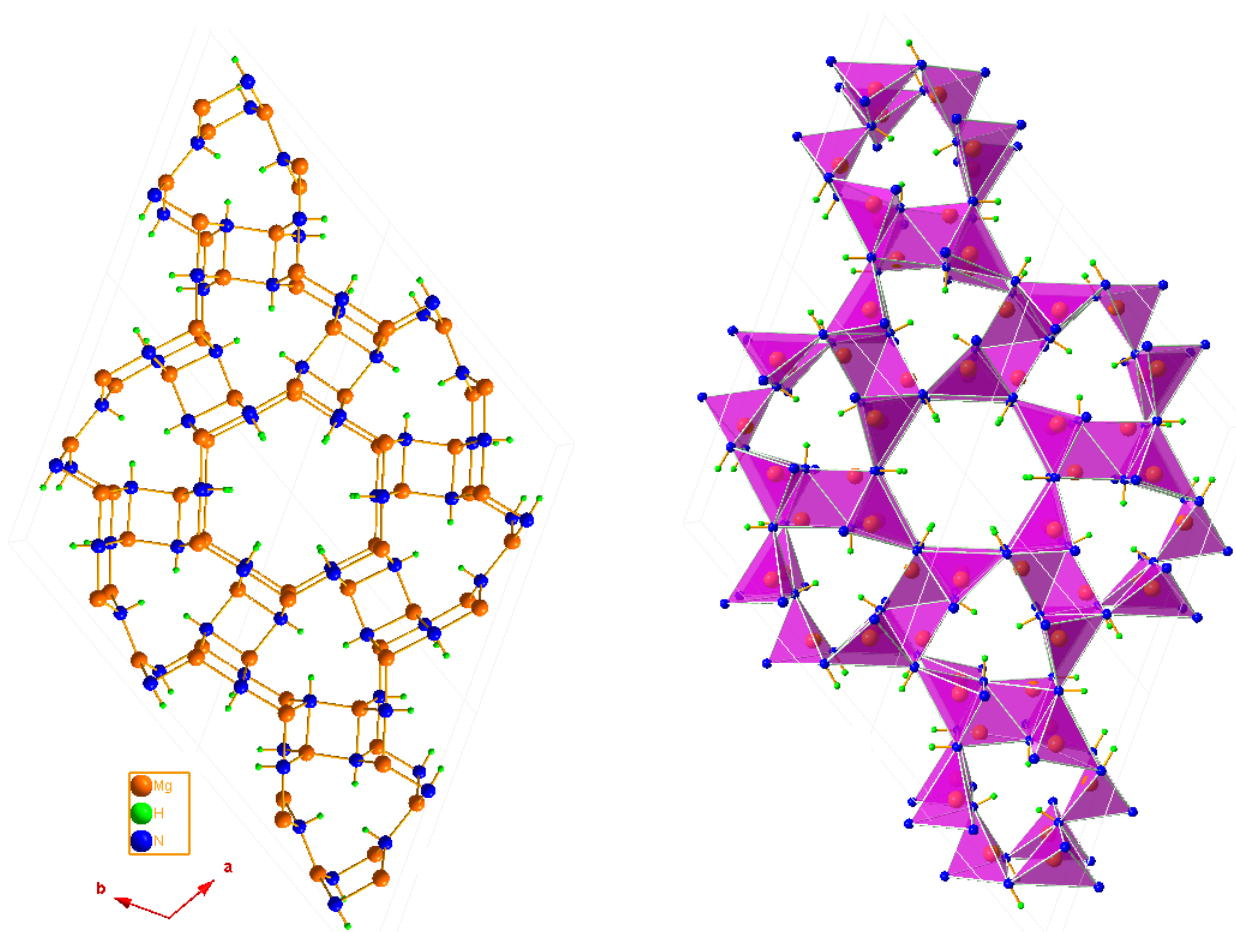
Figure 5. A sketch of the imide structure with hexagonal and triangular cavities showing the deuterium atoms pointing to the center of each hole.

−Emilio Napolitano−
Application of the Diffraction Technique in Solid State Chemistry from
"ab-initio" Structure Solution to Final Structure Refinement
−Powder and Single Crystal–
Doctoral Thesis in Sciences and Chemical Technology, XXIV cycle
University of Sassari

Pag. 92

The deuterium atoms are located inside the channels, and the N-H bonds length show different values, around 0.98618(1) Å to 1.0178(1) Å inside the triangular cavities, and from 1.0250(2) Å to 1.0476(2) Å in the hexagonal ones (table 7.)

Neutron-298K	Length Å	angle	Synchrot-298K	Length Å	angle	Synchrot 100K	Length Å	angle
N-H$_T$	0.98618(1)	----	N-H$_T$	0.972(1)	----	N-H$_T$	1.0178(1)	----
N-H$_H$	1.0250(2)	----	N-H$_H$	1.0554(2)	----	N-H$_H$	1.0476(2)	----
Mg-N$_T$	2.0947(1)	----	Mg-N$_T$	2.1094(2)	----	Mg-N$_T$	2.0873(0)	----
Mg-N$_H$	2.0751(1)	--------	Mg-N$_H$	2.0677(2)	----	Mg-N$_H$	2.0662(1)	----
Mg-N-H$_T$	----	97.237(1)°	Mg-N-H$_T$	----	97.511(2)°	Mg-N-H$_T$		96.335(1)°
Mg-N-H$_H$	----	116.753(2)°	Mg-N-H$_H$	----	116.142(2)°	Mg-N-H$_H$		116.153(1)°

Table 7. Principle bonds length and angle for the Imide crystal structure (Neutron, Synchrotron at room and 100K)

The magnesium ions are surrounded by 4 N atoms, in a sort of distorted tetrahedral coordination (Figure 5) with Mg-N distances ranging from 2.07(1) Å to 2.14(9) Å; slightly longer than in magnesium amide and magnesium nitride. The minimum Mg-Mg distance is found for the edge sharing MgN$_4$ tetrahedral and is around 2.70(9) Å; similar to the shortest Mg-Mg distance in magnesium nitride, rather than the one reported for magnesium amide (around 3.40 Å).

The nitrogen atom shows two different coordination environment, always surrounded by four magnesium atoms and one hydrogen but with different geometry conformation (Figure 6).

The coordination sphere of both the nitrogen atoms distorted trigonal bipyramid, but the difference is on its base, one has two magnesium atoms on the equatorial plane and one deuterium pointing to the hexagonal cavity (Figure 6_1), and the other nitrogen has on the equatotial plane three magnesium (Figure 6_2) atoms and the deuterium in apical position, pointing to the triangular cavity.

–Emilio Napolitano–
Application of the Diffraction Technique in Solid State Chemistry from
"ab-initio" Structure Solution to Final Structure Refinement
–Powder and Single Crystal–
Doctoral Thesis in Sciences and Chemical Technology, XXIV cycle
University of Sassari

Pag. 93
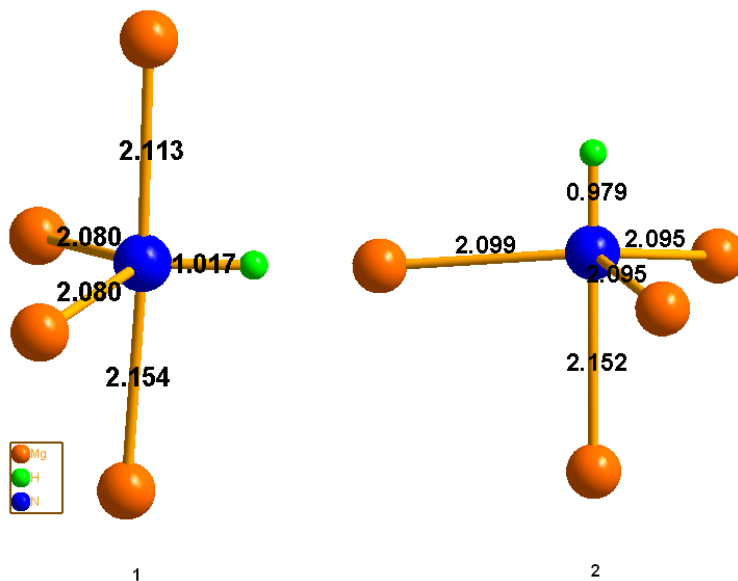
Figure 6. Nitrogen with two different coordination environment.

The nitrogen-deuterium distances are of the order of 1.00 Å well in agreement with other known alkali and alkaline earth imide structures. All the N-H groups point toward the hexagonal and triangular cavities with hydrogen atoms H1 (always connected to N1 atoms) pointing toward the triangular cavities and occupies Wyckoff site k and with hydrogen atoms H2 (always connected to N2 atoms) pointing toward hexagonal cavities occupies the Wyckoff site j (Figure 7.).

−Emilio Napolitano–
Application of the Diffraction Technique in Solid State Chemistry from
"ab-initio" Structure Solution to Final Structure Refinement
–Powder and Single Crystal–
Doctoral Thesis in Sciences and Chemical Technology, XXIV cycle
University of Sassari

Pag. 94
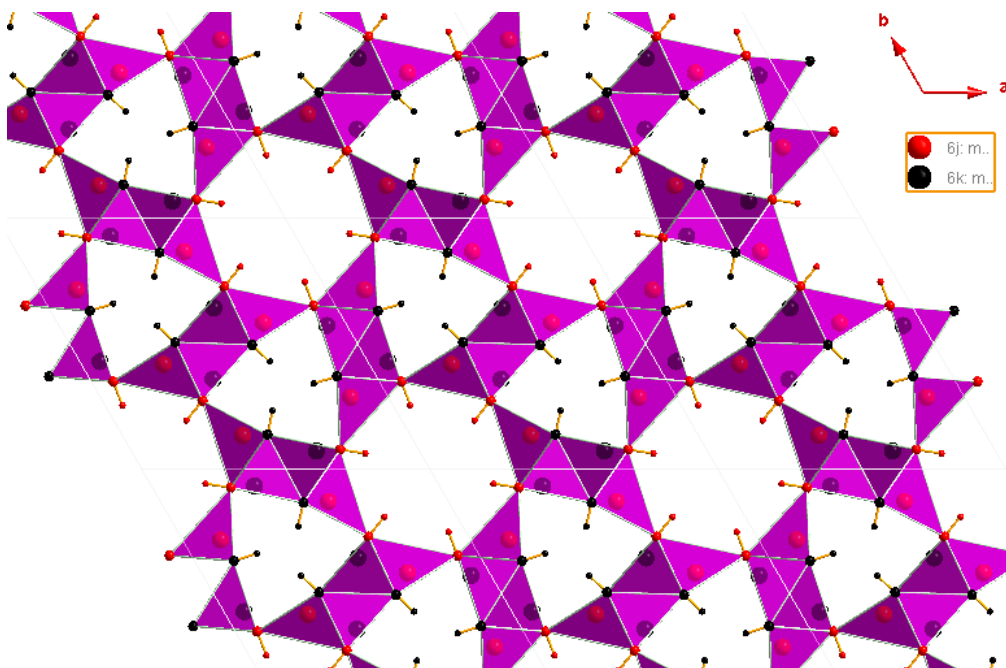
Figure 7. Wyckoff sites occupation

Atom	Wick	x/a	y/b	z/c	B_{Iso} [Å²]
Mg1	6j	0.58627	0.86538	0	0.77(4)
Mg2	6k	0.93004	0.57233	1/2	0.3(4)
N1	6j	0.64992	0.72687	0	0.77(8)
N2	6k	0.49553	0.86208	1/2	0.14(3)
D1	6j	0.94187	0.74909	0	3.0
D2	6k	0.42855	0.76782	1/2	3.0

Table 8. Atomic coordinate Imide 298K Synchrotron source

Atom	Wick	x/a	y/b	z/c	B_{Iso} [Å²]
Mg1	6j	0.584(6)	0.8677(7)	0	0.8(1)
Mg2	6k	0.9285(7)	0.5721(6)	1/2	0.9(1)
N1	6j	0.6517(4)	0.7279(4)	0	0.68(7)
N2	6k	0.4954(4)	0.8633(4)	1/2	1.02(7)
D1	6j	0.9402(6)	0.745(6)	0	2.3(1)
D2	6k	0.9402(6)	0.745(6)	1/2	3.1(2)

Table 9. Atomic coordinate Imide 298K Neutron source

Atom	Wick	x/a	y/b	z/c	B_{Iso} [Å²]
Mg1	6j	0.58359	0.86702	0	0.3(5)
Mg2	6k	0.93153	0.57369	1/2	0.46(6)
N2	6j	0.65097	0.72686	0	0.01(1)
N1	6k	0.49823	0.86668	1/2	0.5(1)
D2	6j	0.94187	0.74909	0	3.0
D1	6k	0.42855	0.76782	1/2	3.0

Table 10. Atomic coordinate Imide 100K Synchrotron source

−Emilio Napolitano−
Application of the Diffraction Technique in Solid State Chemistry from
"ab-initio" Structure Solution to Final Structure Refinement
−Powder and Single Crystal–
Doctoral Thesis in Sciences and Chemical Technology, XXIV cycle
University of Sassari

Pag. 95

Conclusion

The magnesium imide structure has been solved ab-initio after about forty years since its first synthesis reported by Juza and Jacobs.

A key role during the solution was the chemical knowledge of stoichiometry and reaction pathway. While the indexing step was carried out straightforwardly the recognition of the space group was elusive and this may account for the long time before it final solution.

We should also say that even recent DFT computations alone could not solve unambiguously this problem. One other key step was to insert MgND molecule having a no linear atomic disposition. The availability of neutron plus synchrotron radiation patterns made the rest.

Reference

1. R. Juza. Z. anorg. allg. Chem. 409, 199-214 (1974)
2. Von H. Jacobs und R. Juza. Zeitschrift fur anorganische und allgemeine Chemie. Band 370. 1969.
3. M. Lappert, P. Power, A. Protchenko, A. Seeber   Metal Amide Chemistry; Wiley: New York, 2009
4. http://ie.jrc.ec.europa.eu/
5. http://www.ill.eu/instruments-support/instruments-groups/instruments/d20/
6. http://www.esrf.eu/UsersAndScience/Experiments/MaterialsScience/ID31/
7. A. Le Bail, Powder Diffraction 19 (2004) 249-254.
8. Werner, P. E., Eriksson, L. & Westdahl, M. *J. of Appl.Cryst.*(1985) 18, 367–370.
9. Visser, J. W. *J. of App. Cryst.* (1969). 2, 89–95
10. Altomare, A., Giacovazzo, C., Guagliardi, A.,Moliterni, A. G. G., Rizzi, R. &Werner, P.-E. (2000). *J. of Appl. Cryst.*, 33, 1180–1186.
11. Ali Boultif and Daniel LoueÈr J. Appl. Cryst. (2004). 37, 724-731.

–**Emilio Napolitano**–
Application of the Diffraction Technique in Solid State Chemistry from
"ab-initio" Structure Solution to Final Structure Refinement
–**Powder and Single Crystal**–
Doctoral Thesis in Sciences and Chemical Technology, XXIV cycle
University of Sassari

Pag. 96

12. Le Bail, Duroy and Fourquet, *Mater. Res. Bull*., 1988, 23, 447-452

13. R. Cerny´ and V. Favre-Nicolin. (2007). Z. Kristallogr. 222, 105.

14. http://www.crystalimpact.com/endeavour/

15. H. Putz, J. C. Schon and M. Jansen, J. Appl. Crystallogr., 1999, 32, 864.

–Emilio Napolitano–
Application of the Diffraction Technique in Solid State Chemistry from
"ab-initio" Structure Solution to Final Structure Refinement
–Powder and Single Crystal–
Doctoral Thesis in Sciences and Chemical Technology, XXIV cycle
University of Sassari

Pag. 97

B48 boron-based compound structure solution.

The structure determination of the compound named B48 was a real challenge because we had to work the solution from a pattern due to a complex mixture of phases.

The subject has been developed within the context of a European project leaded by the Chemistry Department of the University of Turin (Italy), involving various foreign partners, in particular the GKSS Institution at Geesthacht (Germany). The search for an efficient hydrogen storage-and-release process was considering the class of reactive hydrogen composites (RHC)[1,2,3] based on sodium-boron-hydrides as the challenge of the project.

Experimental

The synthetic route of the process was to react $NaH + MgB_2$ under excess of H_2 at high P and T in order to obtain hydrides able decompose easily to the reactants again. The profitability of the process lies in its low temperature of decomposition.

The powder analyzed was multi-phase to the point that four compounds were identified in the sample plus further un-indexed peaks following the reaction[3]:

1) $NaH + MgB2$ (excess of H_2 at high P and T) $\rightarrow NaBH_4 + NaMgH_3 +$ other unknown peaks
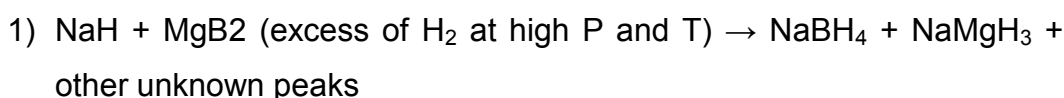
This course of the reaction has been duplicated in two different laboratories Turin[4] and Geesthacht[5].

In Figure 1 we report the powder patterns collected at Turin and Geesthacht for reaction 1 conducted under 50 bar of H_2 at 300 °C. Efforts to examine a third pattern collected at the synchrotron source for the same purposes have revealed Geesthacht inadequate.

–Emilio Napolitano–
Application of the Diffraction Technique in Solid State Chemistry from
"ab-initio" Structure Solution to Final Structure Refinement
–Powder and Single Crystal–
Doctoral Thesis in Sciences and Chemical Technology, XXIV cycle
University of Sassari

Pag. 98
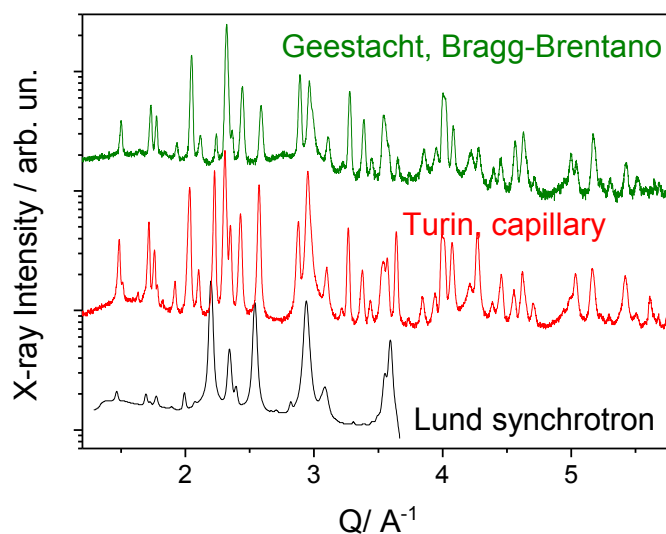
Figure 1. Comparison among patterns taken with conventional apparatuses and at a synchrotron source (bottom pattern) for the products of reaction (1). It is clear that the collection strategy must be carried out coherently to the problem in hand. Note the Q scale $4(\pi/\lambda) \cdot \sin\vartheta$ in order to carry out a one-to-one comparison of pattern taken using a different constant wavelength. The patterns of Geesthacht and Turin were collected with the same instrument (Pananalytical) but the specimen holders were a plate support and a capillary in the two cases, respectively.

As we said both patterns of Turin and Geesthacht show the presence of NaH, MgB_2, $NaMgH_3$ and $NaBH_4$ with extra unindexed peaks, having approximately the same sequence.

Nevertheless, it seems worth to point out some slight differences between the two experiments.

Data processing

A relatively easy identification of the four phases was possible with the pattern acquired by the Turin group using the Search-Match procedure. From analysis of the peak positions and from whole powder-pattern fitting the lattice parameters of the four phases turned out to be those reported in the literature at room

−**Emilio Napolitano**−
Application of the Diffraction Technique in Solid State Chemistry from
"ab-initio" Structure Solution to Final Structure Refinement
−**Powder and Single Crystal**−
Doctoral Thesis in Sciences and Chemical Technology, XXIV cycle
University of Sassari

Pag. 99

temperature, without significant zero-shift of the 2θ scale of abscissa. The correct alignment is granted by the capillary centered in the beam.

The same result could be retrieved from the Geesthacht pattern only after shifting the 2θ-scale of a value 0.20°. This was due to a misalignment of the sample holder with respect to the Bragg-Brentano parafocussing geometry.

However, as it can be seen from the patterns proposed again in Fig. 2, the sample prepared in Geesthacht shows a limited presence of NaH with respect to that prepared in Turin. Whether this simplification occurred by chance or not, the pattern of Geesthacht may be more appealing for the scope of indexing the peaks not covered by the known phases, once its "zero-shift" is removed correctly and the contribution of other phases are eliminated from the pattern.

Before to start the indexing step, a qualitative analysis of powder X-ray pattern has been performed.

Pre-processing data before starting the search match was executed: subtraction of background and $K\alpha_2$ stripping with Rachinger method, data smoothing were avoided because of the good signal/noise ratio of the experimental pattern. The peaks position found with the "second derivate method", created a list of 2θ Bragg-reflections with no sufficient precision on the 2θ value. Using all the classical indexing softwares, TREOR[6], ITO-15[7] and DICVOL06[8] generated very poor outputs due to the approximated peak location.

For overcoming this trouble the Maud-software[9] has been run for finding more reliable 2θ values for the peaks.

In practice the peak-positions have been obtained by the second derivate approach, and then they have been refined with a least-square method with a Le Bail type approach. The reflection-list generated was input in Dicvol06 and McMaille[9] (Tab.1).

The two softwares converged to the same solution with high figure of merit.

Software	IN	FoM M_{20}	Vol	a/Å	b/Å	c/Å	α	β	γ	Symmetry
McMaille	20	205	390.707	7.3104	7.3104	7.3104	90.00	90.00	90.00	Cub
Dicvol06*	12	166	392.970	7.3246	7.3246	7.3246	90.00	90.00	90.00	Cub
mean-val			391.838	7.3175	7.3175	7.3175	90.00	90.00	90.00	Cub

Table 1. Indexing result-Dicvol06 shows a FoM M_{12}

The 20 d-values created same problems to Dicvol06 software, but reducing them to the 12 judged unambiguous in the difference pattern conducted finally reliable cell parameter of a primitive cubic sequence.

The Whole-Powder Pattern Indexing approach[10,11], implemented in Maud-software[9], was used to validate the lattice constants obtained. This method does not need any peaks-list[11,12,13], it uses a the Genetic Algorithm, based on the exploration of the hypersurface {a,b,c,α,β,γ} describing the cell until to find the minimum Rw(a,b,c,α,β,γ) value. This approach works similar to McMaille, but it makes use of the experimental pattern instead of a hypothetical synthetic powder profile where the intensity value is given only in correspondence of a $2\theta_{hkl}$.

The genetic algorithm is based on evolutionary principles, in which the best member of a population, trial lattice parameters {a, b, c, α, β, γ}, has allowed to evolve through several generations, using the evolutionary operations of coupling, mutation and natural selection until to converge to the global minimum R_w(a, b, c, α, β, γ).

−Emilio Napolitano−
Application of the Diffraction Technique in Solid State Chemistry from
"ab-initio" Structure Solution to Final Structure Refinement
−Powder and Single Crystal−
Doctoral Thesis in Sciences and Chemical Technology, XXIV cycle
University of Sassari

Pag. 101
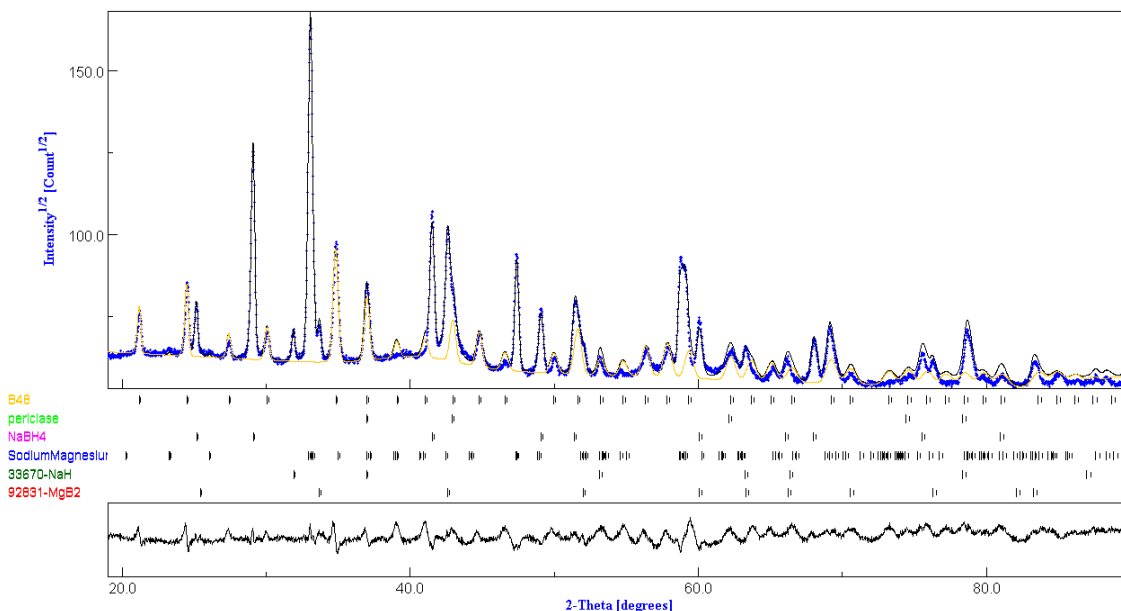
Figure 2. Whole Powder Pattern Indexing in cubic crystal system. The yellow curve is calculated on the basis of a cubic sequence.

Rwp(%)	a/Å	b/Å	c/Å	α	β	γ	Symmetry
6.432774	7.3251104	7.3251104	7.3251104	90.00	90.00	90.00	Cub
8.095087	5.174627	5.174627	5.174627	90.00	90.00	90.00	Cub
8.569465	7.3246	7.3246	7.3246	90.00	90.00	90.00	Cub
9.275568	3.6570878	3.6570878	3.6570878	90.00	90.00	90.00	Cub
12.43702	7.3175	7.3175	7.3175	90.00	90.00	90.00	Cub

Table 2. Whole Powder Pattern Indexing in cubic crystal system. The solution to check on the basis of the agreement factor is dependent upon the user, but the lattice parameter of 7.325 A is the first to consider in the proposed list.

Cubic tetragonal and orthorhombic cells were explored with such method, for each crystal system the starting population was divided in many non-overlapping sub-populations, running in parallel-independent tasks.

The indexing has been confirmed for a cubic crystal system with lattice parameter a=7.326 (2) Å and R_{wp} = 6.51%.(Fig.2; Tab 2)

−**Emilio Napolitano**−
Application of the Diffraction Technique in Solid State Chemistry from
"ab-initio" Structure Solution to Final Structure Refinement
−**Powder and Single Crystal**−
Doctoral Thesis in Sciences and Chemical Technology, XXIV cycle
University of Sassari

Pag. 102

The tetragonal, hexagonal and orthorhombic outputs have been discarded because of high R_{wp} values.

The lattice parameters have been refined with a Le Bail fit[13] until a convergence to a = 7.319 Å (Fig. 3).
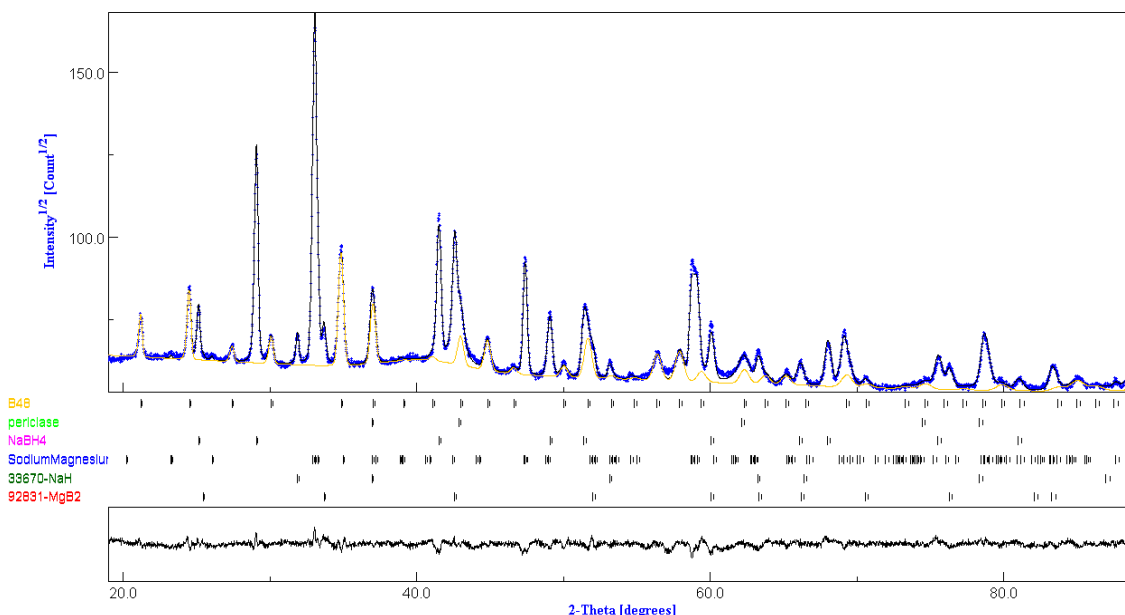
Figure 3. Whole powder pattern indexing, convergence achieved with only one Le Bail fit iteration.

The relatively short lattice parameters suggest to start with the space group P23. From the stoichiometry of the reaction and taking in consideration the phases present in the sample, a phase with a single element was hypothesized that can be likely boron. In facts, from the reactants NaH+MgB2 under H_2, we can hypothesize in a sort of collision theory that a molecule of NaH reacts with MgB_2 and H_2 to give stable $NaBH_4$ but depleting the original crystallite of MgB_2 to unstable fraction of MgB, ready to react with further NaH and H_2 to give $NaMgH_3$. This second reaction leaves boron atoms that can aggregate and grow in microcrystals. It is also possible that parallel the NaH reacts with MgB_2 to create a $NaMgH_3$ first leading in this case to 2 Boron atoms that can aggregate in a sort

−Emilio Napolitano−
Application of the Diffraction Technique in Solid State Chemistry from
"ab-initio" Structure Solution to Final Structure Refinement
−Powder and Single Crystal−
Doctoral Thesis in Sciences and Chemical Technology, XXIV cycle
University of Sassari

Pag. 103

of competitive chain reaction. These two competitive reactions (the first consecutive and the second direct) are responsible for the formation of the two hydrides but inestricably lead to free boron which is likely to occur separately. From literature we have at least four boron structures, namely:

1) "An accurate refinement of the beta-rhombohedral boron structure", Acta Cryst B, (1977), 33, 1951-1954, the habit is reported with S.G R-3m n. 166 in IT, density = 2.21 g/cc; a = 10.9251(2) Å b = 10.9251(2) Å, c = 23.8143(8) Å , γ = 120°. The same pattern is obtained with data reported in Phase Transition (1992), 38, 127-220 where density is 2.28 g/cc, lattice parameters a = b = c = 10.17 Å and $\gamma = 65.12°$, the unit cell volume is 1/3 of the previous value. This structure was the subject of a further article by Kolakowski where the reported density is 2.35 g/cm^3. However, some B-B distances are calculated to be 1.16 Å, the unrealistic values suggesting occupation factors reduced to 0.5 for some Wyckoff sites. This of course implies a correction for the total density value.

2) "The structure of tetragonal boron", Journal of the American Chemical Society (1958), 80, 4507-4515, Space Group P42/nnm, tP50, density = 2.32 g/cc; a = 8.75 Å, c = 5.06 Å;

3) "The crystal structure of a simple rhombohedral form of boron", in Acta Cryst. (1959), 12, 503-506, again S. G. R-3m (hR12), n. 166, a = b = c = 5.057(3) Å α = β = γ = 58.06(5)°; density = 2.46 g/cc;

4) Crystal structure of tetragonal boron related to alpha-Al B12, Journal of Solid State Chemistry (1979), 28, 289-301, a = b = 10.14(1) Å c = 14.17(1) Å, density = 2.34, G. S. P43, tP190

–Emilio Napolitano–
Application of the Diffraction Technique in Solid State Chemistry from
"ab-initio" Structure Solution to Final Structure Refinement
–Powder and Single Crystal–
Doctoral Thesis in Sciences and Chemical Technology, XXIV cycle
University of Sassari

Pag. 104

In summary the density values reported for the boron allotropes range from a lower value of 2.21 g/cm^3 to an upper value of 2.32 g/cm^3. The content inside the cell was realistically estimated to be 48 atoms of boron, for a calculated density of 2.198 g/cm^3.

Integrated intensity values vs Bragg peak positions and cell constants were used as input for Endeavour, kept them fixed and equal to the values obtained through the previous profile analysis. Starting with the P23 space group and a random configuration of the boron atoms inside the cell, the simulated-annealing algorithm run until to converge to a solution with Rw value 7.22 and cost-function 0.84403.

Atom	Wyck	Site	x/a	y/b	z/c	U [Å^2]
B1	12j	1	0.50640	0.24240	0.10380	1.1000
B2	12j	1	0.23330	0.76180	0.01560	1.1000
B3	12j	1	0.36480	0.44630	0.24650	1.1000
B4	12j	1	0.23270	0.60360	0.14940	1.1000

Table 3. Endeavour structure solution obtained for the suspected "Boron" cubic phase. The simulated annealing process confirmed the P23 Space group, 48 atoms in the cell distributed in four 12j Wyckoff sites

A parallel computation with the P23 space group was performed with Maud, using the experimental pattern instead of simplified columnar powder profile like in Endeavour.

The global optimization has been performed using the Hybrid Algorithm implemented in Maud-software. Lattice constants and profile parameters obtained with the previous Le Bail fit have been kept fixed and boron atoms have been inserted in random general (x, y, and z) positions.

Choosing the population size and the number of generation, the algorithm has able to select the individuals with the best genome (new x,y,z coord. atom,

–Emilio Napolitano–
Application of the Diffraction Technique in Solid State Chemistry from
"ab-initio" Structure Solution to Final Structure Refinement
–Powder and Single Crystal–
Doctoral Thesis in Sciences and Chemical Technology, XXIV cycle
University of Sassari

Pag. 105

intensity computed), so the population evolves based on evolutionary rules and a fitness criteria based on R_w.

The computation converged until a R_w = 4.610% and a W_{ss} = 35770.8808

Atom	Wyck	x/a	y/b	z/c	U [Å²]
B1	12j	0.73642	0.63309	0.97086	1.0
B2	12j	0.50224	0.71560	0.74838	1.0
B3	12j	0.78270	0.09555	0.40051	1.0
B4	12j	0.94695	0.26399	0.86837	1.0

Table 4. Maud structure solution for space group P23 after fixing the cell constant and attributing the 48 atomic boron general positions in Wyckoff sites 12j.

The observed reflections were compatible with the P23 space group, but also with the Pm3, P432, Pm3m and P43m. Le Bail fit has been performed and the outputs are very close to the primitive one. These values are expected because of the reflections are completely overlapped at identical Bragg angles.

The structure solutions have been performed for these space groups but the R_w were higher than the previous solution, and the chemical structures had a no chemical sense.

As it was mentioned earlier, the observed reflections were compatible also with the Pa-3 space group. Again, Maud was run to search a solution within this space group and returned a sensible solution in terms of two general positions in Wyckoff sites with multiplicity 24(d).

Atom	Wyck	Site	x/a	y/b	z/c	U [Å²]
B1	24d	1	0.15749	0.45779	0.81197	1.0
B2	24d	1	0.66497	0.04035	0.73108	1.0

Table 5. Atomic parameter for the structure solution in Pa-3 space group.

–Emilio Napolitano–
Application of the Diffraction Technique in Solid State Chemistry from
"ab-initio" Structure Solution to Final Structure Refinement
–Powder and Single Crystal–
Doctoral Thesis in Sciences and Chemical Technology, XXIV cycle
University of Sassari

Pag. 106

This solution may be appealing because the number of positional variables are reduced to 6 with respect to the previous description under P23 needing 12. Nevertheless, the definite checking of this ambiguity would eventually come from a Rietveld refinement, corroborated by an analysis of the interatomic distances.

The two structures in P23 space group were then imported in Maud[9] for the least-square global refinement.

Structural, microstructural and scale factor parameters for each phase component the sample under the isotropic displacement assumption have been refined. The least squared fit converged quickly to low residuals for each approach here considered.

B48	Rwp%	Rp%	Rwpb%	Rpb%	GoF	d/gcm^{-1}
Endeavour	3.03467	2.38442	3.76229	2.90212	1.940	2.1978
Maud	3.02955	2.37882	3.71769	2.87902	1.938	2.1977

Table 6. Rietveld refinement parameters comparison between Endeavour and Maud crystal models.

−Emilio Napolitano–
Application of the Diffraction Technique in Solid State Chemistry from
"ab-initio" Structure Solution to Final Structure Refinement
–Powder and Single Crystal–
Doctoral Thesis in Sciences and Chemical Technology, XXIV cycle
University of Sassari

Pag. 107

	Phase	Wt%	sd %	a	b	c	Crystallite Å	sd%
Endeavour	B48	62.6	19.0*	7.3191(9)	7.3191(9)	7.3191(9)	Val>2000	~10
	NaMgH$_3$	13.0	4.0	5.4706(6)	7.7091(1)	5.4187(3)	Val>2000	"
	NaBH$_4$	12.8	4.0	6.1789(5)	6.1789(5)	6.1789(5)	1642.5	"
	MgB$_2$	7.6	2.3	3.7622(9)	3.7622(9)	3.0884(9)	575.6	"
	Periclase	3.2	1.0	4.2356(4)	4.2356(4)	4.2356(4)	150.0	"
	NaH	0.8	0.2	4.8899(5)	4.8899(5)	4.8899(5)	1526.1	"
Maud-HR	B48	62.4	0.7	7.3192(1)	7.3192(1)	7.3192(1)	Val>2000	~10
	NaMgH$_3$	12.9	0.1	5.4706(4)	7.7091(3)	5.4187(6)	Val>2000	"
	NaBH$_4$	12.8	0.1	6.1789(6)	6.1789(6)	6.1789(6)	1546.6	"
	MgB$_2$	7.7	0.1	3.0885(1)	3.0885(1)	3.5284(6)	561.4	"
	Periclase	3.2	0.1	4.2352(2)	4.2352(2)	4.2352(2)	150.0	"
	NaH	0.8	0.4	4.8899(2)	4.8899(2)	4.8899(2)	1435.5	"

Table 7. Quantitative Rietveld analysis for both the inputted models. The so higher sd % for the B48 (Endeavour) could be compatible with an software bug.
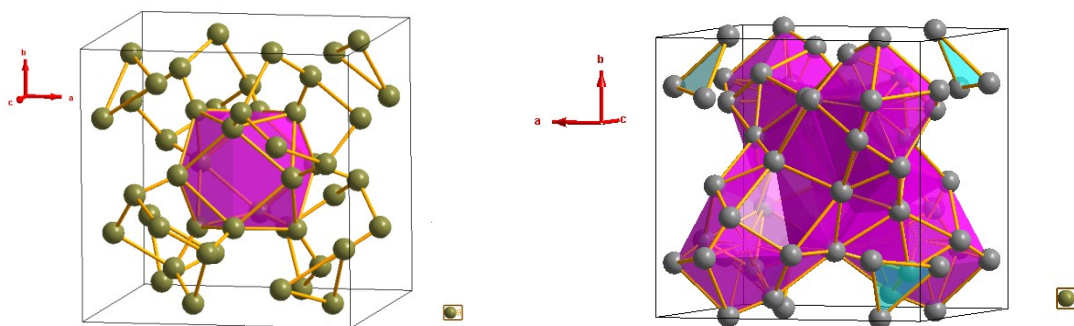
Figure 4. Maud Structural models after Rietveld refinement and Endeavour. The atomic arrangement in the both solution is very close but the solution with MAUD appears to have converged to a configuration with a dodecahedron-like core usual in Boron-based structures.

−Emilio Napolitano–
Application of the Diffraction Technique in Solid State Chemistry from
"ab-initio" Structure Solution to Final Structure Refinement
−Powder and Single Crystal–
Doctoral Thesis in Sciences and Chemical Technology, XXIV cycle
University of Sassari

Pag. 108

Conclusion

Waiting for a better synthesis pathway to obtain a single phase and a better data collection up to high 2θ values for a more confident atomic-position determination, the two structural models here obtained (S.G. P23), on the hypothesis of a Boron phase with 48 atoms inside the unit cell, are the most plausible ones. In facts they give sensible interact distances of 1.65 Å also found in other boron allotropes.

References

1. D. Pottmaier, C. Pistidda, E. Groppo, S. Bordiga, G. Spoto, M. Dornheim, M. Baricco. International J. of Hydrogen Energy 36 (2011) 7891-7896

2. S. Garroni, C. Milanese, A. Girella, A. Marini, G. Mulas, E. Menéndez, C. Pistidda M. Dornheim, S. Suriñach, M.D. Baro´. International J. of Hydrogen Energy 35 (201 0) 5434-5441.

3. Pistidda, C.; Garroni, S.; Minella, C. B.; Dolci, F.; Jensen, T. R.; Nolis, P.; Bosenberg, U.; Cerenius, Y.; Lohstroh, W.; Fichtner, M.; Baró, M. D.; Bormann, R. d.; Dornheim, M.,. The J. of Physical Chem. C, 2010, 114, (49), 21816-21823.

4. Dipartimento di Chimica IFM, NIS Centre of Excellence, Universita` di Torino, Via Pietro Giuria, 7/9, I-10125 Turin, Italy.

5. Institute of Materials Research, GKSS Research Centre Geesthacht GmbH, Max-Planck-Straße 1, D-21502 Geesthacht, Germany.

6. Werner, P. E., Eriksson, L. & Westdahl, M. J. of Appl.Cryst.(1985) 18, 367–370.

7. Visser, J. W. J. of App. Cryst. (1969). 2, 89–95

–Emilio Napolitano–
Application of the Diffraction Technique in Solid State Chemistry from
"ab-initio" Structure Solution to Final Structure Refinement
–Powder and Single Crystal–
Doctoral Thesis in Sciences and Chemical Technology, XXIV cycle
University of Sassari

Pag. 109

8. Ali Boultif and Daniel LoueÈr J. Appl. Cryst. (2004). 37, 724-731.

9. Maud: Materials Analysis Using Diffraction, version 2.33, 2011, http://www.ing.unitn.it/~maud/

10. A. Le Bail, Powder Diffraction 19 (2004) 249-254.

11. B. M. Kariuki, S. A. Belmonte, M. I. McMahon, R. L. Johnston, K. D. M. Harris & R. J. Nelmes. J. Synchrotron Rad. 6 (1999) 87-92.

12. European Powder Diffraction Conference (EPDIC 10), Geneva 1-4-Sept-2006.

13. A.Le Bail, H. Duroy, J.L. Fourquet, J. Solid State Chem., (1992), 98, 151.

14. Young, R.A.(1993), The Rietveld Method, Oxford: University Press. (ISBN 0 19 855577 6) Chapter 2.

15. Rietveld,H.M.(1967). Acta Crystallogr.,22,151-2.

16. Rietveld,H.M.(1969). J. Appl. Crystallogr.,2,65-71.

–Emilio Napolitano–
Application of the Diffraction Technique in Solid State Chemistry from
"ab-initio" Structure Solution to Final Structure Refinement
–Powder and Single Crystal–
Doctoral Thesis in Sciences and Chemical Technology, XXIV cycle
University of Sassari

Pag. 110

(-)-10-iodo camphor. $C_{10}H_{15}O$-I structure solution.

The camphor and derivatives compounds have been used from several years as building blocks for the synthesis of chiral auxiliaries in asymmetric catalysis and as ligands in enantioselective synthesis reactions[1,2,3].

In particular, the (-)-10-iodo camphor, easily obtainable from commercial reagents, can be processed in different reactions because it contains an halogen and a carbonyl function, rendering this a versatile chiral auxiliary molecule.

Even if this is a well-known compound in organic synthesis, the crystal structure with the iodine substituent wasn't explored until nowadays.

The (-)-10-iodo camphor powder was gently supplied by Dr. Salvatore Baldino from the Chemistry Department of University of Sassari (Italy) after a work aimed to synthesize an intermediate for further reactions.

Data collection

The diffraction data have been collected on the beamline XRD1[4] at Elettra Synchrotron Light Facility in Trieste (Italy) and on the BM1B[5] High Resolution Powder Diffraction beamline at the European Synchrotron Facility (ESRF) in Grenoble (France). Both the measurements have been performed in transmission geometry with a MarResearch CCD detector at beamline XRD1 (Elettra) and with a scintillator detector on BM1B beamline (ESRF).

The two data collections offer different advantages: the use of two dimensions detector in Elettra allows a fast and simultaneous acquisition of the Debye rings over a wide 2θ range. This involves diffraction data with a better statistics and

–Emilio Napolitano–
Application of the Diffraction Technique in Solid State Chemistry from
"ab-initio" Structure Solution to Final Structure Refinement
–Powder and Single Crystal–
Doctoral Thesis in Sciences and Chemical Technology, XXIV cycle
University of Sassari

Pag. 111

better integrated intensity, simply in a single shot, avoiding any motion of the detector.

On the other hand the use of the scintillator detector at ESRF guarantees a better d-resolution and peak-width.

In both cases the specimen has been gently grinded in an agate mortar and pestle, and loaded in a glass capillary of 0.3 mm of diameter, a capillary spinning was performed during the data acquisition to obtain a better statistics.

A NIST powder standard has been used to calibrate the sample-to-detector distance and to refine instrumental parameters, typically SRM 660a and LaB_6 at Elettra and NIST 640a silicon sample at ESRF respectively, using a pseudo-Voigt peak-shape function for the fitting.

Data processing

The 2D image was processed by integrating the intensities along radial slices every 5°using Maud-software[6] (Lutterotti) [7] creating 72 patterns (Figure 1), intensity vs 2θ.

This allowed the possibility to optimize the centre by tilting the position of the image, the camera radius and to refine the detector distance with the final Rietveld refinement.

–Emilio Napolitano–
Application of the Diffraction Technique in Solid State Chemistry from
"ab-initio" Structure Solution to Final Structure Refinement
–Powder and Single Crystal–
Doctoral Thesis in Sciences and Chemical Technology, XXIV cycle
University of Sassari

Pag. 112
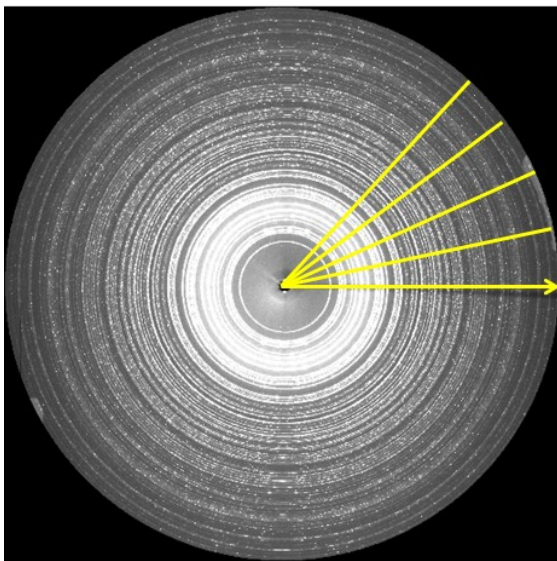
Figure 1. 2D transmission pattern (Elettra), the image has been integrated each 5° from the centre, creating 72 patterns.

This data set was used for the structure solution because of the better statistics and the final least square refinement was performed joining it with the ESRF diffraction pattern analysis procedure.

Before to start the indexing step, a qualitative analysis of X-ray powder pattern has been performed to find and identify possible unexpected compounds affecting the purity of the product.

The sample has been purified several times during the synthesis, nor reactants neither secondary products have been found. Once established that the sample was single phase, the first 20 peaks have been selected for the indexing step and used as input for the classical indexing softwares: McMaille[8], Treor[9], Ito-15[10], N-Treor[11], Dicvol06[12].

All the outputs converged to the same solution as shown by the output collected in the following Table 1.

–Emilio Napolitano–
Application of the Diffraction Technique in Solid State Chemistry from
"ab-initio" Structure Solution to Final Structure Refinement
–Powder and Single Crystal–
Doctoral Thesis in Sciences and Chemical Technology, XXIV cycle
University of Sassari

Pag. 113

Software	IN	FoM M_{20}	Vol	a	b	c	α	β	γ	Symmetry
McMaille	20	84.6	1040.79	10.5022	11.1180	8.9137	90.00	90.00	90.00	ort
ITO-15	19	70.3	1043.73	10.5114	11.1293	8.923	90.00	90.00	90.00	ort
N-Treor	20	60.0	1036.47	10.4864	11.1036	8.9015	90.00	90.00	90.00	ort
Dicvol06	20	26.4	1036.50	10.4892	11.1027	8.9002	90.00	90.00	90.00	ort
Treor 90	18	16	1039.48	10.4956	11.1139	8.9112	90.00	90.00	90.00	ort

Table 1. Indexing results from ESRF pattern, after application of the 5 packages available from the net free-of-charge. IN stay for indexed peaks, FoM for Figure of Merit, Vol for cell volume. Lattice parameters a, b, c, α, β γ, have the usual meaning. No doubt that we are dealing with an orthorhombic system.

Once identified the powder Laue Class mmm, a whole-powder-pattern decomposition[13] has been performed with the primitive group. Lattice parameters and intensities have been refined through a least squares fitting, and the peak positions have been constrained by the unit cell values.

The diffraction patterns showed systematic absence for the rules h00: h=2n+1, 0k0; k=2n+1; 00l: l=2n+1, three sets of mutually perpendicular nonintersecting screw axes have been identified. These observations were compatible with the $P2_12_12_1$ space group.

Pycnometer density measurement of 1.7733 g/cm^3, suggests a number of asymmetric unit Z=4. The exact calculated density is 1.7679 g/cm^3.

The structure solution step has been performed using the 2D pattern, which was statistically representative of the entire sample, because of the geometry of acquisition of the diffraction data. A total of 72 patterns were used to find right position of the atoms inside the cell.

The manipulation of 2D image diffraction data and the structure solution have been performed with the Maud software[6].

–Emilio Napolitano–
Application of the Diffraction Technique in Solid State Chemistry from
"ab-initio" Structure Solution to Final Structure Refinement
–Powder and Single Crystal–
Doctoral Thesis in Sciences and Chemical Technology, XXIV cycle
University of Sassari

Pag. 114

"*A-priori*" chemical information was used, a fragment has been placed inside the cell, in that way a substantial decrease in the number of parameters to be optimized and a speed up in the computation process were obtained.

The C-C, C-H, C=O bonds have an average length of 1.55 Å 1.06 Å and 1.20 Å respectively.

For obtaining a better description of the solid state structure, two objects were entered in random position inside the cell, the fragment $C_{10}H_{15}O$ and the Iodium atom.

Only 9 parameters need an optimization, 6 for the organic rigid-body (3 positional x, y, z and 3 orientational θ, φ, ψ), plus the 3 coordinates describing the I atom position, instead of 72 atomic coordinates describing independently the 24 atomic positions of the compound.

Table 2. Starting random atom positions of the fragment.

Element	x (rel.)	y(rel.)	z(rel.)
I1	0.8144	0.8743	0.9123
O1	0.6391	0.3355	0.4617
C1	0.5832	0.4302	0.4847
C2	0.6285	0.5598	0.4582
C3	0.4445	0.4472	0.5317
C4	0.504	0.6248	0.5004
C5	0.4439	0.5589	0.6365
C6	0.4061	0.6083	0.3693
C7	0.3591	0.4781	0.3951
C8	0.3939	0.3325	0.6111
C9	0.5288	0.5399	0.778
C10	0.3109	0.5942	0.6996
H1	0.7095	0.5786	0.5394
H2	0.6901	0.5837	0.3703
H3	0.5155	0.7128	0.5354
H4	0.3227	0.6729	0.3958
H5	0.4233	0.6519	0.2619
H6	0.3856	0.4196	0.3005
H7	0.2551	0.4681	0.4219
H8	0.493	0.472	0.8557
H9	0.6244	0.5136	0.7341
H10	0.5368	0.628	0.8356
H11	0.2748	0.5302	0.7848
H12	0.3254	0.6844	0.7535
H13	0.2439	0.6021	0.607
H14	0.4558	0.3231	0.7115
H15	0.2958	0.3569	0.6471

The whole-powder-pattern structure solution started keeping fixed the instrument function, obtained separately with a standard LaB_6 sample of known lattice parameters determined previously with a Le Bail fit,. During the global optimization a single value of the isotropic displacement parameter (B_{iso} = 3 Å^2) has been kept fixed common to all atoms.

–Emilio Napolitano–
Application of the Diffraction Technique in Solid State Chemistry from
"ab-initio" Structure Solution to Final Structure Refinement
–Powder and Single Crystal–
Doctoral Thesis in Sciences and Chemical Technology, XXIV cycle
University of Sassari

Pag. 115
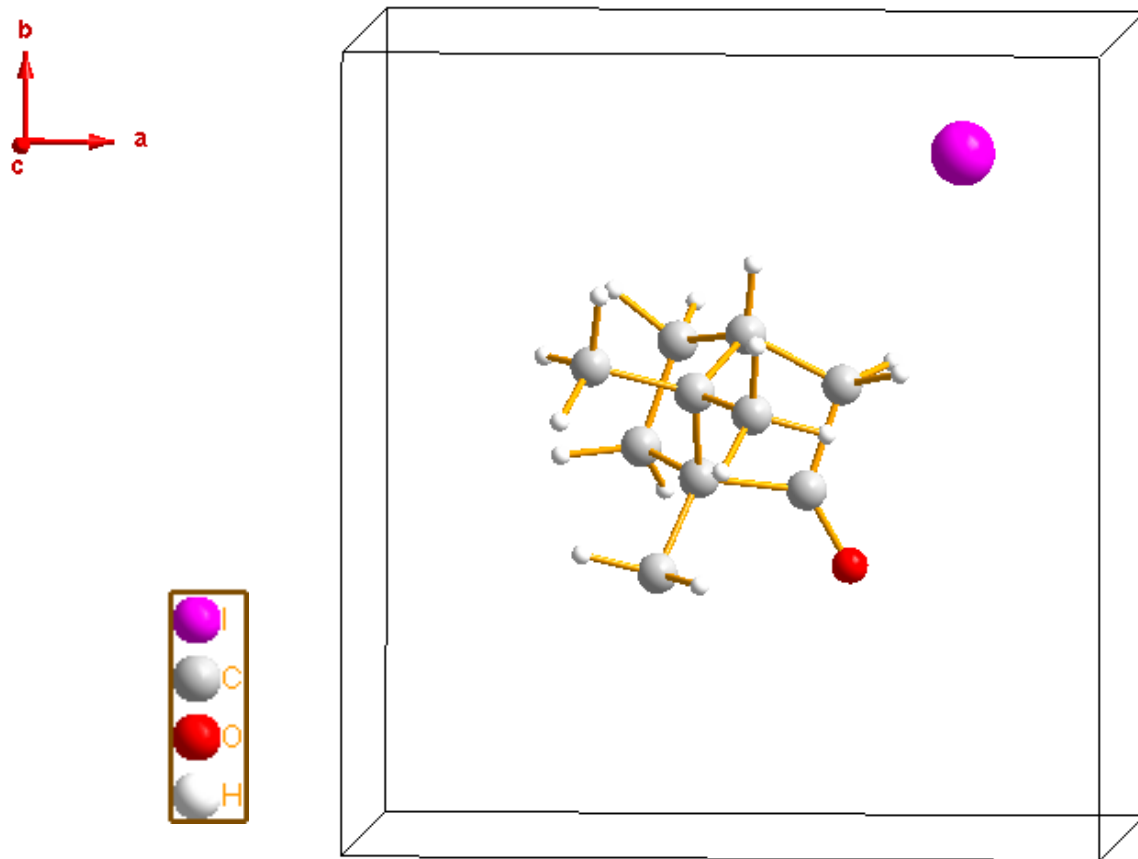
Figure 2. Fragment in starting random configuration inside the unit cell.

Starting from a random configuration of the two bodies inside the cell, the global optimization has been performed using the Hybrid Algorithm implemented in Maud-software, the calculus proceeded over all the 72 patterns concurrently analyzed, calculating for each one the structure factors for each new atom position created, until to find the structure solution.

The model optimization displayed a good match between the observed and calculated profiles with a final Rw = 15.07%.

–Emilio Napolitano–
Application of the Diffraction Technique in Solid State Chemistry from
"ab-initio" Structure Solution to Final Structure Refinement
–Powder and Single Crystal–
Doctoral Thesis in Sciences and Chemical Technology, XXIV cycle
University of Sassari

Pag. 116
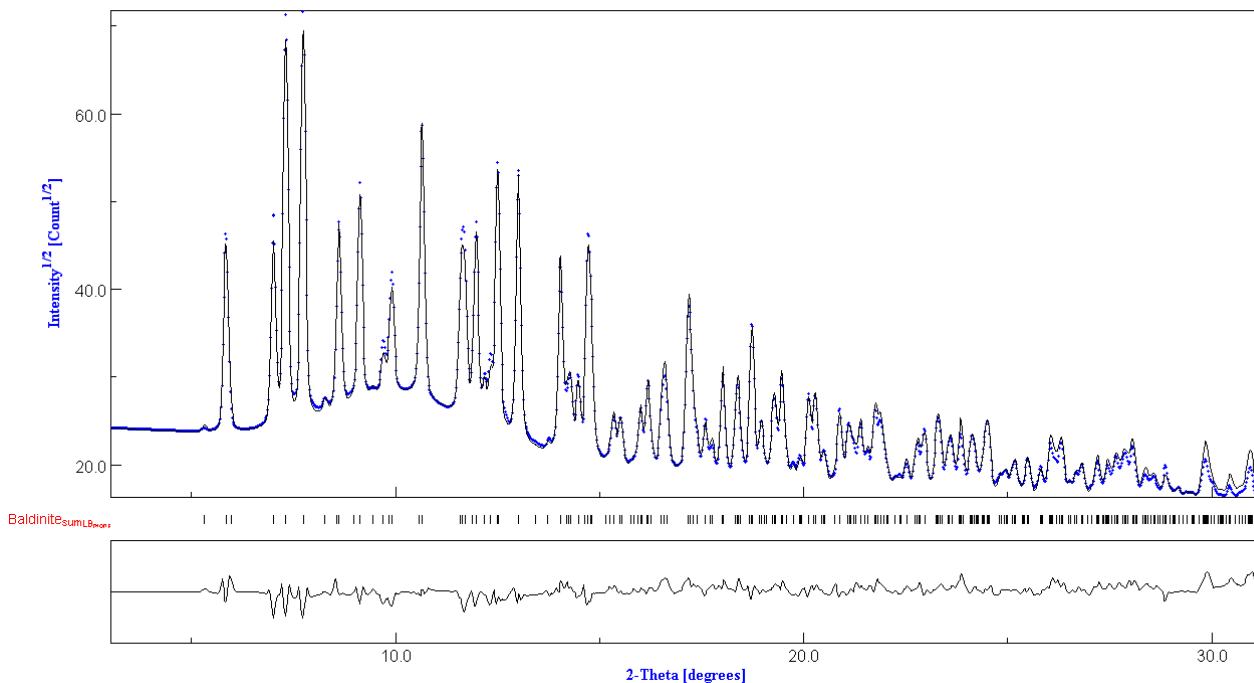
Figure 3. Summed view pattern, 2D data collection + structure solution calculated after the the fit.

The Rietveld refinement has been performed combining two data sets, namely the first from Elettra, λ = 0.70953 Å, with the best statistics used for the structure solution and the second from ESRF, λ = 0.50300 Å with the better resolution for accurate cell parameter determination.

Starting from profile parameter previously determined for both the data sets with the NIST standards, structural, microstructural and overall isotropic displacement atomic parameters have been refined.

The final value of R_{wp} obtained was 11.36% and a GoF = 2.747 (Table 3)

−Emilio Napolitano–
Application of the Diffraction Technique in Solid State Chemistry from
"ab-initio" Structure Solution to Final Structure Refinement
−Powder and Single Crystal–
Doctoral Thesis in Sciences and Chemical Technology, XXIV cycle
University of Sassari

Pag. 117

Patterns	Rwp%	Rp%	Rwpb%	Rpb%
Elettra	10.8751	7.47779	15.9507	10.5663
ESRF	16.6302	12.5216	18.7521	14.3354
Combined	11.3625	7.8162	16.3978	10.9704

Table 3. Values of Elettra , ESRF and combined Rietveld refinement.

A texture analysis using *E-WIMV* algorithm implemented in Maud-software was included Into the Rietveld refinement. This allowed to calculate a reliable Oriented Distribution Function (Figure 5.).
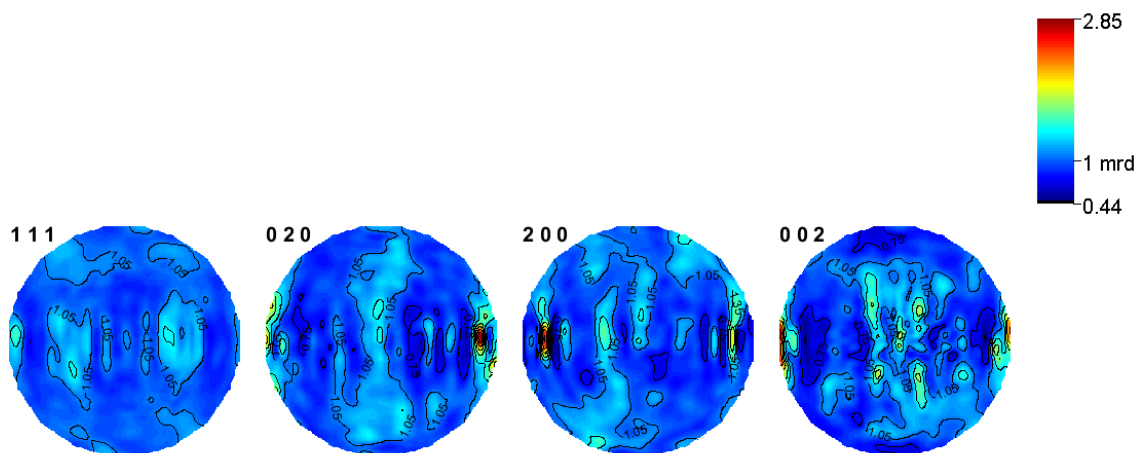
Figure 5. Reconstructed pole figures from ODF obtained by the Rietveld-texture Joint refinement.

In the following we are reporting some screen-shots illustrating the step procedure followed by us.

−**Emilio Napolitano**−
Application of the Diffraction Technique in Solid State Chemistry from
"ab-initio" Structure Solution to Final Structure Refinement
−**Powder and Single Crystal**−
Doctoral Thesis in Sciences and Chemical Technology, XXIV cycle
University of Sassari

Pag. 118

2D Multiplot for 2D plot
measured data and fit
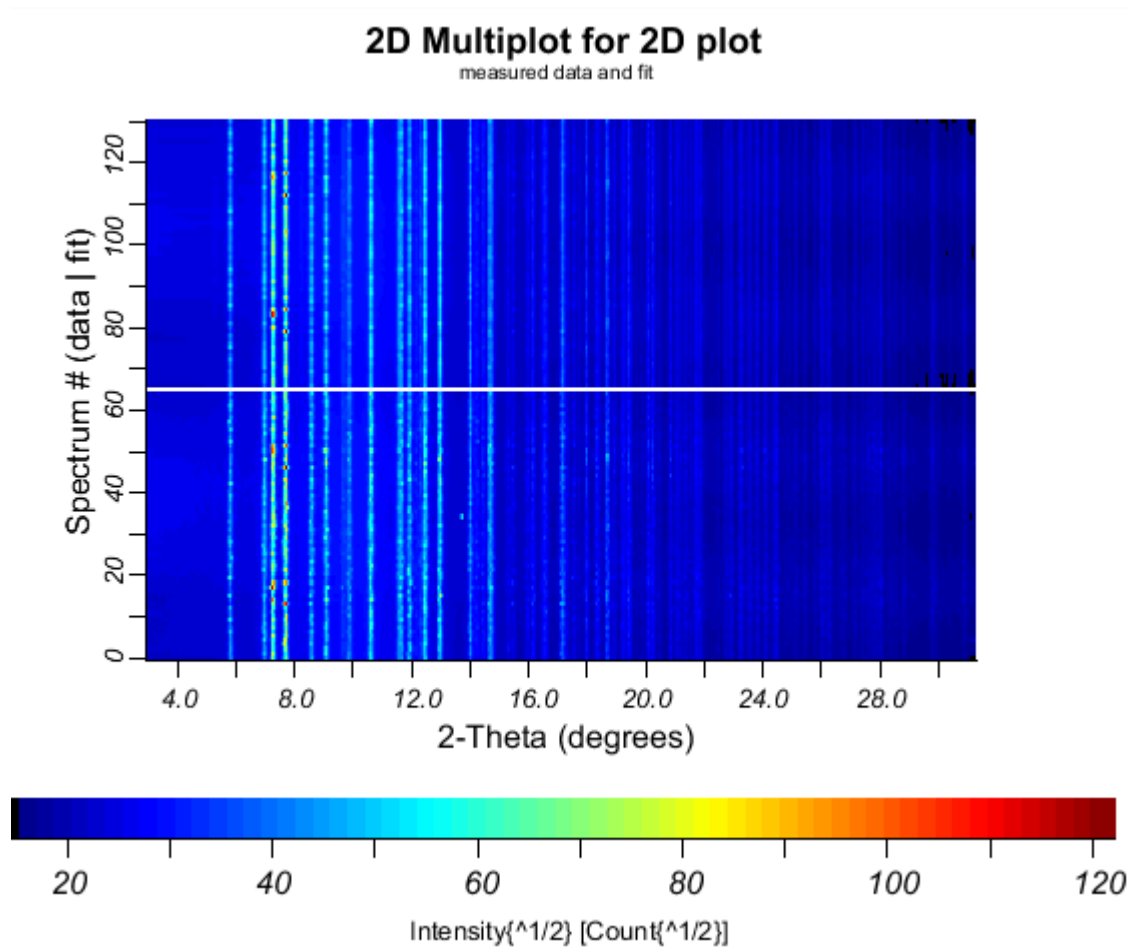
Figure 5 a. 2D Pattern after joint refinement, on the top the computed pattern of each of the 72 sectors extracted from the plate (at the bottom).

–Emilio Napolitano–
Application of the Diffraction Technique in Solid State Chemistry from
"ab-initio" Structure Solution to Final Structure Refinement
–Powder and Single Crystal–
Doctoral Thesis in Sciences and Chemical Technology, XXIV cycle
University of Sassari

Pag. 119
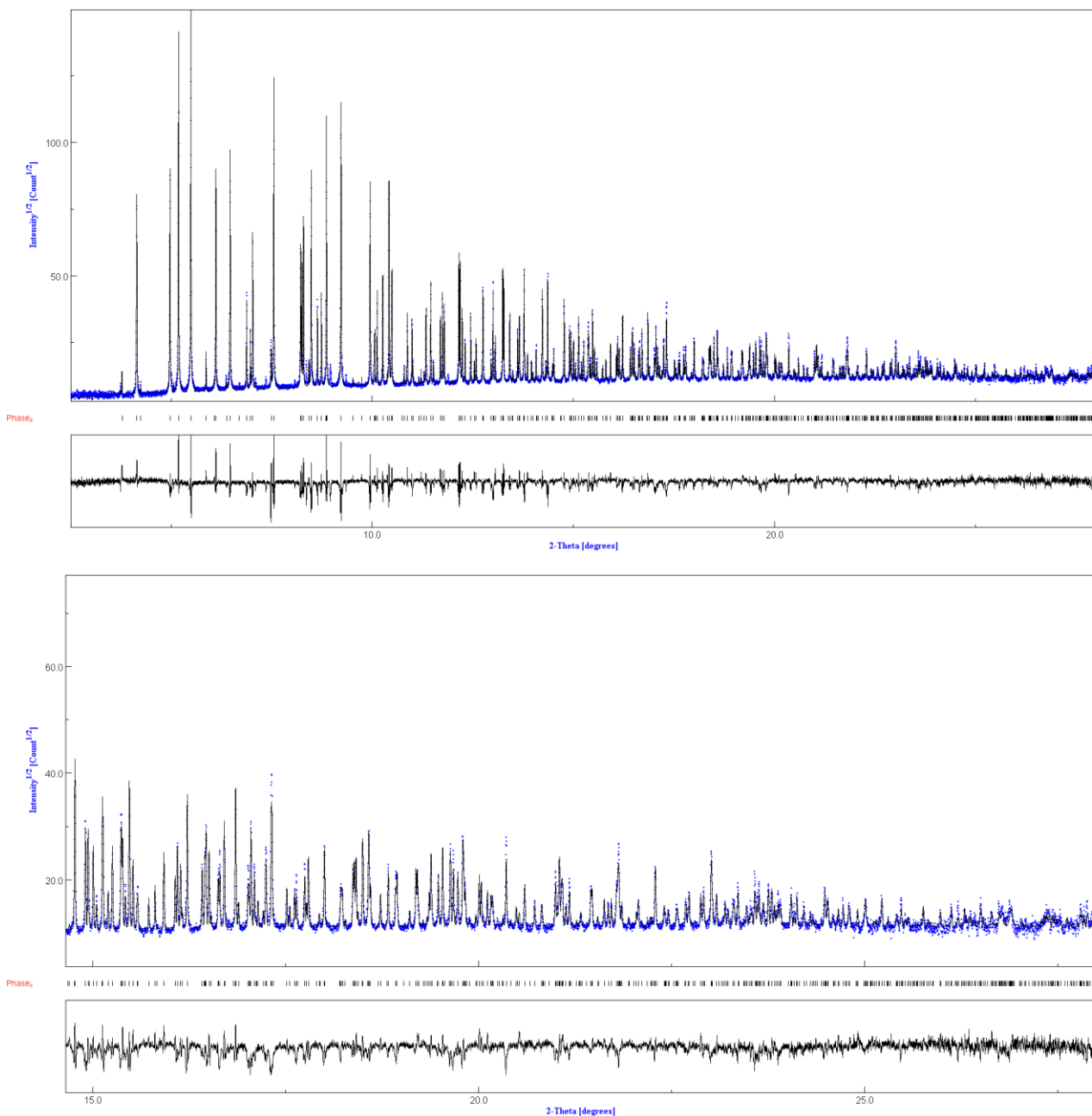
Figure 6b. ESRF Whole Pattern view(i), high angle zoom(ii). Note the y-scale expressed in units of square root of intensity data to fulfill the condition of homogeneous standard deviation for the experimental data.

–Emilio Napolitano–
Application of the Diffraction Technique in Solid State Chemistry from
"ab-initio" Structure Solution to Final Structure Refinement
–Powder and Single Crystal–
Doctoral Thesis in Sciences and Chemical Technology, XXIV cycle
University of Sassari

Pag. 120
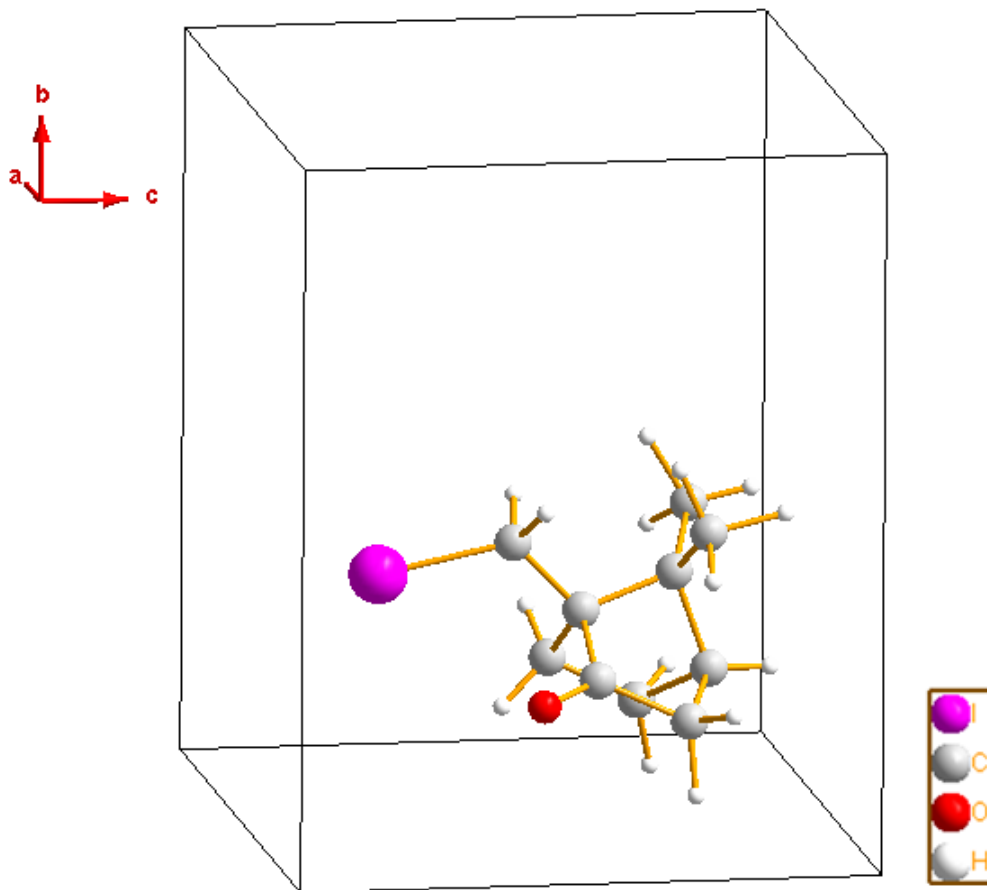
Figure 7. Asymmetric unit inside the unit cell after Join refinement.

–Emilio Napolitano–
Application of the Diffraction Technique in Solid State Chemistry from
"ab-initio" Structure Solution to Final Structure Refinement
–Powder and Single Crystal–
Doctoral Thesis in Sciences and Chemical Technology, XXIV cycle
University of Sassari

Pag. 121

Refinement final output indices for single datasets

Patterns	Rwp%	Rp%	Rwpb%	Rpb%
Elettra	10.8751	7.47779	15.9507	10.5663
ESRF	16.6302	12.5216	18.7521	14.3354
Combined	11.3531	7.8162	16.3978	10.9704

Table 4. Rietveld values for single and combined refinement data set. As discussed in the text, the Elettra experiment gives better agreement indices because of the low-resolution in terms of peak width. Conversely, the high resolution of the ESRF experiment is more challenging for accurate determination of the lattice parameters and atomic fractional coordinates, on the basis of the peak shape.

Atom	x/a	y/b	z/c	B_{iso} [Å²]
I1	0.75402	0.28454	0.28718	3.79(2)
C0	0.14007	0.34890	0.35710	3.79(2)
O3	0.06733	0.36852	0.46356	3.79(2)
C1	0.14259	0.40928	0.19844	3.79(2)
C2	0.26181	0.27453	0.36174	3.79(2)
C4	0.27075	0.36216	0.13899	3.79(2)
C7	0.27829	0.22852	0.19828	3.79(2)
C8	0.37611	0.42473	0.24132	3.79(2)
C10	0.37736	0.36277	0.39499	3.79(2)
C11	0.24902	0.17588	0.48190	3.79(2)
C12	0.15661	0.15191	0.16431	3.79(2)
C13	0.39597	0.15736	0.14982	3.79(2)
H9	0.27662	0.36329	0.03350	3.0
H5	0.05572	0.38736	0.14026	3.0
H6	0.11119	0.50636	0.19272	3.0
H14	0.47174	0.39674	0.17023	3.0
H15	0.40111	0.52042	0.21272	3.0
H16	0.35626	0.42451	0.47734	3.0
H17	0.46563	0.30741	0.41442	3.0
H18	0.15523	0.06391	0.21482	3.0
H19	0.07276	0.20320	0.17391	3.0
H20	0.16705	0.12976	0.03088	3.0
H21	0.38922	0.06298	0.22285	3.0
H22	0.39669	0.13861	0.04281	3.0
H23	0.47768	0.20097	0.20392	3.0
H25	0.17446	0.12198	0.44122	3.0
H26	0.34599	0.12838	0.46132	3.0
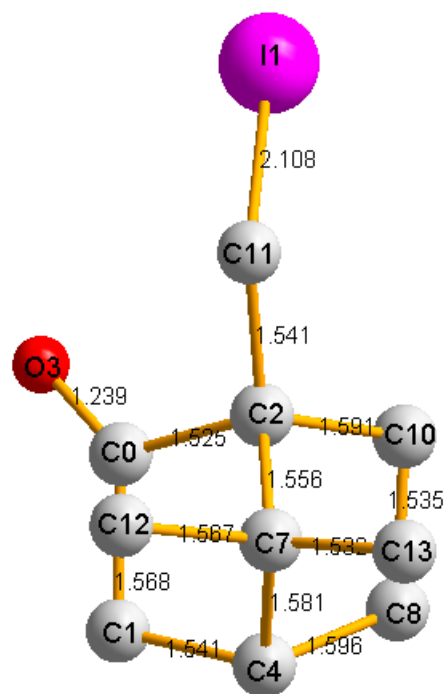
Table 5. Atomic coordinates of the refined model. The values for Biso were attributed empirically on the isotropic assumption.

−Emilio Napolitano–
Application of the Diffraction Technique in Solid State Chemistry from
"ab-initio" Structure Solution to Final Structure Refinement
−Powder and Single Crystal–
Doctoral Thesis in Sciences and Chemical Technology, XXIV cycle
University of Sassari

Pag. 122

The structure looks "tensioned", with light deviation from "standard" bond length and angles, and this is a probable reason of its low melting point (T_m = 350 K). Mild distortions on the bornane skeleton are present, in particular the two methyl groups (C12-C13) were tilted in a clock-way manner respect to a normal axis to C7 (Figure 8).
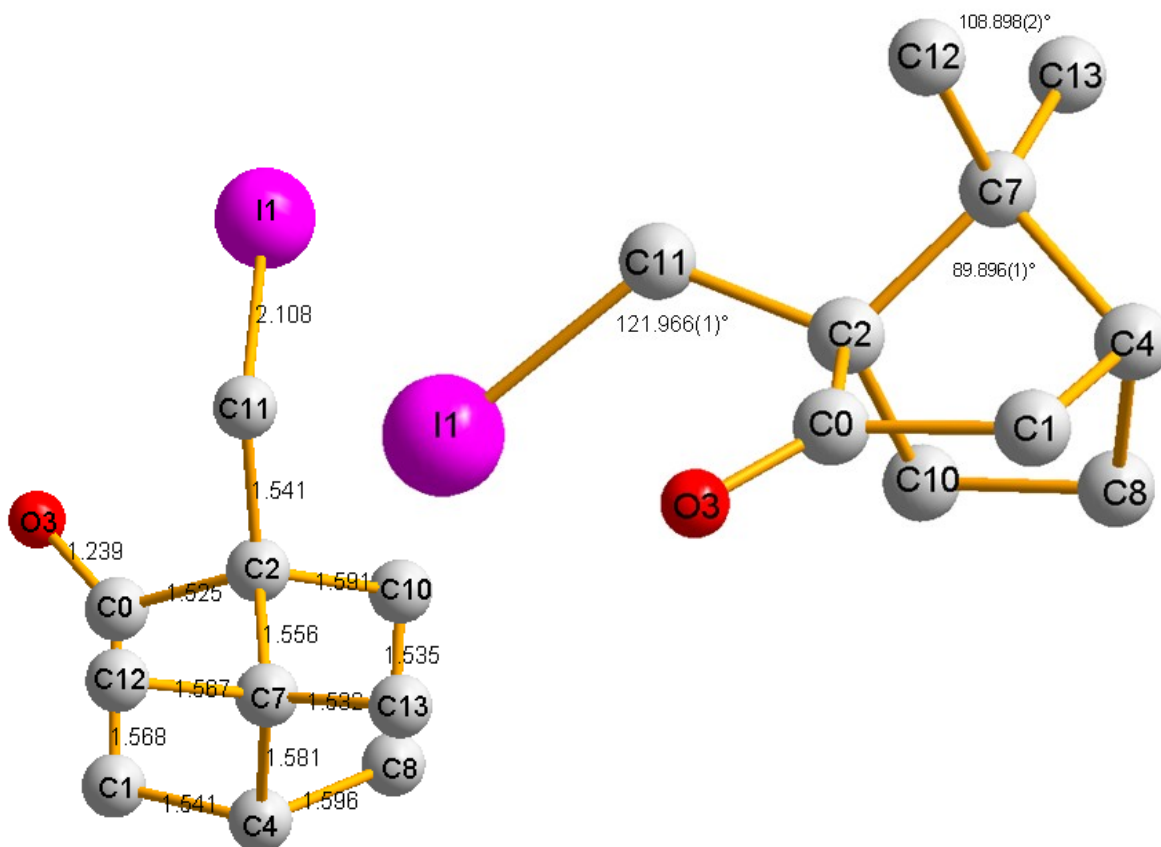
Figure 8. Lateral view of the cyclohexane boat (i).View of the iodo-camphor(ii) normal to the C7(Me)$_2$ bridge.

–Emilio Napolitano–
Application of the Diffraction Technique in Solid State Chemistry from
"ab-initio" Structure Solution to Final Structure Refinement
–Powder and Single Crystal–
Doctoral Thesis in Sciences and Chemical Technology, XXIV cycle
University of Sassari

Pag. 123

The bond length C_4-C_8 C_0-C_1 and C_2-C_{10} are slightly longer than the tabulated single crystal values. We are currently establishing whether this discrepancy is attributable to sensible chemical effects rather than being numerical artefacts.

Conclusion

In summary, the iodo-camphor was solved ab-initio from synchrotron powder data collected at two different stations in Elettra and ESRF respectively.

The present solution is different from an analogous study carry out in 2002[13] at low temperature (Journal of Solid State Chemistry 163, 253-258 (2002) doi:10.1006/jssc.2001.9400) where the S-camphor was solved in the Orthorhombic Space Group $P2_12_12_1$, a=8.9277(2)Å, b=27.0359(5) Å, c=7.3814(1)Å, B overall=0.49(1) Å^2, V=1781.6(1) Å^3, ρ = 1.135 g /cm^3, Z=8.

References

1. Shin-ichi Watanabe, Risa Hasebe, Jun Ouchi, Hideko Nagasawa, Tadashi Kataoka Tetrahedron Letters 51 (2010) 5778–5780.
2. Chelucci Giorgio, Baldino Salvatore. Tetrahedron: Asymmetry 17 (2006)1529–1536.
3. Sell Thorsten; Laschat Sabine; Dix Ina; Jones Peter G.*Eur. J. Org. Chem.* 2000, 4119-4124.
4. http://www.elettra.trieste.it/experiments/beamlines/xrd1/index.html
5. http://www.esrf.eu/UsersAndScience/Experiments/CRG/BM01/bm01b
6. Maud: Materials Analysis Using Diffraction, version 2.33, 2011, http://www.ing.unitn.it/~maud/

–Emilio Napolitano–
Application of the Diffraction Technique in Solid State Chemistry from
"ab-initio" Structure Solution to Final Structure Refinement
–Powder and Single Crystal–
Doctoral Thesis in Sciences and Chemical Technology, XXIV cycle
University of Sassari

Pag. 124

7. L. Lutterotti, M. Bortolotti, G. Ischia, I. Lonardelli and H.-R. Wenk, "Rietveld texture analysis from diffraction images", Z. Kristallogr.,Suppl. 26, 125-130, 2007.

8. A. Le Bail, Powder Diffraction 19 (2004) 249-254.

9. Werner, P. E., Eriksson, L. & Westdahl, M. *J. of Appl.Cryst.*(1985) 18, 367–370.

10. Visser, J. W. *J. of App. Cryst.* (1969). 2, 89–95

11. Altomare, A., Giacovazzo, C., Guagliardi, A.,Moliterni, A. G. G., Rizzi, R. &Werner, P.-E. (2000). *J. of Appl. Cryst.*, 33, 1180–1186.

12. Ali Boultif and Daniel LoueÈr J. Appl. Cryst. (2004). 37, 724-731.

13. A.Le Bail, H. Duroy, J.L. Fourquet, J. Solid State Chem., (1992), 98, 151.

14. Michela Brunelli, Andrew N. Fitch, Asiloe H J. Mora.J. of Solid State Chem. 163, 253-258 (2002)

–Emilio Napolitano–
Application of the Diffraction Technique in Solid State Chemistry from "ab-initio" Structure Solution to Final Structure Refinement –Powder and Single Crystal– Doctoral Thesis in Sciences and Chemical Technology, XXIV cycle University of Sassari

Pag. 125

[P(Ph)₃CH₂CN]·BF₄ single crystal structure determination.

In organometallic and organic field phosphonium salts play an important role like starting reagent in the well-known Wittig[1-2] reaction, a useful pathway to synthetize compounds containing C=C double bonds[3].

[P(Ph)₃CH₂CN]·BF₄ is a phosphonium salt synthesized by Dr. Facchin from Institute of Science and molecular technologies of the University of Padova.
The scheme of reaction is briefly reported below:

$$PPh_3 + BrCH_2CN \xrightarrow[\text{refl. 8h}]{CH_3NO_2} Ph_3PCH_2CN^+ \, Br^- \downarrow \xrightarrow[\text{NaBF}_4]{(CH_3)_2CO \text{ ref.20h}} Ph_3PCH_2CN^+BF_4 + NaBr \downarrow$$

$$Ph_3PCH_2CN^+BF_4^- \xrightarrow[\text{Et}_2O]{CH_3Cl} Ph_3PCH_2CN^+BF_4^- \downarrow$$
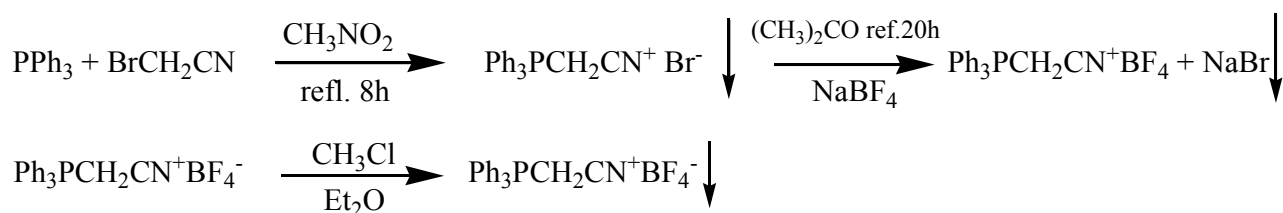
The [P(Ph)₃CH₂CN]·BF₄ compound was synthetized in 1996 by Dr. Facchin during a collaboration at the DIMTI in Trento (Italy).
This compound was stored until few months ago in brown glass sample holder inside a dry box.

Data collection

The powder sample is composed by thousands of needle shaped crystals (light yellow). Selected one preliminary X-ray diffraction investigation was performed at room temperature, using Mo K$_\alpha$ radiation.
A single crystal of suitable size 771x51.4x128.5 µm³ was selected for structure analysis. Two data collection has been performed, one at 293K and another at 120K.

–Emilio Napolitano–
Application of the Diffraction Technique in Solid State Chemistry from
"ab-initio" Structure Solution to Final Structure Refinement
–Powder and Single Crystal–
Doctoral Thesis in Sciences and Chemical Technology, XXIV cycle
University of Sassari

Pag. 126

After a preliminary evaluation of cell parameters dimension and quality of the diffraction spots, a suitable data collection strategy has been defined.

A scanning angle of 0.8° and a Dx (detector-sample distance) value of 40 mm have been chosen; ω and ϕ scans with an exposure times of 60s/° have been used to collect data. The diffracted intensities were collected up to θ= 34.99° for a resolution of 0.62 Å.
A total of 25418 reflections were collected, 9420 independent reflections with I≥3σ(I) were finally obtained.

The compound was composed by C, O, N and H atoms each with light scattering power. For obtaining more confident diffraction data, atomic position and atomic displacement parameters, the room temperature data acquisition has been followed by a data collection performed at 120K.

Data processing

The frames were integrated with the Bruker SAINT[4] software package using a narrow-frame algorithm.
Data were corrected for absorption effects using the multi-scan method (SADABS)[5].

The indexing step for both the data sets, using the Apex2 suite[6](from Bruker AXS), converged to a monoclinic system. The cell parameters values are: a= 15.0762(1) Å, b= 9.3173(2) Å, c= 27.7461(2) Å and β= 94.416(5)° for a volume value of 3885.8(9) Å^3 (298K).

–Emilio Napolitano–
Application of the Diffraction Technique in Solid State Chemistry from
"ab-initio" Structure Solution to Final Structure Refinement
–Powder and Single Crystal–
Doctoral Thesis in Sciences and Chemical Technology, XXIV cycle
University of Sassari

Pag. 127

A predictable shrinkage for the lattice parameters has been detected in the sample cooled down to 120K: a = 14.9648(12) Å (-0.74%), b = 9.2338(8) Å (-0.89%), c = 27.383(2) Å (-1.31%) and β= 94.3113(14)°(-0.11%) and volume value 3773.1(5) Å^3(-2.9%) (120K).

The observed extinction rules[7] h0l: h+l=2n+1, 0k0: k=2n+1 were consistent with the space group P12$_1$/n1, and no polymorph transition has been observed.

Two structural models considering the P12$_1$/n1 space group has been built up with direct method[8] implemented in Sir2011[9] software. The calculus converged with two chemically correct structural models, leading to a reliability factor of ~20 % and ~21% respectively for low and room temperature data set. For the structure refinement the low temperature model has been selected because of its better quality of diffraction data. This model was then introduced in the refinement program Jana2006[10]; all the atomic positions were refined, and then anisotropic displacement parameters (ADP) are considered for all the atoms. The refinement leads to an agreement factor equal to 11%. Fourier differences were then calculated allowing the location of all the hydrogen atoms. The final refinement procedure leads to R=5.54% and R$_w$= 5.86%. Structural parameters are summarized in Appendix-A.

–Emilio Napolitano–
Application of the Diffraction Technique in Solid State Chemistry from
"ab-initio" Structure Solution to Final Structure Refinement
–Powder and Single Crystal–
Doctoral Thesis in Sciences and Chemical Technology, XXIV cycle
University of Sassari

Pag. 128
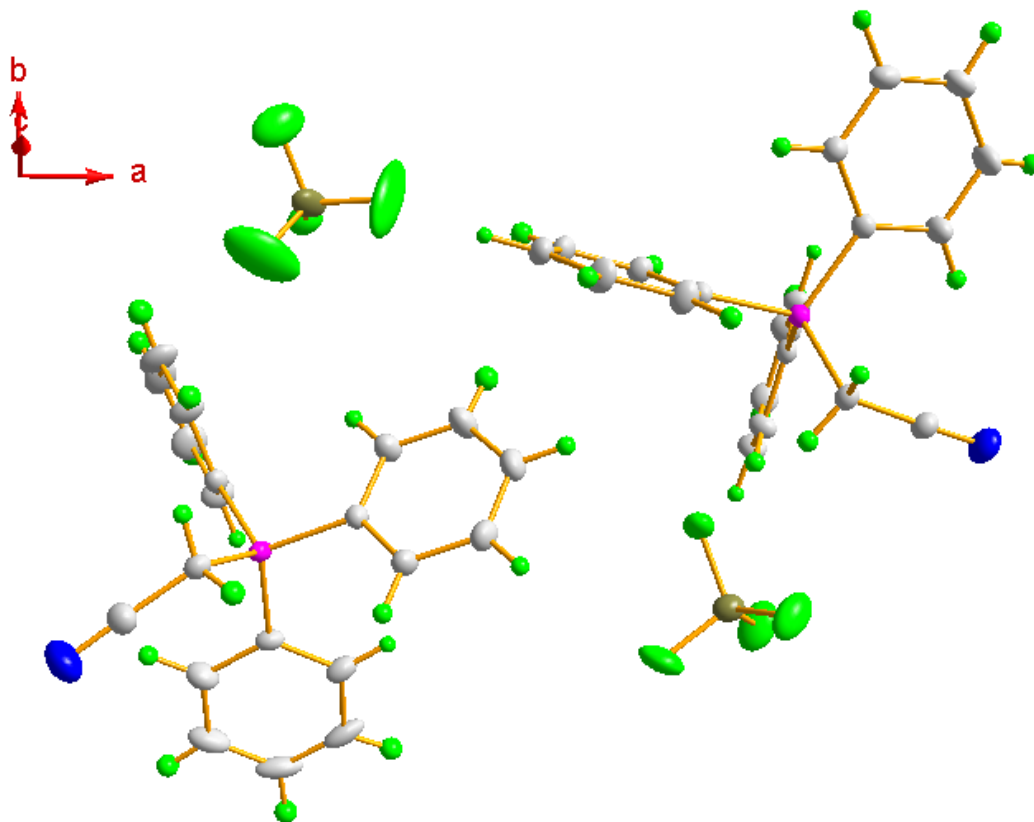
Figure 1. Asymmetric unit [P(Ph)₃CH₂CN]·BF₄ after refinement.[11]

−**Emilio Napolitano**−
Application of the Diffraction Technique in Solid State Chemistry from
"ab-initio" Structure Solution to Final Structure Refinement
−**Powder and Single Crystal**−
Doctoral Thesis in Sciences and Chemical Technology, XXIV cycle
University of Sassari

Pag. 129
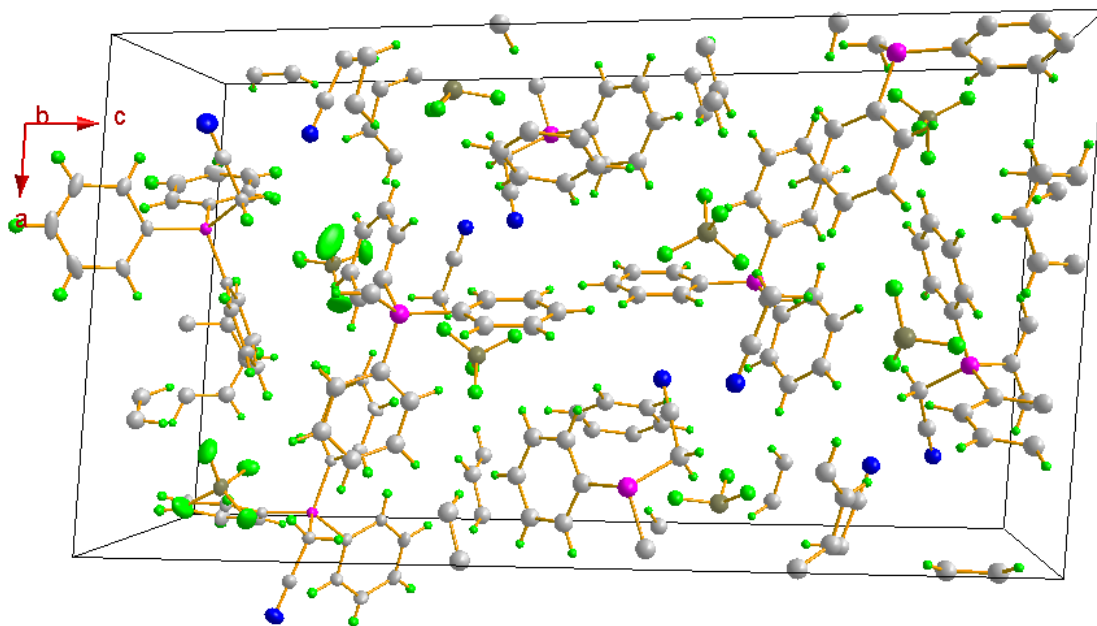
Figure 3. Unit cell content view.

Conclusion

The phosphonium salt $[P(Ph)_3CH_2CN]\cdot BF_4$ showed to be a stable compound, in facts no polymorph transition has been observed from 298K down to 120K and no presence of impurity like phosphine oxide has been detected, only a shrinkage of lattice parameters (~ - 1%) has been found.

The structure determined at low temperature shows standard bond and angle values, and this makes us confident about atomic positions.

Different values for non-bonding inter molecular F···H separation have been found, typically distances of 2.2324(1) Å 2.366(3) Å (the two shortest values), one distance of 2.5323(2) Å and one more at 2.76 Å which is slightly larger than the sum of Van der Waals radii for H and F atoms equivalent to 2.55 Å. This generates a slightly larger anisotropic atomic displacement for fluorine atoms interested by this chemical surrounding because of the weak interaction of the electron clouds.

−Emilio Napolitano−
Application of the Diffraction Technique in Solid State Chemistry from
"ab-initio" Structure Solution to Final Structure Refinement
−Powder and Single Crystal−
Doctoral Thesis in Sciences and Chemical Technology, XXIV cycle
University of Sassari

Pag. 130

References

1. S. Trippett and D. M. Walker. J. Chem. Soc., 1959, 3874-3876

2. http://www.nobelprize.org/nobel_prizes/chemistry/laureates/1979/wittig-cv.html

3. J.Clayden, N. Greeves, S. Warren, P. Wothers. Organic Chemistry, Oxford University Press, 2000, Ch.14.

4. Bruker (2007). *Saint software*. Bruker AXS Inc., Madison, Wisconsin, USA.

5. Sheldrick, G. M. (2002). SADABS. Bruker AXS Inc., Madison, Wisconsin, les Etats Unis.

6. Bruker (2005). *APEX2*. Bruker AXS Inc., Madison, Wisconsin, USA.

7. International Table for Crystallography. Vol A, Fifth Revised Ed. Theo Hahn, Ed., Published for the International Union of Crystallography by Springer, Berlin (2002).

8. M. C Burla, C. Giacovazzo, G. Polidori. J. Appl. Cryst. (2011). 44, 193–199

9. Burla, Camalli, Carrozzini, Cascarano, Giacovazzo, Polidori & Spagna (2003). *J. Appl. Cryst.* **36**, 1103

10. Petrıcek, V., Dusek, M. & Palatinus, L. (2006). *Institute of Physics, Praha, Czech Republic*, JANA2006, The crystallographic computing system.

11. Diamond ver. 3.2g was used for visualization -Brandenburg, K. & Putz, H. (2005).DIAMOND Version 3. -Crystal Impact GbR, Postfach 1251, D-53002 Bonn,Germany

–Emilio Napolitano–
Application of the Diffraction Technique in Solid State Chemistry from
"ab-initio" Structure Solution to Final Structure Refinement
–Powder and Single Crystal–
Doctoral Thesis in Sciences and Chemical Technology, XXIV cycle
University of Sassari

Pag. 131

C$_{21}$H$_{36}$NO$_3$ and C$_{27}$H$_{37}$NO$_5$ single crystal structure determination.

The 1-azabicyclic alkaloid systems A (C$_{21}$H$_{36}$NO$_3$) and B (C$_{27}$H$_{37}$NO$_5$) were resolved by single crystal X-ray analysis. These structures were synthesized as intermediates in the syntheses of enantiomeric pure polyhydroxylated alkaloid.

The compound A incorporate a pyrrolo-[1,2a]-azocine backbone and the compound B a indolizidine one; both substructures are present in many natural substances with different biological properties, including the anticancer and antiviral ones. [1]

A   B
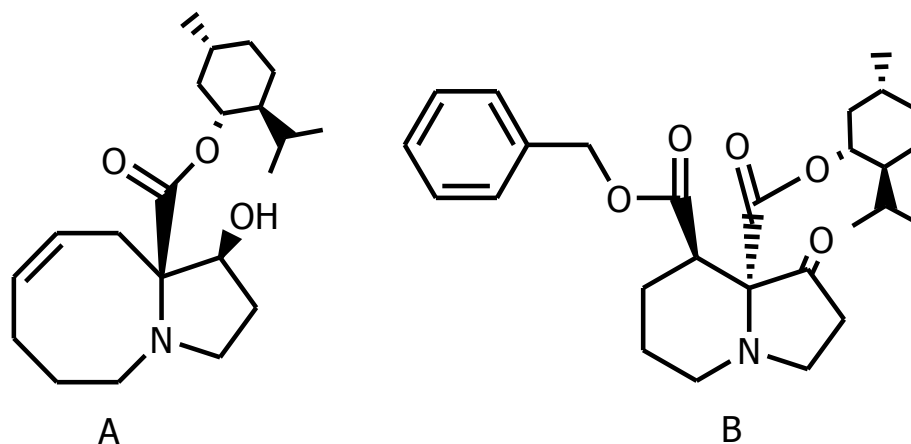
Both compounds were synthesized with high stereoselectivity through carbenoidic cascade processes, starting from L-Proline, by Dr. D. Muroni (Department of Chemistry, University of Sassari). The introduction in the early steps of the syntheses of the chiral auxiliary (-)-menthyl, which is not chemical involved in the course on the syntheses, allowed the purification of the two compounds by recrystallization. The XR analyses, which were in accordance with the NMR data, confirmed the configuration of stereocenters on natural menthol, and it was possible to give the absolute configuration of new stereocenters,

–Emilio Napolitano–
Application of the Diffraction Technique in Solid State Chemistry from
"ab-initio" Structure Solution to Final Structure Refinement
–Powder and Single Crystal–
Doctoral Thesis in Sciences and Chemical Technology, XXIV cycle
University of Sassari

Pag. 132

whose configuration were those expected from the known stereochemical pathway of reactions.

$C_{21}H_{36}NO_3$

For the crystal structure analysis a single crystal of suitable size 359.8x128.5x128.5 μm^3 (colorless) has been selected. Two data collections have been performed, one at 293K and another at 120K.

After a preliminary evaluation of cell parameters dimension and quality of the diffraction spots performed at room temperature, a suitable data collection strategy has been defined. A scanning angle of 0.5° and a Dx (detector-sample distance) value of 40 mm have been chosen; ω and φ scans with an exposure times of 30s/° have been used to collect data. The diffracted intensities were collected up to θ= 30.02° for a resolution of 0.71 Å for an overall number of 21850 reflections; 3753 independent reflections with I≥3σ(I) were finally obtained.

The frames were integrated with the Bruker SAINT[2] software package using a narrow-frame algorithm.

Data were corrected for absorption effects using the multi-scan method (SADABS)[3].

The organic sample was composed by C, O, N and H atoms each with light scattering power. For obtain more confident diffraction data, atomic position and atomic displacement parameters, the room temperature data acquisition has been followed by a data collection performed at 120K.

−Emilio Napolitano−
**Application of the Diffraction Technique in Solid State Chemistry from
"ab-initio" Structure Solution to Final Structure Refinement
−Powder and Single Crystal−
Doctoral Thesis in Sciences and Chemical Technology, XXIV cycle
University of Sassari**

Pag. 133

The indexing step of both the data sets, using the Apex2 suite[4] (from Bruker AXS) converged to an orthorhombic crystal system with lattice parameters: a= 10.8837(13) Å, b= 7.8540(9) Å, c= 24.201(3) Å and $\alpha=\beta=\gamma=90.00°$ and a volume value of 2068.7(4) Å^3 for the 293K data collection.

An expected shrinkage (~-1%) of cell parameters have been observed for the 120K data acquisition, a= 10.7804(8) Å (-0.767%), b= 7.7938(7) Å (-0.949%), c= 23.8862(2) Å (-1.3019 %) and $\alpha=\beta=\gamma=90.00°$ and a volume value 2006.925 Å^3 (-2.98% in comparison with the volume measured at room temperature).

The compound did not show polymorphic transition. A total of 1851 frames were collected, a sections of the reciprocal space calculated from these series of experimental frames are sufficiently accurate to obtain an overall view of the reciprocal space. The observed condition limiting the possible reflections, h00: l=2n, 0k0: k=2n and 00l: l=2n are consistent with the space group[5] $P2_12_12_1$.

A structural model considering the $P2_12_12_1$ space group has been built up using a direct method implemented[6] into Sir2011[7]. The structure solution has been performed for both the two data collected at RT and 120K. The first model leaded to a reliability factor of ~21% (293K) and ~19% (120K). They have been inputted in the refinement program Jana2006[8]; all the atomic positions have been refined, and then anisotropic displacement parameters (ADP) have been considered for all the atoms. The refinement leads to an agreement factor equal to 12%.

The location of all the hydrogen atoms have been determined with a geometric approach for the room temperature data and by the Fourier differences map for

–Emilio Napolitano–
Application of the Diffraction Technique in Solid State Chemistry from
"ab-initio" Structure Solution to Final Structure Refinement
–Powder and Single Crystal–
Doctoral Thesis in Sciences and Chemical Technology, XXIV cycle
University of Sassari

Pag. 134

the 120K data collection. The final refinement procedure leads to R=5.17% and R_w= 5.37% for the data collected at 293 K, R=4.96% and R_w= 4.74% for 120 K diffraction data.

Conclusion

The structural model shows standard bond lengths and angles, the structural X-ray analysis and the goodness of the data collected both at 293 and 120K confirm the stereochemistry of carbon atoms known from literature in the auxiliary chiral (-)-menthyl: C3 (S), C4, C17 (R)[9].

Two new chiral centers have been identified: C8(S) and C5 (R).

A cis double bond (1.3279(3) Å) has been identified in the azocine ring, in position C12-C15.

Structural parameters are summarized in Appendix-B.

–Emilio Napolitano–
Application of the Diffraction Technique in Solid State Chemistry from
"ab-initio" Structure Solution to Final Structure Refinement
–Powder and Single Crystal–
Doctoral Thesis in Sciences and Chemical Technology, XXIV cycle
University of Sassari

Pag. 135
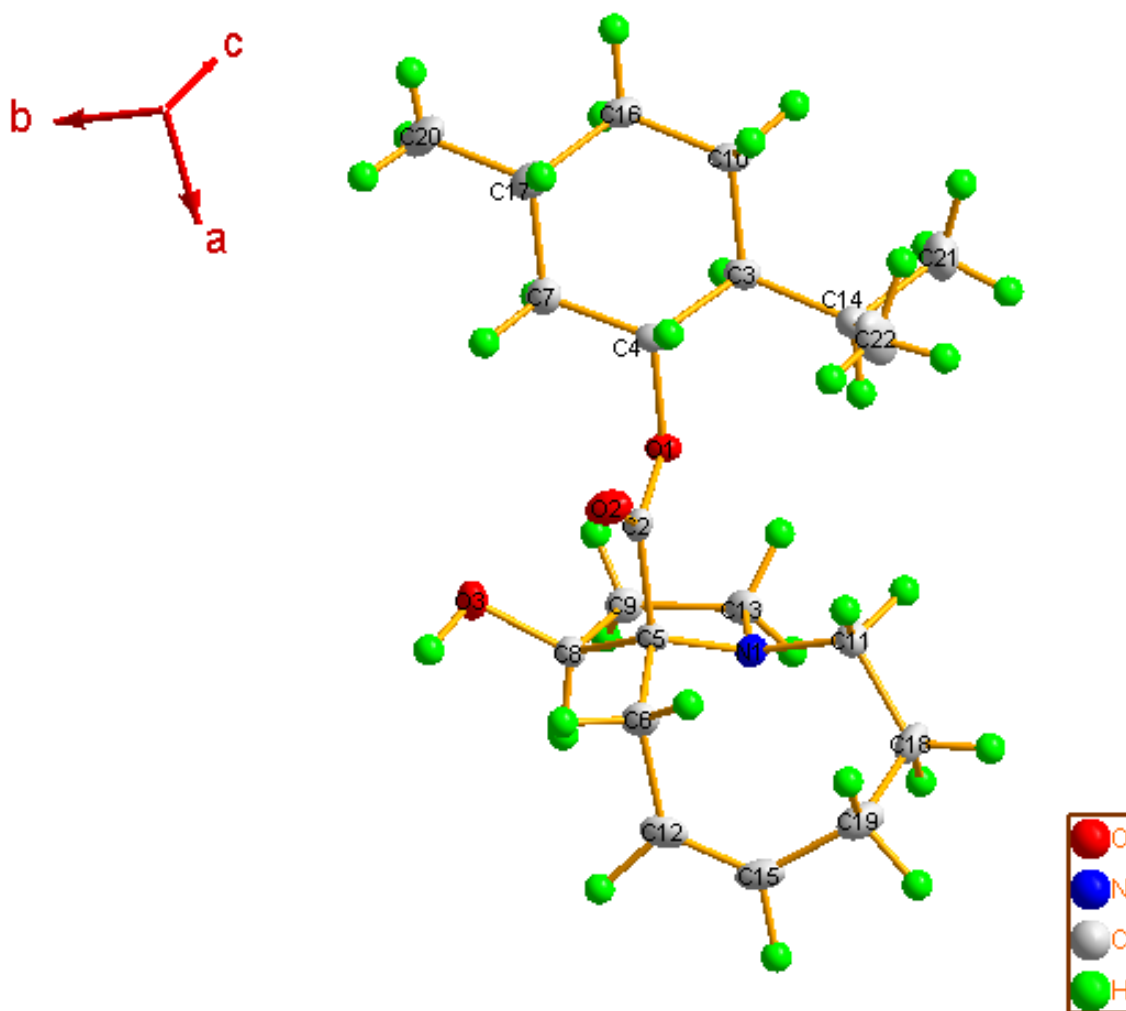
Figure 2. C$_{21}$H$_{36}$NO$_3$ structure model (120K)[11]

−Emilio Napolitano−
Application of the Diffraction Technique in Solid State Chemistry from
"ab-initio" Structure Solution to Final Structure Refinement
−Powder and Single Crystal−
Doctoral Thesis in Sciences and Chemical Technology, XXIV cycle
University of Sassari

Pag. 136

C$_{27}$H$_{37}$NO$_5$

The same procedure has been adopted for the C$_{27}$H$_{37}$NO$_5$ compound.

A single crystal of dimension 257x282.7x308.4 µm^3 (brownish) has been selected for the crystal structure analysis.

After a preliminary evaluation of cell parameters dimension and quality of the diffraction spots performed at room temperature, a suitable data collection strategy has been defined. A scanning angle of 0.8° and a Dx (detector-sample distance) value of 40 mm have been chosen; ω and χ scans with an exposure times of 40s/° have been used to collect data. The diffracted intensities were collected up to θ= 29.97° for a resolution of 0.71 Å for an overall number of 11322 reflections; 3547 independent reflections with I≥3σ(I) were finally obtained.

The frames were integrated with the Bruker SAINT[2] software package using a narrow-frame algorithm.

Data were corrected for absorption effects using the multi-scan method (SADABS)[3].

The organic sample was composed by C, O, N and H atoms each with light scattering power. For obtain more confident diffraction data, atomic position and atomic displacement parameters, the room temperature data acquisition has been followed by a data collection performed at 120K.

The indexing step of both the data sets, using the Apex2 suite[4] (from Bruker AXS) converged to a monoclinic crystal system with lattice parameters:

–Emilio Napolitano–
Application of the Diffraction Technique in Solid State Chemistry from
"ab-initio" Structure Solution to Final Structure Refinement
–Powder and Single Crystal–
Doctoral Thesis in Sciences and Chemical Technology, XXIV cycle
University of Sassari

Pag. 137

a=8.2164(16) Å, b= 16.2695(17) Å, c= 9.5528(13) Å and β= 98.995(11)° and a volume 1261.3(3) Å^3.

An anisotropic shrinkage (average ~-1.87%) of cell parameters have been observed for the 120K data acquisition a= 8.0038(11) Å (-2.58%), b= 16.331(2) Å (+0.378%), c= 9.2290(11) Å (-3.389%) and β= 93.545(7)° (-5.5%) and a volume 1204.0(3) Å^3 (-4.542 %) for the 120K data collection.

A total of 497 frames were collected, a sections of the reciprocal space calculated from these series of experimental frames are sufficiently accurate to obtain an overall view of the reciprocal space.

The compound did not show polymorphic transition, the observed extinction rules[7] h0l: h+l=2n+1, 0k0: k=2n+1, h00: h = 2n +1 and 00l: l = 2n+1 were consistent with the space group P12$_1$/n1.

A structural model considering the P12$_1$/n1 space group has been built up with the direct method implemented[6] into Sir2011[7] for both the two data collection. The first model leaded to a reliability factor of ~22 % (293K) and ~19%(120K) . They have been inputted in the refinement program Jana2006[8]; all the atomic positions have been refined, and then anisotropic displacement parameters (ADP) have been considered for all the atoms. The refinement leads to an agreement factor equal to 15%.

The location of all the hydrogen atoms have been determined with a geometric approach for the room temperature data and by the Fourier differences map for the 120K data collection. The final refinement procedure leads to R=5.17% and

–Emilio Napolitano–
Application of the Diffraction Technique in Solid State Chemistry from
"ab-initio" Structure Solution to Final Structure Refinement
–Powder and Single Crystal–
Doctoral Thesis in Sciences and Chemical Technology, XXIV cycle
University of Sassari

Pag. 138

R_w= 5.37 %for the data collected at 293 K and R=6.40% and R_w= 8.19% for 120 K diffraction data respectively.
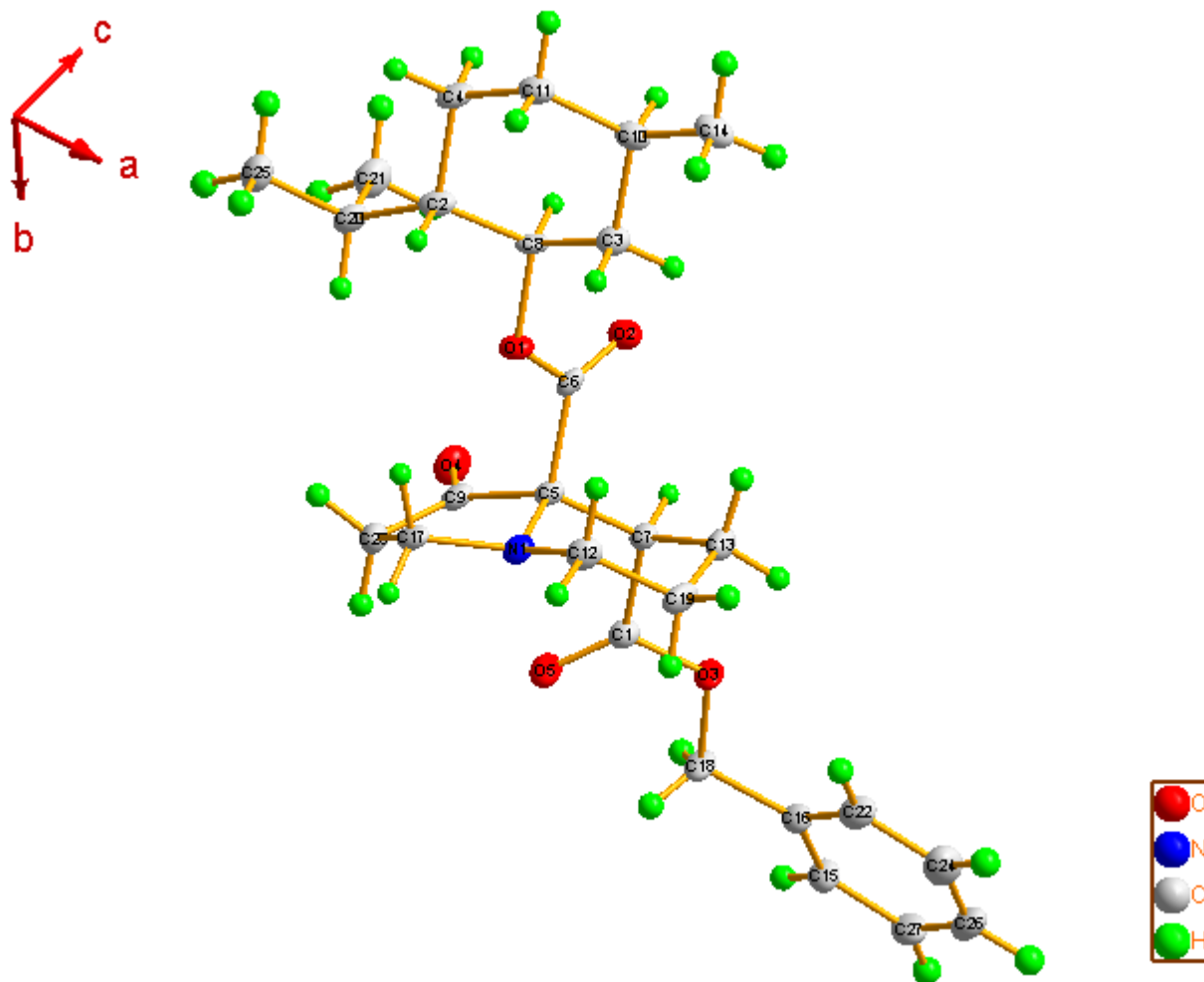
Figure 3 $C_{27}H_{37}NO_5$ Structure model (120K)[11].

−Emilio Napolitano−
Application of the Diffraction Technique in Solid State Chemistry from
"ab-initio" Structure Solution to Final Structure Refinement
−Powder and Single Crystal–
Doctoral Thesis in Sciences and Chemical Technology, XXIV cycle
University of Sassari

Pag. 139

Conclusion

The structural model shows standard bond lengths and angles, the structural XR analysis and the goodness of the data collected both 293 and 120K confirm the stereochemistry of carbon atoms in the auxiliary chiral (-)-menthyl: C2 (S), C8, C1 (R)[9].

Two new chiral centers have been identified: C5(S) and C7(R).
Structural parameters are summarized in Appendix-C

Reference

1. P. Compain, O. R. Martin, Iminosugars: From Synthesis to Therapeutic Applications, Wiley, Chichester, 2007.
2. Bruker (2007). *Saint software*. Bruker AXS Inc., Madison, Wisconsin, USA.
3. Sheldrick, G. M. (2002). SADABS. Bruker AXS Inc., Madison, Wisconsin, les Etats Unis.
4. Bruker (2005). *APEX2*. Bruker AXS Inc., Madison, Wisconsin, USA.
5. International Table for Crystallography. Vol A, Fifth Revised Ed. Theo Hahn, Ed., Published for the International Union of Crystallography by Springer, Berlin (2002).
6. M. C Burla, C. Giacovazzo, G. Polidori. J. Appl. Cryst. (2011). 44, 193–199
7. Burla, Camalli, Carrozzini, Cascarano, Giacovazzo, Polidori & Spagna (2003). *J. Appl. Cryst.* **36**, 1103
8. Petrıcek, V., Dusek, M. & Palatinus, L. (2006). *Institute of Physics, Praha, Czech Republic*, JANA2006, The crystallographic computing system.

–Emilio Napolitano–
Application of the Diffraction Technique in Solid State Chemistry from "ab-initio" Structure Solution to Final Structure Refinement –Powder and Single Crystal– Doctoral Thesis in Sciences and Chemical Technology, XXIV cycle University of Sassari

Pag. 140

9. V. Adovasio, N. Nardelli, G. Chelucci, A. Saba. Acta Cryst. (1995). C51, 2166-2169

10. Cui-Lian Xu, Shan-Yu Liu, Gang Chen, Guo-Yu Yang[a] and Ming-Qin Zhao Acta Cryst. (2009). E65, o2431

11. Diamond ver. 3.2g was used for visualization -Brandenburg, K. & Putz, H. (2005).DIAMOND Version 3. -Crystal Impact GbR, Postfach 1251, D-53002 Bonn, Germany

–Emilio Napolitano–
Application of the Diffraction Technique in Solid State Chemistry from
"ab-initio" Structure Solution to Final Structure Refinement
–Powder and Single Crystal–
Doctoral Thesis in Sciences and Chemical Technology, XXIV cycle
University of Sassari

Pag. 141

Conclusion

In this PhD thesis we have paid attention to the methods available for structural determination in new materials with a wide application range.

The subject of our investigations involved materials for energy and environment care applications, fossil bones, organic and inorganic compounds. All of them in common required a satisfactory solution of their structure. Being able to solve successfully these problems has meant essentially to become acquainted with the diffraction techniques, whether applied in a laboratory scale rather than at Large Scale facilities like the Synchrotron radiation and Neutron source installations.

The complexity of theory and instrumentation was accompanied by the sparse availability of very refined software made available from various authors, whose development is permanently in progress.

In particular, part of this work was dedicated to improve the well-known software MAUD, early used for structure refinement, in order to encompass the more flexible whole-powder-pattern fitting including indexing and structure solution in direct space method, suggesting and testing various modification made by Dr. Lutterotti.

As further development for the structure solution, the classical ability to solve the structure from single-crystal data has implemented simultaneously in order to take advantage of the complementary merits of each approach.

Also, the performance has been tested, when possible, about the various approaches to solve the structure in the real or reciprocal space (direct space methods vs direct methods).

–Emilio Napolitano–
Application of the Diffraction Technique in Solid State Chemistry from
"ab-initio" Structure Solution to Final Structure Refinement
–Powder and Single Crystal–
Doctoral Thesis in Sciences and Chemical Technology, XXIV cycle
University of Sassari

Pag. 142

During the development of these abilities we have addressed the problem to determine the role of phase composition, structure and microstructure of powder materials, especially in terms of average crystallite size extension and lattice microstrain.

Chapter 1. We showed a kinetic study on the phase transformation processes undergone by titanium dioxide powders during the mechanical treatment. X-ray diffraction has been employed to carry out a quantitative characterization of the powder structural evolution by using the so-called Rietveld approach. It is found that the polymorph anatase phase transforms into the high-pressure TiO_2-II form, which in turn transforms into rutile. The kinetic curves have been suitably interpolated by model curves, which allowed the rough evaluation of the apparent rate constants of the phase transformation processes from reactant powders to intermediate and then to final product.

Another application of this kind was dealing with diagenetic and taphonomy effects in palaeontological bones referred to European dinosaurs.

Chapter 2. The diffraction techniques have demonstrated unsurpassed with respect to other spectroscopies in order to give general insights of the bone condition after excavations, that witnesses the post-mortem changes to which the bones could be subjected in the course of the eras. Of course the concomitant approach with other techniques is fundamental in order to describe appropriately the physical and chemical state of these precious fossils.

Chapter 3.This study concerns the structure solution of a simple but still undetermined compound like the magnesium imide MgNH. Although its hexagonal structure was indexed successfully in 1969, the location of atoms in the unit cell was missed because of a wrong attribution of the space group. This

–Emilio Napolitano–
Application of the Diffraction Technique in Solid State Chemistry from
"ab-initio" Structure Solution to Final Structure Refinement
–Powder and Single Crystal–
Doctoral Thesis in Sciences and Chemical Technology, XXIV cycle
University of Sassari

Pag. 143

problem could be easily solved thanks to the modern numerical tools now available, combined with a basic knowledge of the compound chemistry.

Chapter 4. Two boron crystal structures has been proposed like possible solution of a polycrystalline sample composed by different phases. Un-indexed peaks from a complex pattern were successfully attributed to a cubic Boron-based phase, using a whole powder pattern algorithm implemented in Maud. This was precipitated after the hydrogenation reaction of MgB_2 and NaH mixture carried out under extreme conditions in order to propose a hydrogen storage-and-release mechanism within the subject of complex reacting hydrides.

Chapter 5. Structure solution of the iodo-camphor has been solved. This compound is relatively common substrate used in many organic reactions, it was solved ab-initio from synchrotron powder data collected at two different stations in Elettra-Trieste and ESRF-Grenoble respectively. Indexing, structure solution and Rietveld refinement have been performed using Maud software.

Chapter 6. Structure determination of the phosphonium salt $[P(Ph)_3CH_2CN]\cdot BF_4$ has been performed from single crystal data. Two diffraction experiments have been carried out at room temperature and 120K. The compound appeared to be stable, no polymorph transition has been observed. The crystal structure corresponds to a monoclinic one with space group $P12_1/n1$.

Chapter 7. Structure determination of the $C_{21}H_{36}NO_3$ and $C_{27}N_{37}NO_5$ compounds has been carried out with single crystal approach.

The solution achieved suggests standard bond lengths and angles. The structural X-ray analysis and the good quality of the data collected both at 293K and 120K, confirm the stereochemistry of carbon atoms known from literature in the auxiliary chiral (-)-menthyl: C3 (S), C4, C17 (R).

–Emilio Napolitano–
Application of the Diffraction Technique in Solid State Chemistry from
"ab-initio" Structure Solution to Final Structure Refinement
–Powder and Single Crystal–
Doctoral Thesis in Sciences and Chemical Technology, XXIV cycle
University of Sassari

Pag. 144

Two new chiral centers have been identified: C8(S) and C5 (R).

A cis double bond (1.3279(3) Å) has been identified in the azocine ring, in position C12-C15.

Furthermore, the data collected both at 293K and 120K for the $C_{27}H_{37}NO_5$ compound confirm the stereochemistry of carbon atoms in the auxiliary chiral (-)-menthyl: C2 (S), C8, C1 (R) and the presence of two new chiral centers: C5(S) and C7(R).

−Emilio Napolitano−
Application of the Diffraction Technique in Solid State Chemistry from
"ab-initio" Structure Solution to Final Structure Refinement
−Powder and Single Crystal−
Doctoral Thesis in Sciences and Chemical Technology, XXIV cycle
University of Sassari

Pag. 145

Publication

1. *Emilio Napolitano, Gabriele Mulas, Stefano Enzo, Francesco Delogu.*
   Kinetics of mechanically induced anatase-to-rutile phase transformations under inelastic impact conditions.
   Acta Materialia 2010, 58, 3798–3804.

2. *Francesco Dolci, Emilio Napolitano, Eveline Weidner, Stefano Enzo, Pietro Moretto, Michela Brunelli, Thomas Hansen, Maximilian Fichtner, and Wiebke Lohstroh.*
   Magnesium Imide: Synthesis and Structure Determination of an Unconventional Alkaline Earth Imide from Decomposition of Magnesium Amide
   Inorg. Chem. 2011, 50, 1116–1122.

3. *Giampaolo Piga, Andrés Santos-Cubedo, Antonio Brunetti, Massimo Piccinini, Assumpciò Malgosa, Emilio Napolitano, Stefano Enzo.*
   A multi-technique approach by XRD, XRF, FT-IR to characterize the diagenesis of dinosaur bones from Spain.
   Palaeogeography, Palaeoclimatology, Palaeoecology, 2011, Vol 310, Issues 1-2, Pages 92-107.

–Emilio Napolitano–
Application of the Diffraction Technique in Solid State Chemistry from
"ab-initio" Structure Solution to Final Structure Refinement
–Powder and Single Crystal–
Doctoral Thesis in Sciences and Chemical Technology, XXIV cycle
University of Sassari

Pag. 146

Caen, 25 October 2011

Object: PhD work of Emilio Napolitano

Emilio Napolitano did arrive in Trento in January 2011 to work under supervision of Dr. Luca Lutterotti on crystallographic analyses of organic and non-organic compound as part of his thesis work. He has worked at the beginning on finding the structure of a compound, the so-called B48, as a minor phase inside a sample containing several other phases. The job was not easy but using different crystallographic tools he has done a good job identifying a hypothetical structure that match both the experimental data and the chemistry.

From then he helped a lot the development of Maud, the crystallographic software we develop, by suggestion and testing the various modifications against also other crystallographic software (FullProf, Expo, Endeavour etc.). In March he prepared several samples to measure them at the synchrotron of Elettra in Trieste: Iodate Camphor $C_{10}H_{15}IO$ (Dr. Baldino, Dipartimento di Chimica, Università degli studi di Sassari), $[P(Ph)_3CH_2CN]\cdot BF_4$ (Dr. Facchin, Istituto di Scienze e Tecnologie Molecolari, Università degli Studi di Padova) and dinosaur bones from archeological sites in Spain.

He came to Elettra for the measurements of all these samples plus others and did an excellent job after for the analysis of the collected data.

In April he moved to the CRISMAT laboratory of Ensicaen and Université de Caen-Basse Normandie under supervision of Prof. Daniel Chateigner (and again Luca Lutterotti), to continue his work, and made more experiments/analyses on 4-circles laboratory instruments. He is still working here at CRISMAT until the end of October. In the Caen period he learned how to perform single crystal analyses, and collected several pattern on

−Emilio Napolitano–
Application of the Diffraction Technique in Solid State Chemistry from
"ab-initio" Structure Solution to Final Structure Refinement
−Powder and Single Crystal–
Doctoral Thesis in Sciences and Chemical Technology, XXIV cycle
University of Sassari

Pag. 147

other compounds. He learned also how to solve structures from single crystal data using the Jana package with the help of Dr. Olivier Perez, and got introduced to superspace formalism.

In such period he has solved more structures using conventional and less conventional crystallographic methods, helping the development of some new methodologies like hybrid minimization and single crystal like structure factor extractions using texture.

Among the structures solved by him in this period there are:

- Iodate Camphor
- the organic compounds $C_{21}H_{36}NO_3$ e $C_{27}H_{37}NO_5$ (Dr. Muroni, Dipartimento di Chimica, Università degli studi di Sassari) from single crystal
- $[P(Ph)_3CH_2CN]\cdot BF_4$ solved single crystal and with texture under work

In addition he has done other activities using diffraction to:

- monitor structural parameters of hydride compounds at different hydrations
- pattern collection on $Ca_3Co_4O_9$ and $Ca_3Co_4AgO_9$ compounds

Up to now Emilio Napolitano has done an excellent work and becomes quite an expert in the field of solving structures using diffraction techniques. It is worth to mention his dedication to the research work and all the hours spent to test new routines, programs and verification of the analyses performed through different tools. He always wanted to know more and studied in parallel the basis of the crystallographic foundations and method for a better understanding.

Several of his results are now in preparation in corresponding paper for submission to international journals.

Best Regards,

Prof. Daniel Chateigner
CRIMAT-ENSICAEN
Université de Caen Basse-Normandie
France

Dr. Luca Lutterotti
Dipartimento di Ingegneria dei Materiali
Università degli Studi di Trento
Italy

–Emilio Napolitano–
**Application of the Diffraction Technique in Solid State Chemistry from
"ab-initio" Structure Solution to Final Structure Refinement
–Powder and Single Crystal–
Doctoral Thesis in Sciences and Chemical Technology, XXIV cycle
University of Sassari**

Pag. 148

Appendix

–Emilio Napolitano–
Application of the Diffraction Technique in Solid State Chemistry from
"ab-initio" Structure Solution to Final Structure Refinement
–Powder and Single Crystal–
Doctoral Thesis in Sciences and Chemical Technology, XXIV cycle
University of Sassari

Pag. 149

Appendix - A

Fractional atomic coordinates and isotropic displacement parameters (Å^2) [P(Ph)$_3$CH$_2$CN]·BF$_4$ (120 K)

Atom	Occ	x	y	z	U_{iso}*/U_{eq}
P1	1	0.36088(3)	0.35846(4)	0.071068(13)	0.01515(10)
P2	1	0.96525(3)	0.68596(4)	0.185682(13)	0.01455(10)
F1	1	0.40869(8)	0.98046(10)	0.11568(4)	0.0317(3)
F2	1	0.84675(7)	0.33118(9)	0.14406(4)	0.0339(3)
F3	1	0.93324(9)	0.14088(13)	0.16877(4)	0.0458(4)
F4	1	0.91864(9)	0.20365(14)	0.08843(4)	0.0502(5)
N2	1	1.16121(12)	0.45404(17)	0.17336(6)	0.0361(5)
F5	1	0.80103(9)	0.10525(11)	0.12438(4)	0.0418(4)
N1	1	0.16298(14)	0.12760(19)	0.09403(7)	0.0460(6)
C2	1	1.13988(13)	1.03052(18)	0.26362(6)	0.0275(5)
C3	1	0.82545(12)	0.62462(17)	0.24342(6)	0.0228(4)
F6	1	0.51200(13)	0.9204(3)	0.17756(7)	0.1157(10)
F8	1	0.39145(11)	1.03725(14)	0.19447(5)	0.0585(5)
C6	1	0.64712(13)	0.46125(18)	0.13023(7)	0.0274(5)
C7	1	0.36204(17)	0.05820(18)	-0.06071(6)	0.0379(7)
C8	1	0.85287(10)	0.69815(14)	0.20257(5)	0.0160(4)
C9	1	0.59215(13)	0.57009(19)	0.10969(7)	0.0292(5)
C10	1	0.28229(17)	0.09897(18)	-0.04319(7)	0.0351(6)
C11	1	0.22537(13)	0.19296(18)	0.10603(6)	0.0270(5)
C12	1	1.05228(13)	1.01665(17)	0.27402(6)	0.0259(5)
C13	1	0.99402(13)	0.86647(18)	0.05322(6)	0.0282(5)
C14	1	1.09121(12)	0.47345(16)	0.18603(6)	0.0230(5)
C15	1	0.61387(12)	0.32146(18)	0.13336(6)	0.0252(5)
C16	1	0.50536(12)	0.54052(16)	0.09194(6)	0.0238(5)
C17	1	1.12452(12)	0.83047(18)	0.20782(6)	0.0248(5)
C18	1	0.96932(13)	0.75539(19)	0.02097(6)	0.0278(5)
C-11	1	0.79289(11)	0.78848(15)	0.17547(6)	0.0195(4)
C-20	1	0.23412(15)	0.74554(19)	0.07191(8)	0.0369(6)
C-10	1	0.99832(12)	0.90969(16)	0.25130(6)	0.0200(4)
C-12	1	0.70645(11)	0.80342(16)	0.18925(6)	0.0219(4)
C-14	1	0.73833(12)	0.64081(18)	0.25653(7)	0.0255(5)
C-5	1	0.94325(13)	0.62297(18)	0.03893(6)	0.0264(5)
C-13	1	1.17737(14)	0.93711(19)	0.23069(7)	0.0299(5)
C-4	1	0.44211(17)	0.10782(19)	-0.03942(7)	0.0349(6)

C-17	1	0.47170(11)	0.39997(15)	0.09509(5)	0.0174(4)
C-21	1	0.22084(15)	0.77746(19)	0.02270(8)	0.0369(6)
C-1	1	0.28179(14)	0.19007(18)	-0.00307(6)	0.0282(5)
F7	1	0.37365(17)	0.81145(17)	0.17035(7)	0.1001(9)
C-23	1	0.29110(14)	0.55440(19)	0.00232(7)	0.0299(5)
C-3	1	0.44377(13)	0.19940(17)	0.00150(6)	0.0241(5)
C-19	1	0.27505(13)	0.61659(17)	0.08709(7)	0.0277(5)
C-6	1	0.94313(12)	0.59981(17)	0.08886(6)	0.0219(4)
C-2	1	0.36334(11)	0.23913(15)	0.01968(5)	0.0192(4)
C-16	1	0.52708(12)	0.28967(16)	0.11613(6)	0.0216(4)
B19	1	0.42176(15)	0.93128(19)	0.16385(8)	0.0294(6)
C-15	1	0.67891(12)	0.72990(16)	0.22961(6)	0.0228(5)
C-9	1	1.03475(10)	0.81696(15)	0.21792(5)	0.0171(4)
C-7	1	0.99373(12)	0.84595(16)	0.10330(6)	0.0211(4)
B23	1	0.87640(14)	0.19360(19)	0.13108(7)	0.0238(5)
C-22	1	0.24904(15)	0.6835(2)	-0.01194(8)	0.0381(6)
C-24	1	0.30662(11)	0.27298(16)	0.12101(6)	0.0187(4)
C-18	1	0.30246(11)	0.52001(15)	0.05204(5)	0.0180(4)
C-25	1	1.00255(11)	0.50336(15)	0.20198(6)	0.0184(4)
C-8	1	0.96935(10)	0.71195(15)	0.12121(5)	0.0167(4)
H1-c-16	1	0.5040(14)	0.1921(19)	0.1194(7)	0.026(5)
H1-c2	1	1.1734(14)	1.105(2)	0.2800(8)	0.030(5)
H1-c-11	1	0.8129(15)	0.843(2)	0.1486(8)	0.031(5)
H1-c18	1	0.9730(15)	0.767(2)	-0.0143(8)	0.033(5)
H1-c-22	1	0.2437(19)	0.706(2)	-0.0468(10)	0.059(7)
H1-c-21	1	0.1891(17)	0.864(2)	0.0151(8)	0.043(6)
H1-c16	1	0.4645(14)	0.6153(19)	0.0795(7)	0.025(5)
H1-c7	1	0.3660(16)	-0.009(2)	-0.0884(9)	0.044(6)
H1-c-25	1	0.9609(15)	0.4399(19)	0.1866(7)	0.028(5)
H1-c-5	1	0.9242(13)	0.5501(19)	0.0168(7)	0.024(5)
H1-c-24	1	0.3489(16)	0.210(2)	0.1360(8)	0.038(6)
H1-c-4	1	0.4972(17)	0.087(2)	-0.0499(9)	0.041(6)
H1-c10	1	0.2302(17)	0.061(2)	-0.0595(8)	0.040(6)
H2-c-25	1	1.0040(13)	0.4934(18)	0.2381(7)	0.022(4)
H1-c-10	1	0.9376(15)	0.9003(18)	0.2571(7)	0.025(5)
H1-c-3	1	0.4988(14)	0.2364(18)	0.0149(7)	0.021(4)
H2-c-3	1	0.8680(14)	0.5610(19)	0.2602(7)	0.029(5)
H1-c-15	1	0.6194(13)	0.7403(17)	0.2399(6)	0.016(4)
H1-c-14	1	0.7208(14)	0.5944(19)	0.2822(8)	0.025(5)
H1-c-7	1	1.0117(13)	0.9215(17)	0.1249(7)	0.018(4)
H1-c-12	1	1.0238(14)	1.0852(19)	0.2974(7)	0.024(5)
H1-c-13	1	1.0147(17)	0.963(2)	0.0402(9)	0.046(6)

–Emilio Napolitano–
Application of the Diffraction Technique in Solid State Chemistry from
"ab-initio" Structure Solution to Final Structure Refinement
–Powder and Single Crystal–
Doctoral Thesis in Sciences and Chemical Technology, XXIV cycle
University of Sassari

Pag. 151

H1-c-1	1	0.2222(15)	0.2188(19)	0.0082(8)	0.030(5)
H2-c-15	1	0.6514(13)	0.2498(19)	0.1475(7)	0.023(5)
H1-c-23	1	0.3102(14)	0.4879(19)	-0.0217(7)	0.026(5)
H2-c-13	1	1.2327(16)	0.9451(19)	0.2228(8)	0.029(5)
H1-c17	1	1.1488(14)	0.7679(19)	0.1850(7)	0.028(5)
H1-c-6	1	0.9263(14)	0.508(2)	0.1022(7)	0.030(5)
H1-c6	1	0.7055(15)	0.4826(18)	0.1427(7)	0.026(5)
H2-c-24	1	0.2942(14)	0.3456(19)	0.1419(7)	0.024(5)
H1-c-19	1	0.2879(16)	0.597(2)	0.1212(9)	0.039(6)
H1-c-20	1	0.2182(17)	0.807(2)	0.0957(9)	0.048(6)
H2-c-12	1	0.6619(16)	0.867(2)	0.1700(8)	0.038(6)
H2-c9	1	0.6194(16)	0.666(2)	0.1060(8)	0.044(6)

Anisotropic atomic displacement parameters ($Å^2$) [P(Ph)$_3$CH$_2$CN]·BF$_4$ (120 K)

Atom	U^{11}	U^{22}	U^{33}	U^{12}	U^{13}	U^{23}
P1	0.01584(19)	0.01478(16)	0.01476(16)	0.00156(13)	0.00069(13)	-1.02(12)E-3
P2	0.01367(18)	0.01631(16)	0.01371(16)	0.00017(13)	0.00121(13)	-1.0(12)E-4
F1	0.0412(7)	0.0291(5)	0.0256(5)	0.0034(4)	0.0069(5)	0.0015(4)
F2	0.0283(6)	0.0183(4)	0.0549(7)	-0.0017(4)	0.0016(5)	-0.0036(4)
F3	0.0475(8)	0.0595(7)	0.0287(6)	0.0249(6)	-0.0076(5)	0.0049(5)
F4	0.0494(9)	0.0718(8)	0.0311(6)	0.0177(6)	0.0145(6)	0.0128(5)
N2	0.0294(9)	0.0379(8)	0.0416(9)	0.0095(6)	0.0071(7)	-0.0033(7)
F5	0.0556(8)	0.0284(5)	0.0404(6)	-0.0172(5)	-0.0038(6)	-0.0081(4)
N1	0.0418(11)	0.0522(10)	0.0448(10)	-0.0191(8)	0.0088(9)	-0.0044(8)
C2	0.0293(10)	0.0258(8)	0.0263(8)	-0.0064(6)	-0.0042(7)	-0.0054(6)
C3	0.0218(8)	0.0265(8)	0.0208(7)	0.0036(6)	0.0052(6)	0.0076(6)
F6	0.0372(10)	0.234(2)	0.0730(12)	0.0569(12)	-0.0137(10)	-0.0081(13)
F8	0.0789(11)	0.0658(8)	0.0300(6)	0.0269(7)	-0.0011(7)	0.0026(6)
C6	0.0201(9)	0.0341(9)	0.0273(8)	-0.0027(6)	-0.0035(7)	-0.0017(7)
C7	0.0779(17)	0.0175(7)	0.0173(8)	0.0076(8)	-0.0024(9)	-0.0013(6)
C8	0.0146(7)	0.0178(6)	0.0155(6)	-0.0006(5)	0.0016(5)	-0.0008(5)
C9	0.0261(9)	0.0278(8)	0.0326(9)	-0.0074(7)	-0.0047(7)	0.0032(7)
C10	0.0587(14)	0.0253(8)	0.0201(8)	-0.0102(8)	-0.0053(9)	-0.0015(6)
C11	0.0270(9)	0.0268(8)	0.0280(8)	-0.0033(6)	0.0072(7)	0.0012(6)
C12	0.0312(10)	0.0227(7)	0.0229(8)	0.0034(6)	-0.0037(7)	-0.0063(6)
C13	0.0353(10)	0.0277(8)	0.0213(8)	-0.0025(7)	0.0009(7)	0.0075(6)
C14	0.0224(9)	0.0219(7)	0.0246(8)	0.0048(6)	0.0006(6)	-0.0019(6)

–Emilio Napolitano–
Application of the Diffraction Technique in Solid State Chemistry from
"ab-initio" Structure Solution to Final Structure Refinement
–Powder and Single Crystal–
Doctoral Thesis in Sciences and Chemical Technology, XXIV cycle
University of Sassari

Pag. 152

C15	0.0215(8)	0.0279(8)	0.0253(8)	0.0055(6)	-0.0029(7)	0.0001(6)
C16	0.0246(9)	0.0209(7)	0.0251(8)	-0.0019(6)	-0.0027(7)	0.0038(6)
C17	0.0199(8)	0.0295(8)	0.0252(8)	-0.0036(6)	0.0027(6)	-0.0070(6)
C18	0.0299(10)	0.0379(9)	0.0157(7)	0.0010(7)	0.0017(7)	0.0031(6)
C-11	0.0200(8)	0.0200(7)	0.0186(7)	0.0024(5)	0.0026(6)	0.0021(5)
C-20	0.0477(13)	0.0215(8)	0.0433(11)	0.0121(8)	0.0149(10)	0.0039(8)
C-10	0.0193(8)	0.0229(7)	0.0175(7)	0.0020(5)	0.0003(6)	-0.0026(5)
C-12	0.0178(8)	0.0233(7)	0.0244(7)	0.0044(6)	-0.0004(6)	-0.0012(6)
C-14	0.0229(9)	0.0287(8)	0.0261(8)	0.0004(6)	0.0103(7)	0.0051(6)
C-5	0.0297(10)	0.0299(8)	0.0196(7)	-0.0023(7)	0.0014(7)	-0.0065(6)
C-13	0.0201(9)	0.0389(10)	0.0306(9)	-0.0086(7)	0.0025(7)	-0.0074(7)
C-4	0.0556(14)	0.0277(9)	0.0223(8)	0.0228(8)	0.0093(9)	0.0034(6)
C-17	0.0166(7)	0.0193(6)	0.0162(6)	0.0000(5)	0.0001(5)	-0.0008(5)
C-21	0.0362(11)	0.0247(8)	0.0501(12)	0.0111(7)	0.0061(9)	0.0157(8)
C-1	0.0349(11)	0.0279(8)	0.0211(8)	-0.0060(7)	-0.0023(7)	-0.0016(6)
F7	0.166(2)	0.0586(9)	0.0701(11)	-0.0493(11)	-0.0270(12)	0.0310(8)
C-23	0.0374(11)	0.0286(8)	0.0229(8)	0.0078(7)	-0.0023(7)	0.0025(6)
C-3	0.0322(10)	0.0227(7)	0.0178(7)	0.0088(6)	0.0043(7)	0.0022(5)
C-19	0.0380(11)	0.0199(7)	0.0260(8)	0.0077(6)	0.0073(7)	0.0025(6)
C-6	0.0254(9)	0.0226(7)	0.0177(7)	-0.0044(6)	0.0022(6)	-0.0018(5)
C-2	0.0276(9)	0.0152(6)	0.0149(6)	0.0020(5)	0.0017(6)	-0.0008(5)
C-16	0.0209(8)	0.0194(7)	0.0240(7)	0.0016(5)	-0.0012(6)	0.0006(5)
B19	0.0344(12)	0.0189(8)	0.0332(10)	0.0036(7)	-0.0088(9)	0.0027(7)
C-15	0.0168(8)	0.0231(7)	0.0291(8)	0.0007(6)	0.0051(7)	-0.0041(6)
C-9	0.0175(7)	0.0184(6)	0.0153(6)	-0.0007(5)	0.0010(5)	0.0008(5)
C-7	0.0265(9)	0.0183(7)	0.0184(7)	-0.0009(6)	0.0013(6)	0.0006(5)
B23	0.0297(10)	0.0215(8)	0.0198(8)	0.0028(7)	-0.0008(7)	0.0002(6)
C-22	0.0453(13)	0.0365(10)	0.0316(10)	0.0095(8)	-0.0028(9)	0.0139(8)
C-24	0.0207(8)	0.0169(6)	0.0186(7)	0.0029(5)	0.0028(6)	0.0011(5)
C-18	0.0177(7)	0.0160(6)	0.0200(7)	0.0006(5)	0.0001(6)	0.0022(5)
C-25	0.0179(8)	0.0177(6)	0.0194(7)	0.0025(5)	0.0005(6)	0.0004(5)
C-8	0.0144(7)	0.0209(7)	0.0149(6)	0.0012(5)	0.0019(5)	0.0003(5)

–Emilio Napolitano–
Application of the Diffraction Technique in Solid State Chemistry from
"ab-initio" Structure Solution to Final Structure Refinement
–Powder and Single Crystal–
Doctoral Thesis in Sciences and Chemical Technology, XXIV cycle
University of Sassari

Pag. 153

Appendix - B

Fractional atomic coordinates and isotropic displacement parameters (Å^2) $C_{21}H_{36}NO_3$ (120 K).

Atom	x	y	z	U_{iso}*/U_{eq}
O1	0.42300(10)	0.13367(16)	0.87519(5)	0.0197(4)
O3	0.54453(12)	0.46906(17)	0.82629(5)	0.0270(4)
O2	0.41147(11)	0.10129(18)	0.78184(5)	0.0275(5)
N1	0.67942(13)	0.06939(19)	0.86739(6)	0.0189(5)
C2	0.47202(16)	0.1300(2)	0.82383(7)	0.0177(5)
C3	0.26773(16)	0.0058(3)	0.93486(7)	0.0205(6)
C4	0.28887(15)	0.1046(2)	0.88036(7)	0.0193(6)
C5	0.61321(15)	0.1647(2)	0.82468(7)	0.0177(5)
C6	0.66445(16)	0.1277(3)	0.76551(7)	0.0230(6)
C7	0.22270(17)	0.2769(3)	0.88012(8)	0.0243(6)
C8	0.63654(16)	0.3512(3)	0.84413(7)	0.0199(6)
C9	0.63903(17)	0.3406(3)	0.90812(7)	0.0226(6)
C10	0.12688(17)	-0.0237(3)	0.94026(8)	0.0266(6)
C11	0.67762(17)	-0.1185(2)	0.86622(8)	0.0237(6)
C12	0.80393(18)	0.1375(3)	0.76217(8)	0.0264(6)
C13	0.67032(16)	0.1543(3)	0.92197(7)	0.0216(6)
C14	0.34512(17)	-0.1601(3)	0.93834(8)	0.0270(6)
C15	0.87866(17)	0.0060(3)	0.77275(8)	0.0280(7)
C16	0.05443(17)	0.1437(3)	0.93821(8)	0.0281(7)
C17	0.08252(18)	0.2495(3)	0.88583(8)	0.0288(7)
C18	0.80133(18)	-0.1981(3)	0.85000(8)	0.0281(7)
C19	0.83916(18)	-0.1733(3)	0.78841(8)	0.0312(7)
C20	0.0140(2)	0.4208(3)	0.88677(10)	0.0455(9)
C21	0.3221(2)	-0.2550(3)	0.99331(10)	0.0415(8)
C22	0.3273(2)	-0.2777(3)	0.88870(10)	0.0454(9)
H1-c20	0.0404	0.5038	0.9197	0.037995
H1-c19	0.9195	-0.2551	0.7801	0.037995
H2-c20	0.0286	0.4909	0.8535	0.037995
H1-c18	0.8706	-0.1513	0.875	0.037995
H1-c21	0.3752	-0.3559	0.9936	0.037995
H2-c21	0.236	-0.3279	0.9938	0.037995
H2-c18	0.9787	0.0116	0.768	0.037995
H3-c20	-0.0656	0.4115	0.8876	0.037995
H3-c18	0.8253	-0.3209	0.8584	0.037995
H3-c21	0.3383	-0.1722	1.0296	0.037995

–Emilio Napolitano–
Application of the Diffraction Technique in Solid State Chemistry from
"ab-initio" Structure Solution to Final Structure Refinement
–Powder and Single Crystal–
Doctoral Thesis in Sciences and Chemical Technology, XXIV cycle
University of Sassari

Pag. 154

H4-c20	0.1005	-0.1037	0.9754	0.037995
H1-c16	-0.0467	0.1197	0.9415	0.037995
H1-c17	0.0504	0.1697	0.8506	0.037995
H1-c22	0.2464	-0.3443	0.8991	0.037995
H1-c10	0.0853	-0.1189	0.9099	0.037995
H1-c12	0.8548	0.2591	0.7492	0.037995
H1-c7	0.2481	0.3473	0.9122	0.037995
H2-c19	0.7684	-0.2139	0.7631	0.037995
H1-c9	0.6898	0.4199	0.9249	0.037995
H2-c7	0.2423	0.3452	0.8443	0.037995
H1-c14	0.4351	-0.136	0.9387	0.037995
H2-c16	0.0844	0.2361	0.9713	0.037995
H2-c9	0.5595	0.383	0.9237	0.037995
H1-c13	0.7508	0.1306	0.9454	0.037995
H1-c11	0.6587	-0.1672	0.9064	0.037995
H2-c13	0.6079	0.1023	0.9509	0.037995
H1-c8	0.7299	0.39	0.8339	0.037995
H2-c22	0.3419	-0.2384	0.852	0.037995
H1-c3	0.2918	0.0956	0.9677	0.037995
H3-c22	0.3625	-0.3872	0.8898	0.037995
H1-c4	0.2615	0.0216	0.849	0.037995
H2-c11	0.6187	-0.1677	0.839	0.037995
H1-c6	0.6338	0.2185	0.7373	0.037995
H1-o3	0.5669	0.5031	0.7864	0.037995
H2-o6	0.6419	0.0118	0.7525	0.037995

Anisotropic atomic displacement parameters ($\mathring{A}^2$) $C_{21}H_{36}NO_3$ (120 K).

Atom	U^{11}	U^{22}	U^{33}	U^{12}	U^{13}	U^{23}
O1	0.0153(6)	0.0253(8)	0.0185(7)	-0.0003(6)	0.0021(5)	0.0009(6)
O3	0.0316(7)	0.0230(8)	0.0263(7)	0.0072(6)	0.0062(6)	0.0077(6)
O2	0.0193(7)	0.0425(10)	0.0206(7)	0.0016(6)	-0.0017(6)	-0.0019(7)
N1	0.0182(7)	0.0193(9)	0.0193(8)	0.0015(6)	0.0004(6)	0.0001(7)
C2	0.0199(9)	0.0159(10)	0.0171(9)	0.0049(8)	0.0016(8)	0.0016(8)
C3	0.0193(9)	0.0218(11)	0.0202(10)	-0.0012(8)	0.0030(8)	-0.0017(9)
C4	0.0143(9)	0.0227(11)	0.0210(10)	-0.0013(8)	0.0015(7)	-0.0005(8)
C5	0.0153(9)	0.0202(10)	0.0175(9)	-0.0003(7)	0.0026(7)	0.0026(9)
C6	0.0239(10)	0.0262(12)	0.0190(9)	0.0019(9)	0.0049(8)	-0.0002(9)
C7	0.0252(10)	0.0247(12)	0.0230(10)	0.0031(9)	0.0009(8)	0.0031(9)
C8	0.0185(9)	0.0172(10)	0.0241(10)	0.0003(8)	0.0031(8)	0.0034(8)
C9	0.0239(10)	0.0219(11)	0.0221(10)	-0.0003(9)	0.0024(8)	-0.0042(9)

–**Emilio Napolitano**–
Application of the Diffraction Technique in Solid State Chemistry from
"ab-initio" Structure Solution to Final Structure Refinement
–**Powder and Single Crystal**–
Doctoral Thesis in Sciences and Chemical Technology, XXIV cycle
University of Sassari

Pag. 155

C10	0.0172(9)	0.0263(12)	0.0364(12)	-0.0032(9)	0.0055(8)	0.0016(10)
C11	0.0215(9)	0.0205(11)	0.0289(10)	-0.0003(8)	-0.0019(8)	0.0030(9)
C12	0.0250(10)	0.0350(13)	0.0192(9)	-0.0066(10)	0.0068(8)	-0.0053(10)
C13	0.0216(10)	0.0260(11)	0.0172(9)	0.0001(9)	-0.0004(8)	0.0012(8)
C14	0.0214(10)	0.0229(11)	0.0366(11)	0.0033(9)	0.0069(9)	0.0057(10)
C15	0.0180(9)	0.0399(14)	0.0263(11)	-0.0009(9)	0.0054(8)	-0.0087(10)
C16	0.0192(10)	0.0296(12)	0.0356(12)	0.0027(9)	0.0067(8)	0.0009(10)
C17	0.0198(10)	0.0357(13)	0.0309(12)	0.0047(9)	-0.0024(8)	-0.0001(10)
C18	0.0236(10)	0.0194(11)	0.0413(12)	0.0074(8)	-0.0017(9)	-0.0010(9)
C19	0.0218(10)	0.0324(13)	0.0395(12)	0.0033(9)	0.0019(9)	-0.0112(11)
C20	0.0268(11)	0.0537(18)	0.0559(16)	0.0181(11)	0.0052(11)	0.0170(13)
C21	0.0437(14)	0.0324(14)	0.0483(14)	0.0073(12)	0.0048(12)	0.0154(11)
C22	0.0688(17)	0.0200(13)	0.0475(15)	0.0037(12)	0.0196(13)	-0.0027(10)

Geometric parameters (Å) $C_{21}H_{36}NO_3$ (120 K)

Atom1-2	Bond/ Å
O1-C2	1.336(2)
O1-C4	1.469(2)
O3-C8	1.418(2)
O2-C2	1.218(2)
N1-C5	1.450(2)
N1-C11	1.464(2)
N1-C13	1.465(2)
C2-C5	1.546(2)
C3-C4	1.530(3)
C3-C10	1.541(2)
C3-C14	1.541(3)
C4-C7	1.520(3)
C4-H1	1.0326(18)
C5-C6	1.545(2)
C5-C8	1.546(3)
C6-C12	1.508(3)
C6-H1	1.0319(19)
C6-H2	0.985(2)
C7-C17	1.532(3)
C7-H1	0.9825(19)
C7-H2	1.0290(19)
C8-C9	1.531(2)
C9-C13	1.527(3)

–Emilio Napolitano–
Application of the Diffraction Technique in Solid State Chemistry from
"ab-initio" Structure Solution to Final Structure Refinement
–Powder and Single Crystal–
Doctoral Thesis in Sciences and Chemical Technology, XXIV cycle
University of Sassari

Pag. 156

C9-H1	0.9179(19)
C9-H2	0.9912(19)
C10-C16	1.522(3)
C11-C18	1.521(3)
C11-H2	0.9877(18)
C12-C15	1.328(3)
C13-H1	1.0495(17)
C13-H2	1.0465(18)
C14-C21	1.527(3)
C14-C22	1.511(3)
C14-H1	0.9876(19)
C15-C19	1.508(3)
C16-C17	1.528(3)
C17-C20	1.526(3)
C18-C19	1.539(3)
C18-H1	1.023(2)
C18-H3	1.012(2)
C19-H2	1.024(2)
C20-H2	0.976(2)
C20-H3	0.861(2)
C21-H1	0.972(2)
C22-H1	1.045(2)
C22-H2	0.942(2)
C22-H3	0.934(2)

Geometric parameters (°) $C_{21}H_{36}NO_3$ (120 K)

Atom1-2-3	Angle/°
C2-O1-C4	117.60(13)
C5-N1-C11	119.51(14)
C5-N1-C13	111.20(14)
C11-N1-C13	117.87(14)
O1-C2-O2	123.26(15)
O1-C2-C5	111.94(14)
O2-C2-C5	124.80(16)
C4-C3-C10	107.04(14)
C4-C3-C14	112.83(15)
C10-C3-C14	113.82(16)
O1-C4-C3	107.21(13)

–Emilio Napolitano–
Application of the Diffraction Technique in Solid State Chemistry from
"ab-initio" Structure Solution to Final Structure Refinement
–Powder and Single Crystal–
Doctoral Thesis in Sciences and Chemical Technology, XXIV cycle
University of Sassari

Pag. 157

O1-C4-C7	109.00(15)
O1-C4-H1-c4	108.50(14)
C3-C4-C7	112.22(15)
C3-C4-H1-c4	104.99(16)
C7-C4-H1-c4	114.59(15)
N1-C5-C2	113.83(14)
N1-C5-C6	111.84(14)
N1-C5-C8	100.97(13)
C2-C5-C6	107.90(14)
C2-C5-C8	109.18(14)
C6-C5-C8	113.10(15)
C5-C6-C12	113.30(14)
C5-C6-H1-c6	110.80(16)
C5-C6-H2-o6	111.79(16)
C12-C6-H1-c6	104.47(16)
C12-C6-H2-o6	106.00(17)
H1-c6-C6-H2-o6	110.15(17)
C4-C7-C17	109.83(16)
C4-C7-H1-c7	111.09(17)
C4-C7-H2-c7	111.35(16)
C17-C7-H1-c7	106.45(16)
C17-C7-H2-c7	110.39(16)
H1-c7-C7-H2-c7	107.60(19)
O3-C8-C5	113.89(14)
O3-C8-C9	110.32(14)
C5-C8-C9	104.61(15)
C8-C9-C13	105.74(15)
C8-C9-H1-c9	114.22(17)
C8-C9-H2-c9	109.97(16)
C13-C9-H1-c9	114.43(17)
C13-C9-H2-c9	115.26(17)
H1-c9-C9-H2-c9	97.36(17)
C3-C10-C16	112.03(17)
N1-C11-C18	113.65(15)
N1-C11-H2-c11	114.17(16)
C18-C11-H2-c11	103.76(16)
C6-C12-C15	123.77(19)
N1-C13-C9	104.56(14)
N1-C13-H1-c13	109.93(15)
N1-C13-H2-c13	117.14(17)
C9-C13-H1-c13	117.73(17)
C9-C13-H2-c13	111.65(16)

–Emilio Napolitano–
Application of the Diffraction Technique in Solid State Chemistry from
"ab-initio" Structure Solution to Final Structure Refinement
–Powder and Single Crystal–
Doctoral Thesis in Sciences and Chemical Technology, XXIV cycle
University of Sassari

Pag. 158

H1-c13-C13-H2-c13	96.38(14)
C3-C14-C21	111.38(16)
C3-C14-C22	113.43(16)
C3-C14-H1-c14	111.84(18)
C21-C14-C22	111.13(18)
C21-C14-H1-c14	104.17(17)
C22-C14-H1-c14	104.29(18)
C12-C15-C19	126.23(18)
C10-C16-C17	112.77(16)
C7-C17-C16	110.09(16)
C7-C17-C20	110.91(18)
C16-C17-C20	111.33(17)
C11-C18-C19	115.13(16)
C11-C18-H1-c18	110.19(17)
C11-C18-H3-c18	124.00(18)
C19-C18-H1-c18	108.71(17)
C19-C18-H3-c18	103.98(17)
H1-c18-C18-H3-c18	91.94(16)
C15-C19-C18	115.36(17)
C15-C19-H2-c19	110.50(18)
C18-C19-H2-c19	109.21(17)
C17-C20-H2-c20	113.6(2)
C17-C20-H3-c20	114.2(2)
H2-c20-C20-H3-c20	103.1(2)
C14-C21-H1-c21	107.5(2)
C14-C22-H1-c22	102.71(19)
C14-C22-H2-c22	120.8(2)
C14-C22-H3-c22	118.8(2)
H1-c22-C22-H2-c22	121.6(2)
H1-c22-C22-H3-c22	83.05(18)
H2-c22-C22-H3-c22	104.7(2)

–Emilio Napolitano–
Application of the Diffraction Technique in Solid State Chemistry from
"ab-initio" Structure Solution to Final Structure Refinement
–Powder and Single Crystal–
Doctoral Thesis in Sciences and Chemical Technology, XXIV cycle
University of Sassari

Pag. 159

Appendix - C

Fractional atomic coordinates and isotropic displacement parameters ($Å^2$) $C_{27}H_{37}NO_5$ (120 K).

Atom	x	y	z	$U_{iso}*/U_{eq}$
O1	0.4123(5)	0.8811	0.2102(3)	0.0184(11)
O2	0.4585(5)	0.9500(2)	0.4197(4)	0.0222(11)
O3	0.7177(3)	1.2104(2)	0.28567(19)	0.0244(12)
O4	0.2120(5)	1.0868(2)	0.2416(4)	0.0261(12)
O5	0.4995(5)	1.1924(2)	0.1271(4)	0.0266(12)
N1	0.5353(3)	1.00701(7)	0.04994(9)	0.0170(12)
C2	0.26377(11)	0.7529(2)	0.2040(2)	0.0196(15)
C7	0.6026(4)	1.07858(9)	0.27694(9)	0.0169(14)
C3	0.55910(13)	0.76309(3)	0.30822(5)	0.0207(16)
C4	0.24457(5)	0.67147(2)	0.28536(4)	0.0217(16)
C5	0.4787(6)	1.0229(3)	0.1917(5)	0.0151(14)
C6	0.4513(6)	0.9478(3)	0.2901(5)	0.0158(14)
C1	0.5972(7)	1.1652(3)	0.2176(5)	0.0183(15)
C8	0.3913(4)	0.80414(11)	0.29020(8)	0.0186(15)
C9	0.3019(2)	1.05868(9)	0.1545(6)	0.0203(15)
C10	0.54759(4)	0.68075(5)	0.38550(4)	0.0211(16)
C11	0.412878(19)	0.62823(4)	0.30717(4)	0.0233(16)
C12	0.69227(3)	0.96608(4)	0.04336(2)	0.0217(16)
C13	0.77827(5)	1.03966(3)	0.27795(5)	0.0224(16)
C14	0.71566(3)	0.63848(3)	0.40620(3)	0.0263(17)
C15	0.9010(6)	1.4128(3)	0.3298(4)	0.0260(17)
C16	0.8895(6)	1.3311(2)	0.2887(2)	0.0210(16)
C17	0.39470(5)	0.98520(4)	-0.05096(8)	0.0194(15)
C18	0.72132(14)	1.29526(6)	0.24386(10)	0.0273(17)
C19	0.82445(4)	1.01885(3)	0.12449(3)	0.0237(16)
C20	0.09808(4)	0.79846(2)	0.16681(4)	0.0210(15)
C21	0.02222(2)	0.835790(14)	0.30495(2)	0.0275(18)
C22	1.0320(5)	1.2837(3)	0.2867(4)	0.0266(18)
C23	0.26028(6)	1.04392(2)	-0.00548(7)	0.0235(16)
C24	1.1842(6)	1.3196(3)	0.3208(4)	0.036(2)
C25	-0.02868(2)	0.743736(12)	0.08619(2)	0.0285(18)
C26	1.1954(6)	1.4013(3)	0.3592(4)	0.036(2)
C27	1.0541(5)	1.4480(3)	0.3624(4)	0.0323(19)
H1c2	0.3026	0.7413	0.1098	0.02351

–Emilio Napolitano–
Application of the Diffraction Technique in Solid State Chemistry from
"ab-initio" Structure Solution to Final Structure Refinement
–Powder and Single Crystal–
Doctoral Thesis in Sciences and Chemical Technology, XXIV cycle
University of Sassari

Pag. 160

H1c7	0.5721	1.0834	0.3755	0.020297
H1c3	0.6361	0.798	0.3629	0.024825
H2c3	0.6025	0.7549	0.2146	0.024825
H1c4	0.2008	0.682	0.3781	0.025993
H2c4	0.1671	0.6368	0.2306	0.025993
H1c8	0.3518	0.8128	0.3851	0.022271
H1c10	0.5144	0.69	0.4824	0.025358
H1c11	0.4499	0.6115	0.2147	0.027922
H2c11	0.3993	0.5784	0.3604	0.027922
H1c12	0.719	0.9606	-0.0561	0.026081
H2c12	0.6868	0.9137	0.09	0.026081
H1c13	0.8594	1.077	0.3214	0.026932
H2c13	0.7807	0.9908	0.3358	0.026932
H1c14	0.7026	0.5875	0.4561	0.031539
H2c14	0.7589	0.6282	0.3132	0.031539
H3c14	0.7922	0.6729	0.4625	0.031539
H1c15	0.8011	1.4448	0.3353	0.031252
H1c17	0.3609	0.9299	-0.0329	0.02328
H2c17	0.4222	0.9976	-0.1483	0.02328
H1c18	0.6358	1.3246	0.2907	0.032748
H2c18	0.7017	1.2996	0.1405	0.032748
H1c19	0.9301	0.9909	0.1286	0.028405
H2c19	0.8399	1.0685	0.0713	0.028405
H1c20	0.1242	0.843	0.1042	0.025188
H1c21	0.1037	0.8705	0.3548	0.033053
H2c21	-0.0755	0.8673	0.2762	0.033053
H3c21	-0.008	0.7924	0.3684	0.033053
H1c22	1.0248	1.2267	0.2619	0.031958
H1c23	0.2685	1.0945	-0.0575	0.028195
H2c23	0.1527	1.0181	-0.0184	0.028195
H1c24	1.2844	1.2875	0.318	0.042603
H1c25	-0.1301	0.7739	0.0642	0.034141
H2c25	0.0156	0.7252	-0.0024	0.034141
H3c25	-0.052	0.6974	0.1456	0.034141
H1c26	1.3029	1.4254	0.3838	0.043133
H1c27	1.0619	1.505	0.3873	0.038818

–Emilio Napolitano–
Application of the Diffraction Technique in Solid State Chemistry from
"ab-initio" Structure Solution to Final Structure Refinement
–Powder and Single Crystal–
Doctoral Thesis in Sciences and Chemical Technology, XXIV cycle
University of Sassari

Pag. 161

Anisotropic atomic displacement parameters (Å^2) $C_{27}H_{37}NO_5$ (120 K).

Atom	U^{11}	U^{22}	U^{33}	U^{12}	U^{13}	U^{23}
O1	0.024(2)	0.0105(17)	0.0211(18)	-0.0018(15)	0.0034(15)	0.0004(14)
O2	0.028(2)	0.0161(18)	0.0225(19)	-0.0024(16)	0.0003(16)	0.0003(15)
O3	0.028(2)	0.0098(18)	0.034(2)	-0.0067(16)	-0.0105(17)	0.0039(15)
O4	0.018(2)	0.027(2)	0.034(2)	0.0041(16)	0.0057(17)	-0.0038(18)
O5	0.026(2)	0.0142(18)	0.039(2)	-0.0034(15)	-0.0084(18)	0.0031(16)
N1	0.017(2)	0.012(2)	0.022(2)	-0.0003(16)	0.0027(17)	-0.0035(16)
C2	0.025(3)	0.012(2)	0.023(3)	-0.001(2)	0.007(2)	-0.001(2)
C7	0.017(3)	0.014(2)	0.020(2)	-0.0027(19)	0.000(2)	0.001(2)
C3	0.021(3)	0.016(3)	0.026(3)	0.000(2)	0.002(2)	0.002(2)
C4	0.024(3)	0.013(3)	0.029(3)	-0.006(2)	0.005(2)	0.001(2)
C5	0.015(2)	0.011(2)	0.020(2)	-0.0013(19)	0.002(2)	-0.0002(19)
C6	0.010(2)	0.013(2)	0.024(3)	-0.0018(19)	0.001(2)	-0.001(2)
C1	0.018(3)	0.014(2)	0.023(2)	0.000(2)	0.001(2)	0.000(2)
C8	0.021(3)	0.012(2)	0.023(2)	-0.003(2)	0.005(2)	0.006(2)
C9	0.018(3)	0.014(3)	0.029(3)	-0.005(2)	0.002(2)	0.002(2)
C10	0.027(3)	0.016(3)	0.020(3)	0.001(2)	0.003(2)	0.003(2)
C11	0.030(3)	0.016(3)	0.024(3)	-0.003(2)	0.001(2)	0.003(2)
C12	0.021(3)	0.019(3)	0.026(3)	0.001(2)	0.007(2)	-0.002(2)
C13	0.015(3)	0.018(3)	0.034(3)	0.000(2)	-0.003(2)	0.004(2)
C14	0.032(3)	0.022(3)	0.025(3)	0.007(2)	0.002(2)	0.006(2)
C15	0.029(3)	0.017(3)	0.031(3)	-0.005(2)	-0.008(3)	0.002(2)
C16	0.026(3)	0.014(3)	0.022(3)	-0.005(2)	-0.005(2)	0.001(2)
C17	0.024(3)	0.013(2)	0.021(2)	-0.007(2)	0.000(2)	0.0000(19)
C18	0.026(3)	0.013(3)	0.042(3)	-0.006(2)	-0.009(3)	0.006(2)
C19	0.013(3)	0.019(3)	0.039(3)	0.000(2)	0.004(2)	0.005(2)
C20	0.017(3)	0.019(3)	0.027(3)	-0.002(2)	0.005(2)	0.001(2)
C21	0.021(3)	0.025(3)	0.037(3)	0.003(2)	0.004(2)	-0.003(2)
C22	0.032(3)	0.021(3)	0.027(3)	-0.006(2)	0.000(3)	-0.002(2)
C23	0.018(3)	0.024(3)	0.027(3)	-0.004(2)	-0.004(2)	0.005(2)
C24	0.027(3)	0.045(4)	0.034(3)	-0.003(3)	0.003(3)	0.004(3)
C25	0.024(3)	0.030(3)	0.030(3)	-0.005(2)	-0.004(3)	-0.001(2)
C26	0.034(4)	0.035(4)	0.038(3)	-0.019(3)	-0.007(3)	0.008(3)
C27	0.042(4)	0.019(3)	0.034(3)	-0.013(3)	-0.010(3)	0.006(2)

−Emilio Napolitano−
Application of the Diffraction Technique in Solid State Chemistry from
"ab-initio" Structure Solution to Final Structure Refinement
−Powder and Single Crystal−
Doctoral Thesis in Sciences and Chemical Technology, XXIV cycle
University of Sassari

Pag. 162

Geometric parameters (Å) $C_{27}H_{37}NO_5$ (120 K).

Atom1-2	Bond/ Å
O1-C6	1.339(6)
O1-C8	1.471(2)
O2-C6	1.195(6)
O3-C18	1.439(4)
O4-C9	1.197(6)
O5-N1	1.196(6)
C1-C5	1.442(5)
C1-C12	1.428(2)
C1-C17	1.4530(19)
C2-C4	1.540(3)
C2-C8	1.505(3)
C2-C20	1.540(2)
C2-H1c2	0.960(2)
C7-C5	1.535(5)
C7-N1	1.514(5)
C7-C13	1.543(3)
C7-H1c7	0.9600(13)
C3-C8	1.497(3)
C3-C10	1.5265(10)
C3-H1c3	0.9600(7)
C3-H2c3	0.9600(6)
C4-C11	1.5229(6)
C4-H1c4	0.9600(4)
C4-H2c4	0.9600(4)
C5-C6	1.552(7)
C5-C9	1.537(5)
C8-H1c8	0.9600(14)
C9-C23	1.512(5)
C10-C11	1.5220(7)
C10-C14	1.5118(7)
C10-H1c10	0.9600(4)
C11-H1c11	0.9600(4)
C11-H2c11	0.9600(6)
C12-C19	1.5236(6)
C12-H1c12	0.9600(3)
C12-H2c12	0.9600(6)
C13-C19	1.5235(6)
C13-H1c13	0.9600(4)

–Emilio Napolitano–
Application of the Diffraction Technique in Solid State Chemistry from
"ab-initio" Structure Solution to Final Structure Refinement
–Powder and Single Crystal–
Doctoral Thesis in Sciences and Chemical Technology, XXIV cycle
University of Sassari

Pag. 163

C13-H2c13	0.9600(5)
C14-H1c14	0.9600(4)
C14-H2c14	0.9600(3)
C14-H3c14	0.9600(4)
C15-C16	1.389(6)
C15-C27	1.369(6)
C15-H1c15	0.960(5)
C16-C18	1.504(5)
C16-C22	1.385(6)
C17-C23	1.5194(8)
C17-H1c17	0.9600(6)
C17-H2c17	0.9600(7)
C18-H1c18	0.9600(11)
C18-H2c18	0.9600(9)
C19-H1c19	0.9600(4)
C19-H2c19	0.9600(4)
C20-C21	1.5694(5)
C20-C25	1.5132(4)
C20-H1c20	0.9600(4)
C21-H1c21	0.9600(3)
C21-H2c21	0.9600(3)
C21-H3c21	0.9600(3)
C22-C24	1.371(6)
C22-H1c22	0.960(5)
C23-H1c23	0.9600(5)
C23-H2c23	0.9600(5)
C24-C26	1.377(8)
C24-H1c24	0.960(5)
C25-H1c25	0.9600(3)
C25-H2c25	0.9600(3)
C25-H3c25	0.9600(3)
C26-C27	1.378(7)
C26-H1c26	0.960(5)
C27-H1c27	0.960(6)

–Emilio Napolitano–
Application of the Diffraction Technique in Solid State Chemistry from
"ab-initio" Structure Solution to Final Structure Refinement
–Powder and Single Crystal–
Doctoral Thesis in Sciences and Chemical Technology, XXIV cycle
University of Sassari

Pag. 164

Geometric parameters (°)$C_{27}H_{37}NO_5$ (120 K).

C6-O1-C8	116.7(3)
C5-C1-C12	117.0(2)
C5-C1-C17	110.4(2)
C12-C1-C17	120.59(8)
C4-C2-C8	107.90(14)
C4-C2-C20	114.52(11)
C4-C2-H1c2	108.6(3)
C8-C2-C20	113.4(2)
C8-C2-H1c2	109.80(16)
C20-C2-H1c2	102.45(16)
C5-C7-N1	110.9(3)
C5-C7-C13	108.9(2)
C5-C7-H1c7	110.2(3)
N1-C7-C13	113.2(3)
N1-C7-H1c7	105.7(2)
C13-C7-H1c7	107.81(17)
C8-C3-C10	111.84(10)
C8-C3-H1c3	109.47(8)
C8-C3-H2c3	109.47(6)
C10-C3-H1c3	109.47(5)
C10-C3-H2c3	109.47(4)
H1c3-C3-H2c3	106.99(9)
C2-C4-C11	110.51(5)
C2-C4-H1c4	109.47(10)
C2-C4-H2c4	109.47(8)
C11-C4-H1c4	109.47(3)
C11-C4-H2c4	109.47(4)
H1c4-C4-H2c4	108.41(4)
C1-C5-C7	110.0(3)
C1-C5-C6	116.7(4)
C1-C5-C9	101.8(4)
C7-C5-C6	106.0(3)
C7-C5-C9	116.7(3)
C6-C5-C9	106.0(4)
O1-C6-O2	124.9(5)
O1-C6-C5	111.0(4)
O2-C6-C5	124.1(5)
O5-N1-C7	127.6(5)

–**Emilio Napolitano**–
Application of the Diffraction Technique in Solid State Chemistry from
"ab-initio" Structure Solution to Final Structure Refinement
–**Powder and Single Crystal**–
Doctoral Thesis in Sciences and Chemical Technology, XXIV cycle
University of Sassari

Pag. 165

O1-C8-C2	107.7(2)
O1-C8-C3	108.3(2)
O1-C8-H1c8	112.47(19)
C2-C8-C3	112.51(16)
C2-C8-H1c8	108.3(2)
C3-C8-H1c8	107.65(15)
O4-C9-C5	124.9(4)
O4-C9-C23	127.3(3)
C5-C9-C23	107.5(3)
C3-C10-C11	109.41(4)
C3-C10-C14	112.63(5)
C3-C10-H1c10	108.93(7)
C11-C10-C14	113.75(6)
C11-C10-H1c10	107.69(4)
C14-C10-H1c10	104.10(4)
C4-C11-C10	113.44(5)
C4-C11-H1c11	109.47(3)
C4-C11-H2c11	109.47(2)
C10-C11-H1c11	109.47(3)
C10-C11-H2c11	109.47(4)
H1c11-C11-H2c11	105.18(6)
C1-C12-C19	107.82(7)
C1-C12-H1c12	109.47(4)
C1-C12-H2c12	109.47(6)
C19-C12-H1c12	109.47(3)
C19-C12-H2c12	109.47(2)
H1c12-C12-H2c12	111.07(6)
C7-C13-C19	111.22(4)
C7-C13-H1c13	109.47(7)
C7-C13-H2c13	109.47(7)
C19-C13-H1c13	109.47(4)
C19-C13-H2c13	109.47(4)
H1c13-C13-H2c13	107.67(4)
C10-C14-H1c14	109.47(3)
C10-C14-H2c14	109.47(3)
C10-C14-H3c14	109.47(4)
H1c14-C14-H2c14	109.47(4)
H1c14-C14-H3c14	109.47(3)
H2c14-C14-H3c14	109.47(3)
C16-C15-C27	120.2(5)
C16-C15-H1c15	119.9(5)
C27-C15-H1c15	119.9(5)

–Emilio Napolitano–
Application of the Diffraction Technique in Solid State Chemistry from
"ab-initio" Structure Solution to Final Structure Refinement
–Powder and Single Crystal–
Doctoral Thesis in Sciences and Chemical Technology, XXIV cycle
University of Sassari

Pag. 166

C15-C16-C18	119.3(4)
C15-C16-C22	120.5(4)
C18-C16-C22	120.2(3)
C1-C17-C23	101.56(8)
C1-C17-H1c17	109.47(7)
C1-C17-H2c17	109.47(7)
C23-C17-H1c17	109.47(4)
C23-C17-H2c17	109.47(5)
H1c17-C17-H2c17	116.37(7)
O3-C18-C16	109.44(18)
O3-C18-H1c18	109.47(13)
O3-C18-H2c18	109.47(11)
C16-C18-H1c18	109.47(16)
C16-C18-H2c18	109.47(13)
H1c18-C18-H2c18	109.50(10)
C12-C19-C13	112.42(3)
C12-C19-H1c19	109.47(4)
C12-C19-H2c19	109.47(3)
C13-C19-H1c19	109.47(3)
C13-C19-H2c19	109.47(3)
H1c19-C19-H2c19	106.36(3)
C2-C20-C21	112.13(9)
C2-C20-C25	111.54(12)
C2-C20-H1c20	106.46(11)
C21-C20-C25	110.33(2)
C21-C20-H1c20	107.77(3)
C25-C20-H1c20	108.40(3)
C20-C21-H1c21	109.47(2)
C20-C21-H2c21	109.47(2)
C20-C21-H3c21	109.47(2)
H1c21-C21-H2c21	109.47(2)
H1c21-C21-H3c21	109.471(19)
H2c21-C21-H3c21	109.471(19)
C16-C22-C24	118.5(5)
C16-C22-H1c22	120.7(4)
C24-C22-H1c22	120.7(4)
C9-C23-C17	104.74(8)
C9-C23-H1c23	109.47(8)
C9-C23-H2c23	109.47(9)
C17-C23-H1c23	109.47(5)
C17-C23-H2c23	109.47(4)
H1c23-C23-H2c23	113.82(5)

–Emilio Napolitano–
Application of the Diffraction Technique in Solid State Chemistry from
"ab-initio" Structure Solution to Final Structure Refinement
–Powder and Single Crystal–
Doctoral Thesis in Sciences and Chemical Technology, XXIV cycle
University of Sassari

Pag. 167

C22-C24-C26	121.1(5)
C22-C24-H1c24	119.5(5)
C26-C24-H1c24	119.5(5)
C20-C25-H1c25	109.47(2)
C20-C25-H2c25	109.47(2)
C20-C25-H3c25	109.47(2)
H1c25-C25-H2c25	109.47(2)
H1c25-C25-H3c25	109.471(18)
H2c25-C25-H3c25	109.47(2)
C24-C26-C27	120.3(4)
C24-C26-H1c26	119.8(5)
C27-C26-H1c26	119.8(5)
C15-C27-C26	119.4(5)
C15-C27-H1c27	120.3(4)
C26-C27-H1c27	120.3(4)

–Emilio Napolitano–
Application of the Diffraction Technique in Solid State Chemistry from
"ab-initio" Structure Solution to Final Structure Refinement
–Powder and Single Crystal–
Doctoral Thesis in Sciences and Chemical Technology, XXIV cycle
University of Sassari

Pag. 168